Impacts of External Variability and Randomness on Infectious Disease Dynamics: A Modelling Study with Applications to COVID-19 and Vaccination Strategies

By

Nyandjo Bamen Hetsron Legrace

A Thesis submitted in fulfillment of the requirements for the degree of:

Doctor of Philosophy in Mathematics (Applied Mathematics)

Department of Mathematics
School of Science
College of Science and Technology
University of Rwanda

August 2025

Copyright

Declaration

I declare that this dissertation contains my work except where acknowledged, and it has been passed through the antiplagiarism system and found to be compliant and this is the approved version of the PhD Thesis: **Impacts of External Variability and Randomness on Infectious Disease Dynamics: A Modelling Study with Applications to COVID-19 and Vaccination Strategies.**

Nyandjo Bamen Hetsron Legrace, Reg. N°: 221000078 Date: October 3, 2025

Name, registration number and signature of the PhD candidate

The PhD Thesis Supervisory Team of Mr. Nyandjo Bamen Hetsron Legrace

Prof. Olivier Menoukeu Pamen Date: October 3, 2025

Name and signature of the Main Supervisor

Prof. Aurelien Tellier Date: October 3, 2025

Name and signature of the Co-supervisor

Prof. Jean Marie Ntaganda Date: October 3, 2025

Name and signature of the Co-supervisor

Dedication

In the memory of my father.

Acknowledgement

The preparation of this thesis was made possible through the collaboration of many individuals whose invaluable support and assistance have been instrumental. I would like to take this opportunity to express my heartfelt gratitude to everyone who contributed in any way to the successful completion of this work.

First and foremost, I extend my deepest thanks to my supervisors, Prof. Olivier MENOUKEU PAMEN, Prof. Aurelien TELLIER, and Prof. Jean Marie NTAGANDA, for their unwavering support, guidance, and encouragement throughout this research journey. Their positive attitude and regular follow-ups on my progress greatly eased the Process.

I would like to thank the examiners of the Synopsis Evaluation, Prof. Boureima SANGARE, Prof. Martial NDEFFO and Prof. Joseph NZABINATA, for their high contribution in the improvement of the quality of this document.

I would like to thank the jury members of the Ph.D defense, Dr. Celestin KURUJYIBWAMI as the chair of the session, Prof. Boureima SANGARE, Prof. Joseph NZABINATA and Dr. Charline UWILINGIYIMANA as examiners, for their useful remarks and comments that contributed to this final version of my manuscript.

I am also profoundly grateful to the UR Centre of Postgraduate Studies, the School of Sciences, and the Department of Mathematics at the University of Rwanda, as well as the College of Registrar, for their guidance and support. Your patience, generosity, and willingness to assist whenever I sought clarification were deeply appreciated.

I am truly grateful for the support of Prof. Antoine TAMBUE and Prof. Gisele MOPHOU who are among the people who initiated this Process. I am equally indebted to my former master's supervisor, Prof. Samuel BOWONG, for introducing me to the field of Mathematical Biology.

This research would not have been possible without financial support. This thesis was funded by a grant from the African Institute for Mathematical Sciences, www.nexteinstein.org, with financial support from the Government of Canada, provided through Global Affairs Canada, www.international.gc.ca, and the International Development Research Centre, www.idrc.ca. It was also supported by the Technical University of Munich (TUM) through the TUM Global Incentive Fund and the TUM Africa Talent Fund, as well by the Deutscher Akademischer Austauschdienst (DAAD) through the DAAD Research Grant. I am sincerely

grateful to the African Institute for Mathematical Sciences Research and Innovation Centre (AIMS RIC), the Technical University of Munich (TUM), and the Deutscher Akademischer Austauschdienst (DAAD) for their funding and training opportunities, which enabled me to pursue this work.

To my fellow participants in the AIMS Doctoral Training Programme in Climate-Related Sciences (ADTP-CS) and our coordinators, Dr. Isambi Sailon MBALAWATA and Dative TUYISENGE, I cherish the amazing moments we shared during various events in Rwanda. My heartfelt thanks also go to my Rwandan colleagues, Marie Aimée and Michel, for their significant contributions at the university level.

I am truly grateful to my research group at AIMS Ghana for their insightful discussions, comments, and suggestions, which helped shape my ideas. I deeply value the friendships and joyful memories we created together in Accra. Special thanks to Wilfried, Some, Rhoss, Moustapha, Bernard, Edward, Lizzy, Abi, Francis, Sorelle, Antoine-Marie, and Olivier. I also appreciate the support of the AIMS Ghana management team for hosting me and facilitating visa arrangements for my travels to conferences and workshops.

My integration into the Popgen group at TUM was both rewarding and seamless, thanks to the warm welcome and support of Silke, Daniela, Usman, Gustavo, Sona, Thibaut, Heng, Kai, Sidra, Kevin, Lukas, Moritz, Hsiang-Ling, Luzie, Miles, and Aurelien. I also had the privilege of attending courses taught by Prof. Donna ANKERST, Prof. Johannes MÜLLER, and Prof. Cristina KUTTLER, whose valuable insights and discussions were greatly enriching me.

I am deeply appreciative of Prof. Ralf Wunderlich for his invitation to the Brandenburgische Technische Universität Cottbus-Senftenberg and for the discussions I had with Florent and Ibrahim during my visit.

A special note of thanks goes to Beryl, Daudel, Ronald, Aicha, Severine, and Guissel for their constant encouragement and companionship, which brought me great comfort and joy. I am also indebted to my other friends whose presence and shared moments have enriched my life immeasurably.

Above all, I am profoundly grateful to my family for their unwavering support, unconditional love, and encouragement throughout my academic journey. To my parents, Mr. and Mrs. BAMEN, I acknowledge the sacrifices you made and the belief you placed in me, which have been a constant source of motivation and strength. Being away from home for extended periods was not easy, but your faith in me carried me through. Finally, to myself I trust the Process and am proud of the journey thus far.

Abstract

Disease dynamics are inherently influenced by the interplay between hosts and parasites. And this interaction may be subject to demographic and environmental variability. As environmental conditions shift and human interventions evolve, understanding these dynamics is crucial for effective disease management. This thesis investigates into the wide area of disease modelling, with a particular emphasis on the impact of external variability and stochasticity on epidemic dynamics within the context of host-parasite. First, we investigate the global stability dynamics and sensitivity of COVID- 19 transmission models considering timely and delayed diagnosis. Through theoretical analysis and numerical simulations, we show that the disease persistence depends on the basic reproduction number, $\mathcal{R}_0$. Our results suggest reducing the inflow of new individuals into the country or ensuring early diagnosis will lower the basic reproduction number and thereby limiting secondary infections and preventing multiple epidemic peaks. Next, we study the impact of imperfect vaccines, vaccine trade-offs, and population turnover on infectious disease dynamics. Using a mathematical model, we compute the basic reproduction number, establish global stability conditions of equilibria and perform sensitivity analysis. We derive conditions for the vaccination coverage and efficiency to achieve disease eradication assuming different intensity of the population turnover (weak and strong), vaccine properties (transmission and/or recovery) and trade-off between the latter. We show that the minimum vaccination coverage increases with lower population turnover, decreases with higher vaccine efficiency (transmission or recovery), and is increased/decreased by up to 15% depending on the vaccine trade-off. We then formulate a stochastic model for disease transmission in heterogeneous populations of vaccinated and unvaccinated hosts. We prove the existence of a unique nonnegative weak solution and derive conditions for extinction and persistence in mean. Simulations illustrate how demographic variability can alter vaccination outcomes and long-term disease persistence. Finally, we outline future research on metapopulation models for malaria forecasting, incorporating temperature variability and some vaccination strategies to account for climate-sensitive transmission regarding a specific vaccine. This extension aims to enhance predictive accuracy and support targeted interventions for malaria control in a changing climate.

List of publications

1. S. E. Moore, **H. L. Nyandjo Bamen**, O. Menoukeu-Pamen, J. K. K. Asamoah, Z. Jin, Global stability dynamics and sensitivity assessment of covid-19 with timely-delayed diagnosis in ghana. Computational and Mathematical Biophysics 10 (1), 87–104 (2022).

2. **Nyandjo Bamen, H.L.**, Ntaganda, J.M., Tellier, A., Menoukeu Pamen, O.: Impact of imperfect vaccine, vaccine trade-off and population turnover on infectious disease dynamics. Mathematics 5(11), 1240 (2023).

3. **Nyandjo Bamen, H.L.**, Ntaganda, J.M., Tellier, A., Menoukeu Pamen, O.: Stochastic extinction and persistence of a heterogeneous epidemiological model. Journal of Applied Mathematics and Computing 70(6), 5603–5628 (2024)

Table of contents

List of abbreviations

NPI: **N**on-**P**harmacological **I**ntervention
LHS: **L**atin **H**ypercube **S**ampling
PRCC: **P**artial **R**ank **C**orrelation **C**oefficient
DFE: **D**isease-**F**ree **E**quilibrium
EE: **E**ndemic **E**quilibrium
GAS: **G**lobally **A**symptotically **S**table
LAS: **L**ocally **A**symptotically **S**table
ODE: **O**rdinary **D**ifferential **E**quation
SDE: **S**tochastic **D**ifferential **E**quation
a.s.: **a**lmost **s**urely

List of tables

List of figures

Chapter 1

General introduction

1.1 Background

The diversity of host defenses against parasitism reflects the complex and dynamic nature of host-parasite interactions. In natural systems, hosts have developed a wide range of defense mechanisms, which can be classified into immune and behavioral defenses. Immune defenses, include resistance which refers to the ability to prevent or limit infection and tolerance, which refers to the ability to minimize damage caused by an infection. These mechanisms provide direct biological protection against parasites. Behavioral defenses, on the other hand, involve strategies like social avoidance [61], where individuals distance themselves from infected conspecifics, and mate choice, where potential mates are selected based on traits indicative of parasite resistance. At the same time, parasites have developed a diverse array of strategies to exploit hosts [107], including variations in virulence (ranging from highly virulent to avirulent), infection duration (chronic or acute infections), life cycle complexity (involving one or multiple variants), and transmission mechanisms (airborne, environmental, social, or sexual) [77]. These variations in parasitic traits have likely emerged through coevolution with their hosts, as both parties adapt to the changing pressures exerted by the other.

This reciprocal interaction has been observed across various systems including, viral and bacterial parasites of animals [39], bacterial, fungal, and animal parasites of plants [44, 57], and viral parasites of bacteria [96]. Given the ubiquitous presence of parasites and their significant impact on host fitness, host-parasite interaction is considered as one of the major forces in shaping the Earth's biodiversity. This evolutionary arms race impacts the biological and ecological traits of both hosts and parasites, and leads to maintenance of significant diversity in antagonistic species. In turn this diversity plays a crucial role in determining the spread and persistence of infectious diseases [82, 117].

Mathematical modelling has been a fundamental tool in advancing our understanding of host-parasite interactions [28], contributing to a robust and evolving body of theoretical work. These models allow researchers to investigate the complex dynamics between hosts

and parasites, providing insights into the causes and consequences of their reciprocal evolutionary interactions. By translating biological processes into mathematical framework, these models can simulate various scenarios, such as how different defense strategies in hosts or transmission mechanisms in parasites influence the coevolutionary landscape. Early mathematical models, such as those developed by Anderson and May [10, 11, 13], provided foundational insights into the population-level dynamics in host-parasite interactions. These models highlighted how factors such as parasite virulence, host resistance, and transmission rates influence the invasion, persistence and spread of infectious diseases. Building upon this groundwork, more recent models have incorporated genetic and evolutionary dynamics, enabling deeper exploration of how host and parasite traits coevolve over time [31, 47].

1.2 Problem statement

In the field of mathematical epidemiology, many researchers have predominantly used deterministic models to provide valuable insights for policymakers [29, 50, 69], despite the fact that they assume predictable outcomes based on initial conditions. Besides, host-parasite interactions in a stochastic setting have received considerably less attention. However, in a rapidly changing world, the delicate balance between hosts and parasites is increasingly subject to disruption by external variability and stochastic (random) factors such as demographic variability, environmental changes, and human interventions, which can lead to unexpected outcomes, such as sudden disease outbreaks or the emergence of new pathogen strains, challenging our ability to effectively manage and control [6, 102, 116, 113].

In this thesis, we consider there are no significant mutations or adaptations on parasites that alter their ability to infect or exploit hosts. The evolutionary pressure is unidirectional, with hosts being the primary drivers of change by developing defenses such as vaccines [87], non-pharmacological interventions (NPIs) [55], antiviral drugs, antibiotics (for bacterial infections), or other treatments to combat infections [85]. We explore how the absence of parasite evolution and the presence of host driven defenses interact with random factors that can significantly influence the course of epidemics. Understanding these dynamics is crucial for designing effective public health strategies, especially in an area marked by rapid environmental changes, increased global mobility, and varying levels of healthcare access. Since not all individuals respond to vaccines or NPIs in the same way, stochastic variations in immune responses, behavior, and compliance with interventions can lead to heterogeneous outcomes, where some populations experience higher rates of infection despite widespread preventative measures. Fluctuations in environmental conditions (temperature, humidity) or

social behavior (seasonal gatherings) can also introduce randomness into epidemiological dynamics [41]. For example, a heatwave might cause more people to gather indoors, increasing the likelihood of transmission, or it can extend the active season for vectors such as mosquitoes, increasing the transmission window for diseases like malaria and dengue [105]. Additionally, changes in abiotic factors, such as temperature or humidity can disrupt the timing of host-parasite interactions, potentially increasing the overlap between susceptible hosts and infectious parasites, further exacerbating disease risks.

Despite the wealth of literature on human disease epidemiology, there are two types of unresolved questions in the study of the impact of stochastic processes on disease dynamics. The key general, yet only partially answered, question is to assess whether deterministic models can predict accurately disease epidemiology and dynamics, or if stochastic processes affect the behavior and outcome/severity of an epidemics. A most efficient disease control method is vaccination. The efficacy of a vaccination campaign depends on the efficiency of the vaccine in reducing symptoms, transmission and decreasing virulence, but also on population demography, age structure, and social constraints. Thus the questions I want to answer are:

1. What is the influence of population characteristics on efficacy of vaccination?

2. Do stochastic processes affect the predicted impact of vaccination in controlling the disease compared to the deterministic developed models?

Two gaps in knowledge need to be filled. First, key biological characteristics of disease epidemiology models need to be studied. What characteristics of the population influence the most efficiency of a vaccination campaign ? What is the influence of stochasticity due to random external factors on disease transmission and disease dynamics in a population with vaccination ? Second, at the mathematical level, stochastic models have relied on incomplete posedness and unknown steady state behavior. Therefore a key question is: What is the impact of stochasticity in changing the behavior of the stochastic model compared to the equivalent deterministic model ?

1.3 General objective

The main objective of this thesis is to explore how external variability and random factors influence the dynamics of host-parasite systems, particularly in cases where parasites do not evolve.

1.3.1 Specific objectives

Specifically, this study aims to:

1. Assess the impact of timely and delayed diagnosis on the spread of COVID-19 in Ghana
2. Evaluate how variations in vaccine efficacy mechanisms and population demographic dynamics affect the effectiveness of vaccination policies
3. Investigate how demographic stochasticity affects the extinction and persistence of infectious diseases

1.4 Thesis Contribution

This thesis makes several original contributions to the mathematical modelling of host-parasite systems and the potential role that can play external variability and random factors. The key contributions are as follows:

- We developed new deterministic or stochastic models that capture the dynamics of host-parasite interactions under varying external influences such as delayed diagnosis, environmental transmission pathways, demographic variability, or different vaccine efficiency properties.
- In the deterministic framework, we constructed appropriate Lyapunov function candidates to rigorously analyze the global stability of equilibrium points.
- Sensitivity analysis of the COVID-19 model revealed that key parameters such as the transmission rate of exposed individuals, transmission and decay rate of virus in the environment and the proportion of infectious with timely diagnosis have significant impacts on the epidemic dynamics.
- For the imperfect vaccination model, explicit threshold conditions involving the proportion of vaccinated individuals required for disease eradication with imperfect vaccine.
- The stochastic model underwent comprehensive theoretical analysis, including rigorous proofs of the existence and uniqueness of weak solutions, demonstration of stochastic ultimate boundedness, and identification of conditions under which the disease either becomes extinct or persists in mean.

- Overall, the thesis provides evidence-based insights that are relevant for informing public health interventions and control strategies under various real world constraints and uncertainties.

1.5 Thesis outlines

The thesis is organized in five chapters as follow:

- In Chapter 1, we present the introduction where we give a context of the published results.
- In Chapter 2, we present the literature review.
- In Chapter 3, we present the methodology used to achieve our objectives.
- In Chapter 4, we present our published findings.
- In Chapter 5, we conclude and give some perspectives of future works.

Chapter 2

Literature review

COVID-19 was declared a pandemic in the first quarter of 2020 by the World Health Organization (WHO) see, e.g. [92]. The disease affects different people in different ways with most infected people developing mild to moderate illness. Most common symptoms are fever, dry cough and tiredness while less common symptoms include aches and pains, sore throat, diarrhoea, conjunctivitis, headache, loss of taste or smell, a rash on skin or discolouration of fingers or toes [92, 93]. It is well understood that the elderly with underlying medical problems are the most vulnerable people. COVID-19 is transmitted by means of contact (direct or indirect), droplet spray in short range transmission and aerosol in long-range transmission (airborne transmission) [81]. Globally, there were $100,285,517$ confirmed cases with $2,149,461$ confirmed death cases as on 26th January, 2021 [93].

In Africa, there were a total of $3,472,023$ confirmed cases with $86,060$ confirmed death cases where Ghana is among the top ten (10) most infected countries as on 26th January, 2021 [93]. As on 26th January, 2021, Ghana had $62,135$ confirmed cases with 372 confirmed death cases. The first confirmed cases in Ghana were recorded on 12th of March, 2020 from two people who had returned from Norway and Turkey [37]. Several works have been studied concerning COVID-19 including a human-to-human model analysis for some African countries [15, 34, 52, 86]. The transmission dynamics in Wuhan has also been studied and presented in several articles with control measures and basic reproduction number well analyzed, see e.g. [40, 84, 100]. In [80], the control strategies to curb the virus using data from Wuhan were presented. Measures to control the spread of COVID-19 are mostly avoiding human-to-human contacts, personal protection and environmental disinfection. The diagnosis of COVID-19 is difficult and the incubation period of $2-14$ days or $0-24$ days is longer than most known coronaviruses or similar viruses which usually ranges between 1 to 10 days [70]. Due to the long incubation period, it results in a delay in diagnosis. This delay allows for human-to-human transmission as well as human-environment-human transmission. Therefore, evaluating the impact of delayed diagnosis is essential for understanding the transmission dynamics of COVID-19 and for designing effective control strategies.

In addition, vaccination is one of the most effective public health policies for protecting humans and animals from infectious diseases. Global vaccination campaigns have helped eradicate diseases such as smallpox, measles, poliomyelitis and rinderpest in most parts of the world, ultimately saving the lives of millions of humans and animals. By definition, a perfect vaccine would keep vaccinated individuals from becoming infected when exposed to the pathogen. An imperfect vaccine, however, does not prevent vaccinated individuals from becoming infected upon pathogen exposure but may still be beneficial in various ways [12]. For example, imperfect vaccines may provide benefits such as preventing infection, limiting parasite within-host growth and thus reducing the damage done to the host [110] or preventing transmission by infected hosts [48]. As we have seen recently with the epidemic of COVID-19, imperfect vaccines can be used to reduce the number of infected individuals and also to protect individuals at risk of developing a more lethal form of the infection. The use of imperfect vaccines may be advantageous when the vaccination efficiency is volatile and decreases due to the appearance of new variants of the virus [33, 54, 56].

The effectiveness of a given vaccine is determined not only by its biochemical and immunological properties but also by how the vaccine is deployed and what other health management (biosecurity) measures are in place. Maintaining herd immunity during a disease outbreak, for example, has been promoted as a highly effective disease control strategy [22, 35, 72]. However, a continuous influx of new susceptible, possibly unvaccinated individuals contributes to the long-term persistence of the disease in the population [98, 101]. The frequent introduction of pathogens into a partially immune population (with an intermediate level of population immunity) can lead to longer-lasting epidemics and/or a higher total number of infectious individuals than the introduction into a naive population [98]. This phenomenon is named “epidemic enhancement” [98]. More generally, the population turnover rate, that is, the rate at which individuals can enter and exit the considered population, may affect the effectiveness of control strategies [27, 63, 88]. In humans and also domesticated animals, population turnover takes the form of immigration and emigration in and out of the population, as well as the birth and death of individuals. The turnover is an often neglected factor in epidemiology when generalising predictions of disease modelling from human to domesticated and wild animal populations.

Moreover, a second parameter of importance in studying the efficiency of vaccination strategies is the existence of biological trade-offs in the epidemiology of infectious diseases. The prime example is the trade-off between parasite virulence and transmission rate, which raises challenges for vaccine manufacturing. Indeed, in the seminal paper by [48], vaccines affecting disease transmission are predicted to possibly lead to a decrease

in parasite virulence, while other types of vaccines (reducing within-host growth rate) may lead to an increase in parasite virulence and thus the counter-effect of a worst epidemiological outcome. Interestingly, much work has been devoted to generating precise predictions for virulence evolution in known parasite species by incorporating empirical characterisations of vaccine effects into models capturing the epidemiological details of a given system [2, 31, 46]. In contrast, the biochemical and immunological trade-offs of the vaccine itself have received little attention. We specifically mean here that vaccination can affect several aspects of the disease dynamics, such as within-host growth and transmission, with possible trade-offs between these characteristics. For example, a vaccine reducing within-host growth may be more or less effective in reducing disease transmission. We, therefore, consider the definition of imperfect vaccines as i) providing partial protection (non-maximal efficiency) against infection (decreasing transmission) and ii) partially enhancing the recovery of infected individuals. We are interested in the possible trade-off between these two properties. There has been remarkably little work performed to generally assess how the interplay between different vaccine properties, trade-offs and vaccination strategies influences the burden of the epidemic in a heterogeneous community/population with imperfect vaccination.

A number of mathematicians have developed diverse epidemic models to analyze and control the spread of transmissible diseases in the community by using a deterministic approach [12, 14, 79, 108]. However, when the number of infectious individuals introduced into a population is small or when the variability in transmission, recovery, recruitment or death impacts the epidemic outcome, the impact of stochasticity cannot be ignored. The outcome of the stochastic epidemic model may, indeed, differ from the deterministic one. Based on their equivalent deterministic counterparts, numerous plausible stochastic epidemic models have been derived. In the specific case of epidemiology, there exists in the literature a variety of approaches using stochastic models for the mathematical modelling of epidemics such as discrete time Markov chain (DTMC) [6], continuous time Markov chain (CTMC) [71] and stochastic differential equations (SDEs) [67]. To cite but a few studies, to include stochastic demographic variability, [71, 115] presented a continuous-time Markov chain model that successfully simulated disease clearance, and identified the main factors determining the probability and time of clearance. Similarly, [67] investigated the situation of white noise stochastic perturbations around the endemic equilibrium state. With a widely used approach, the technique of parameter perturbation, [62, 116] were able to derive SDE epidemic of SIR models, and proved the existence of the positive solution and studied the asymptotic behavior.

Another widely used approach to derive SDE epidemic models was provided in [3]. One advantage of the later modeling approach is that the parameters in the model are better understood because they are generated from basic assumptions. However, it was shown [32] that the derived SDE models from [3] do not preserve the non-negativity of the solutions, especially when population sizes are near zero. A set of explicit necessary and sufficient conditions to be fulfilled so that systems of SDEs have non-negative solutions, is given in [32]. These conditions have been recently used in [5] when describing a new method to derive an SDE epidemic model which preserves the non-negativity of solutions with regard to biological realism. This new approach [5] allows to formulate an Itô SDE for SIR (Susceptible-Infected-Recovered) model that ensures the positivity of the system. This new approach is a modification of the widely used one described in [4, 6, 7, 8] when the SDE models can have solutions that become negative in finite time in the case of population sizes being close to zero [32].

2.1 Deterministic modelling preliminaries

We begin with standard compartmental models such as SIR, SEIR, and their extensions. These models divide the population into compartments and use ordinary differential equations (ODEs) to describe the transitions between states.

2.1.1 Well-posedness for ordinary differential equations

Let D be an open subset of $\mathbb{R}^n$, $I \subset \mathbb{R}$, $f : I \times D \to \mathbb{R}^n$, be a vector-valued function, $f = (f_1, f_2, \cdots, f_n)$. Given the dynamical system

$$\begin{cases} \dfrac{\mathrm{d}x}{dt} & = f(t, x), \\ x(t_0) & = x_0, \end{cases} \tag{2.1}$$

Theorem 1 (Existence and uniqueness of solution [25]) *Let the function f be continuous with respect to t and Lipschitz with respect to x on D. Then the initial value value problem admits a unique solution on I.*

Proposition 1 (Invariance of the non-negative orthant [106]) *Suppose that f in Equation (2.1) has the property that solutions of initial value problems $x(t_0) = x_0 \geq 0$ are unique and for all i $f_i(t, x) \geq 0$ whenever $x \geq 0$ satisfies $x_i = 0$. Then $x(t) \geq 0$ for all $t \geq t_0$ for which it is defined, provided $x(t_0) \geq 0$.*

2.1.2 Basic reproduction number

We are going to present the method proposed by Van den Driessche and Watmough [36] to compute the basic reproduction rate $\mathcal{R}_0$.

In simple models, if there is only one infected compartment, the value of $\mathcal{R}_0$ is the product of the infection rate and the duration of infection. In cases where there are more than one classes of infectives involved, we should following the guidelines. Consider that in the dynamical system (2.1), m compartments representing non-infected. We define X_s to be the set of all disease free states. That is

$$X_s = \{x \geq 0 \mid x_i = 0, i = 1, 2, \cdots, m\}.$$

Let $\mathcal{F}_i(x)$ be the rate of appearance of new infections in compartment i, $\mathcal{V}_i^+(x)$ be the rate of transfer of individuals into compartment i by all other means, and $\mathcal{V}_i^-(x)$ be the rate of transfer of individuals out of compartment i. It is assumed that each function is continuously differentiable at least twice in each variable. The disease transmission model consists of nonnegative initial conditions together with the following system of equations:

$$\begin{cases} \dfrac{\mathrm{d}x}{dt} &= f(t,x) = \mathcal{F}_i(x) - \mathcal{V}_i(x), \quad i = 1, 2, \cdots, n \\ x(t_0) &= x_0, \end{cases} \tag{2.2}$$

where $\mathcal{V}_i(x) = \mathcal{V}_i^+(x) - \mathcal{V}_i^-(x)$ and the functions satisfy assumptions (1)–(5) described below. Since each function represents a directed transfer of individuals, they are all non-negative. Thus,

1. if $x \geq 0$, then $\mathcal{F}_i(x), \mathcal{V}_i^+(x), \mathcal{V}_i^-(x) \geq 0$ for $i = 1, 2, \cdots, n$
2. if $x_i = 0$ then $\mathcal{V}_i^- = 0$. In particular, if $x \in X_s$, $\mathcal{V}_i^- = 0$ for $i = 1, 2, \cdots, m$
3. $\mathcal{F}_i = 0, i > m$
4. if $x \in X_s$ then $\mathcal{F}_i(x) = \mathcal{V}_i^+(x) = 0, i = 1, 2, \cdots, m$
5. if $\mathcal{F}(x)$ is set to zero, then all eigenvalues of the Jacobian matrix of f, $Df(x^*)$ evaluated at the DFE, x^*, have negative real parts.

Under these conditions, for $x^* \in X_s$, the Jacobian matrix F and V are defined as follows

$$F = \left(\frac{\partial \mathcal{F}_i}{\partial x_j}(x^*)\right)_{i,j} \quad \text{and} \quad V = \left(\frac{\partial \mathcal{V}_i}{\partial x_j}(x^*)\right)_{i,j}, \quad 1 \leq i, j \leq m, \tag{2.3}$$

such that F is non-negative and V is invertible.

Matrix FV^{-1} is the next generation matrix and $\mathcal{R}_0$ is its spectral radius,

$$\mathcal{R}_0 = \rho(FV^{-1}).$$

2.1.3 Equilibria and stability

Due to nonlinearities, many dynamical systems cannot be solved analytically. To acquire insight into the long-term behavior of such systems, it is essential to begin by determining rudimentary solutions that can enable us to examine the behavior of all other solutions.

Definition 1 (Equilibrium point) *$x^* \in D$ is an equilibrium point or steady-state of the dynamical system (2.1) if $f(t, x^*) = 0$.*

Definition 2 (Stable solution) *A solution $x^*(t) \in \mathbb{R}^n$ of the dynamical system (2.1) is said to be stable if given $\epsilon > 0$, $\exists \delta(\epsilon, t_0) > 0$ such that for $t \geq t_0$ and for any neighboring solution*

$$\|x(t) - x^*(t)\| < \epsilon \quad \text{whenever} \quad \|x(t_0) - x^*(t_0)\| < \delta.$$

Definition 3 (Lyapunov function [66]) *Given a dynamical system $\frac{dx}{dt} = f(x)$. The function $V : M \subset \mathbb{R}^n \longrightarrow \mathbb{R}$ called Lyapunov function for f, if*

- $V \in C^1(M, \mathbb{R})$
- $V(x) \geq 0$ *on* M.
- *On M we have*

$$\frac{dV}{dt} = \sum_{j=1}^{n} \frac{\partial V}{\partial x_j} f_j(x) \leq 0.$$

Theorem 2 (Lasalle [66]) *Let consider the dynamical system $\frac{dx}{dt} = f(x)$ with an equilibrium x^*, defined on a compact positively invariant set Ω.*

If V a Lyapunov function and moreover the largest invariant set contained in $\mathcal{L} = \left\{x \in \Omega | \quad \frac{dV}{dt}(x) = 0\right\}$ is reduced to $\{x^*\}$, then x^* is globally asymptotically stable in Ω.

2.2 Stochastic differential equation modelling preliminaries

2.2.1 Concepts on probability theory

We introduce some fundamental concepts of probability theory such as probability space, random variable and stochastic process.

Definition 4 (Sample space [73, 91]) *The sample space or universe Ω is a non-empty set representing all possible outcomes. Each element $\omega \in \Omega$ is called an elementary events and is interpreted as a possible outcome of an experiment (test, monitoring, phenomenon).*

Definition 5 ($\sigma-$algebra and measurable space [73, 91]) *A collection $\mathcal{F}$ of subsets (i.e. events) of Ω is called a $\sigma-$algebra and the ordered pair $(\Omega, \mathcal{F})$ is called a measurable space if $\mathcal{F}$ has the following properties:*

1. $\Omega \in \mathcal{F}$.
2. *If $F \in \mathcal{F}$, then the complement of F, denoted F^c, is in $\mathcal{F}$, i.e.,*

$$F^c = \{\omega \in \Omega : \quad \omega \notin F\} \in \mathcal{F}.$$

3. *For any sequence $\{F_n\}_{n=1}^{\infty}$, the union $\cup_{n=1}^{\infty} F_n \in \mathcal{F}$.*

An element of $\mathcal{F}$ is called $\mathcal{F}-$ measurable subset of Ω.

The probability measure P is defined on $\mathcal{F}$.

Definition 6 (Probability measure [73, 91]) *Let $(\Omega, \mathcal{F})$ be a measurable space. The application*

$\mathbb{P} : \mathcal{F} \to [0, 1]$ *is called a probability measure if it satisfies the following properties:*

1. $\mathbb{P}(\Omega) = 1 - \mathbb{P}(\emptyset) = 1$.
2. *If $F_i \cap F_j = \emptyset$ for $i, j = 1, 2, \ldots, i \neq j$ (pairwise disjoint), then*

$$\mathbb{P}(\cup_{n=1}^{\infty} F_n) = \sum_{n=1}^{\infty} \mathbb{P}(F_n),$$

where $F_n \in \mathcal{F}, n = 1, 2, \ldots$.

The probability measure $\mathbb{P}$ along with the measurable space $(\Omega, \mathcal{F})$ defines a probability space, the ordered triple $(\Omega, \mathcal{F}, \mathbb{P})$.

Definition 7 (Filtration [73, 91]) *Let $(\Omega, \mathcal{F}, \mathbb{P})$ be a probability space. The family of $\sigma-$algebra $\mathcal{F}_t, t \geq 0$ is called a filtration if for any $0 \geq s \geq t$, we have*

$$\mathcal{F}_s \subset \mathcal{F}_t \subset \mathcal{F}.$$

The quadruplet $(\Omega, \mathcal{F}, \{\mathcal{F}_t\}_{t \geqslant 0}, \mathbb{P})$ is called a filtered probability space.

Definition 8 (Random variable [73, 91]) *Let $(\Omega, \mathcal{F})$ be a measurable space. A random variable X is a $\mathcal{F}$-measurable function, $X : \Omega \to \mathbb{R}^d, \quad d \geq 1$, i.e.*

$$X^{-1}(B) = \{\omega \in \Omega : X(\omega) \in B\} \in \mathcal{F},$$

$\forall B$ open set of $\mathbb{R}^d$.

Remark 1 *According to the values of $d \geq 1$, X is called*

- *real random variable if $d = 1$,*
- *vector random variable if $d > 1$.*

Definition 9 (Stochastic process [73, 91]) *A stochastic process $X := \{X_t, t \in I\}$ is a family of random variables defined on a common probability space $(\Omega, \mathcal{F}, \mathbb{P})$ and indexed by the index set I.*

Usually I represents time. If $I = \{0, 1, 2, \dots\}$, then the process is called a discrete-time stochastic process. If $I = \mathbb{R}^+$, then the process is called continuous-time stochastic process.

Assuming the state space is $\mathbb{R}^n$, with $n \in \mathbb{N}$. For each time $t \in I$ fixed, we have a random variable

$$\omega \mapsto X_t(\omega) \in \mathbb{R}^n.$$

On the other hand, for a fixed sample point $\omega \in \Omega$, the mapping

$$t \mapsto X_t(\omega), \quad t \in I$$

is the sample trajectory of the process X associated with ω.

Definition 10 (Standard Brownian motion [73, 91]) *The stochastic process $\{W(t), t \geq 0\}$ is called a standard Brownian motion if:*

1. $W(0) = 0$ *a.s.*,
2. $W(t) - W(s) \sim \mathcal{N}(0, t-s)$ *for all* $0 \leq s < t < \infty$,
3. *the increments* $W(t) - W(u)$ *and* $W(u) - W(s)$ *are independent for all* $0 \leq s < u < t$,
4. *the maps* $t \mapsto W(t, \omega)$ *are continuous for all* $\omega \in \Omega$.

2.2.2 Well-posedness of stochastic differential equation model

SDEs model are introduced as a natural extension of ODEs to account for randomness.

Let us consider $T > 0$, $t_0 \geq 0$ and the following d-dimensional SDE

$$\begin{cases} \mathrm{d}X(t) &= f(X(t), t)\mathrm{d}t + g(X(t), t)\mathrm{d}W(t), \quad t \in [t_0, T] \\ X(t_0) &= X_0, \end{cases} \tag{2.4}$$

where $f : \mathbb{R}^d \times [t_0, T] \to \mathbb{R}^d$ the drift and $g : \mathbb{R}^d \times [t_0, T] \to \mathbb{R}^d \times \mathbb{R}^m$ the diffusion, are locally Lipschitz continuous function and W is an m-dimensional standard Wiener process defined on $(\Omega, \mathcal{F}, \{\mathcal{F}_t\}_{t \geqslant 0}, \mathbb{P})$, a complete probability space with a filtration $\{\mathcal{F}_t\}_{t \geqslant 0}$ satisfying the usual conditions (i.e. it is increasing and right continuous and $\mathcal{F}_0$ contains all $\mathbb{P}$-null sets). Set

$\mathbb{R}^d_+ := \{x \in \mathbb{R}^d, x_i \geq 0, 1 \leq i \leq d\}$, we denote by $C^{2,1}(\mathbb{R}^d \times [t_0, T]; \mathbb{R}_+)$ the set of nonnegative function defined on $\mathbb{R}^d \times [t_0, T]$ that are twice continuously differentiable in x and once in t. The differential operator L associated with the diffusion (2.4) is defined by

$$L = \frac{\partial}{\partial t} + \sum_{i=1}^{d} f_i(x,t)\frac{\partial}{\partial x_i} + \frac{1}{2}\sum_{i,j=1}^{d} [g^T(x,t)g(x,t)]_{ij}\frac{\partial^2}{\partial x_i \partial x_j}. \tag{2.5}$$

If L acts on a function $V \in C^{2,1}(\mathbb{R}^d \times [t_0, T]; \mathbb{R}_+)$, then

$$LV(x,t) = V_t(x,t) + V_x(x,t)f(x,t) + \frac{1}{2}trace[g^T(x,t)V_{xx}(x,t)g(x,t)],$$

where $V_t = \frac{\partial V}{\partial t}$, $V_x = (\frac{\partial V}{\partial x_1}, \ldots, \frac{\partial V}{\partial x_d})$ and $V_{xx} = (\frac{\partial^2}{\partial x_i \partial x_j})_{d \times d}$. By Itô's formula, if $x \in \mathbb{R}^d$, then

$$\mathrm{d}V(X(t), t) = LV(X(t), t)\mathrm{d}t + V_x(X(t), t)g(X(t), t)\mathrm{d}W_t.$$

Theorem 3 (Existence and uniqueness of solutions [91]) *If the coefficient functions* f, g *of the SDE* (2.4) *satisfy the conditions:*

1. *(Linear growth condition) There exists a constant* $C_1 < \infty$ *such that*

$$| f(t,x) |^2 + | g(t,x) |^2 \leq C_1(1+ | x |^2)$$

for all $(x,t) \in \mathbb{R}^d \times [t_0, T]$*; and*

2. *(Uniform Lipschitz condition) There exists a constant* $C_2 < \infty$ *such that*

$$| f(t,x) - f(t,y) | + | g(t,x) - g(t,y) | \leq C_2 | x - y |$$

for all $x, y \in \mathbb{R}^d$ *and* $t \in [t_0, T]$.

Then, there exists a unique adapted solution $X(t)$ *to equation* (2.4) *with initial value* X_0 *such that*

$$E[| X(t) |^2] < \infty,$$

for all $t \in [t_0, T]$.

Theorem 4 (Invariance criteria [32]) *Let* $I \subset \{1, 2, \ldots, d\}$ *be a non-empty subset. Then, the set*

$$K^+ := \{x \in \mathbb{R}^d : x_i \geq 0, \quad i \in I\}$$

is invariant for the stochastic system (f, g) *if and only if*

- $f_i(t,x) \geq 0$ *for* $x \in K^+$ *such that* $x_i = 0$,
- $g_{i,j}(t,x) = 0$ *for* $x \in K^+$ *such that* $x_i = 0$, $j \in \{1, 2, \ldots, m\}$,

for all $t \geq 0$ *and* $i \in I$.

Definition 11 (Stochastically ultimate boundedness [113]) . *The solution* $X(t)$ *of system* (2.4) *is said to be stochastically ultimately bounded, if for any* $\epsilon \in (0,1)$*, there is a positive constant* $\delta = \delta(\epsilon)$*, such that for any initial value* $X_0 \in \mathbb{R}^d_+$*, the solution* $X(t)$ *of system* (2.4) *has the property*

$$\limsup_{t \to +\infty} \mathbb{P}\{|X(t)| \geq \delta\} < \epsilon.$$

Chapter 3

Methodology

3.1 General approach

To achieve our objectives, the research employs a combination of mathematical modelling, theoretical analysis, and numerical simulation. Each published work addresses a specific research question through the development of new deterministic or stochastic epidemiological models, supported by rigorous analysis to establish well-posedness of the model, critical conditions of disease spread and extinction and the validity of results within an epidemiological context.

3.2 Methodology on the assessment of COVID-19 with timely-delayed diagnosis

We focused on the transmission dynamics of COVID-19 by incorporating human-environment-human interactions, with a specific emphasis on Ghana. We have mainly considered Ghana from the anglophone west Africa to understand the effect of timely-delayed dynamics in these region in the sub-saharan continent. The study seeks to understand the effects of timely-delayed diagnosis and intervention dynamics in this region of the sub-Saharan continent. After describing the model formulation which takes the form of a deterministic system of nonlinear differential equations, we address the well posedness of the model by ensuring the existence and uniqueness as well as the positivity and boundedness of the solution. Then, we perform a global stability analysis of equilibrium states and carry out the sensitivity analysis of the model to show the most influential parameters on the model output variables. Finally, we fit the model using reported data from March 12 to June 19, 2020 and estimate the unknown parameters of the model. And we present some numerical results.

- **Model Formulation**

Since it has been proven that the delay in diagnosis has an impact on the severity of pulmonary diseases[30, 64], and Rong et al.[100] has studied its impact on the spread of covid-19 in Wuhan, our interest is to adapt their model for the case of Ghana. Then, based on the model formulated in [100], we propose a modified version of the epidemiological compartment model. This modification includes the recruitment of hosts, as people were still traveling within Ghana during the early phase of the pandemic and the natural death. The total human population size denoted as (N) is subdivided into seven compartments : susceptible (S), self-quarantine susceptible (S_q), exposed (E), infectious with timely diagnosis (I_1), infectious with delayed diagnosis (I_2), hospitalized (H) and recovered (R). The viral spread in the environment is denoted by (V). Thus the total human population at time t is given by $N(t) = S(t) + S_q(t) + E(t) + I_1(t) + I_2(t) + H(t) + R(t)$. We also assume that all parameters are non-negative. Disease induced deaths occurs only in I_1, I_2 and H compartments, with death rate denote by d. The overall force of infection is given as

$$\lambda = \beta_e E + \beta_{i_1} I_1 + \beta_{i_2} I_2 + \beta_v V,$$

where β_e, β_{i_1}, β_{i_2} and β_v are transmission rates associated with exposed, timely diagnosed, delayed diagnosed, and virus in the environment compartments, respectively. We refer the interested reader to reference [100] for detailed explanations.

Figure 1 below shows the compartment model describing the interaction between the human population and the pathogens in the environment.

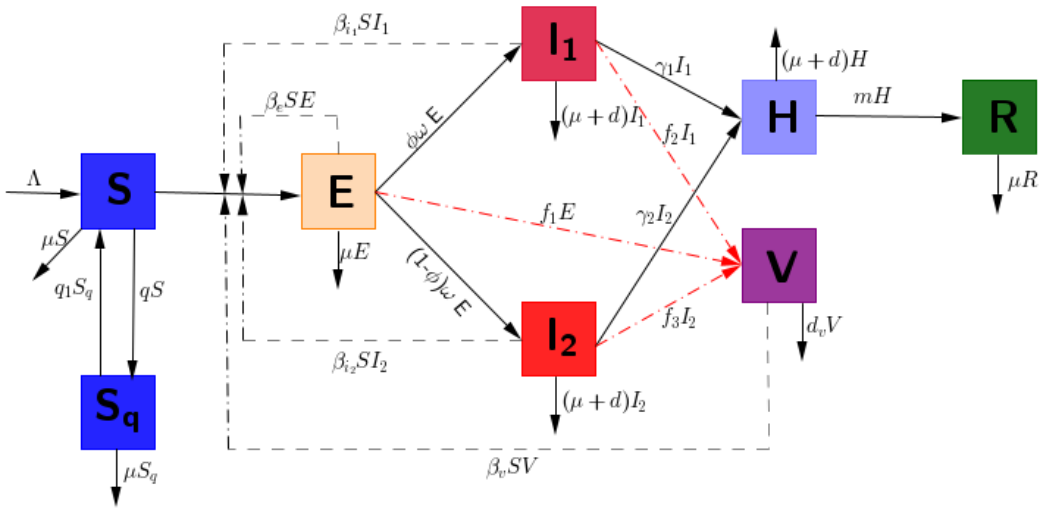

Figure 1: Diagram of COVID-19 Dynamics.

The description of the parameters used in the model for the COVID-19 transmission are given in Table 1. Following the compartmental transition diagram illustrated in Figure 1, the eight state dynamical model describing the transmission dynamics of COVID-19 is

Table 1: Description of parameters.

Parameter	Description
Λ	Recruitment rate
q	Self-quarantined rate of the susceptible
q_1	Transition rate of self-quarantined individuals to the susceptible
β_e	Transmission rate from the exposed to the susceptible
β_{i_1}	Transmission rate from the infectious with timely diagnosis to the susceptible
β_{i_2}	Transmission rate from the infectious with delayed diagnosis to the susceptible
β_v	Transmission rate from virus in the environment to susceptible
$1/\omega$	Incubation period
ϕ	Proportion of the infectious with timely diagnosis
$1/\gamma_1$	Waiting time of the infectious for timely diagnosis
$1/\gamma_2$	Waiting time of the infectious for delayed diagnosis
μ	Natural human death rate
d	Disease-induced death rate
m	Recovery rate of the hospitalized
f_1	Virus released rate of the exposed
f_2	Virus released rate of the infectious with timely-diagnosis
f_3	Virus released rate of the infectious with delayed-diagnosis
d_v	Decay rate of virus in the environment

given as follows

$$
\begin{aligned}
\frac{dS}{dt} &= \Lambda - \lambda S + q_1 S_q - (\mu + q)S, \\
\frac{dS_q}{dt} &= qS - q_1 S_q - \mu S_q, \\
\frac{dE}{dt} &= \lambda S - \omega E - \mu E, \\
\frac{dI_1}{dt} &= \phi\omega E - \gamma_1 I_1 - \mu I_1 - dI_1, \\
\frac{dI_2}{dt} &= (1-\phi)\omega E - \gamma_2 I_2 - \mu I_2 - dI_2, \\
\frac{dH}{dt} &= \gamma_1 I_1 + \gamma_2 I_2 - mH - \mu H - dH, \\
\frac{dR}{dt} &= mH - \mu R, \\
\frac{dV}{dt} &= f_1 E + f_2 I_1 + f_3 I_2 - d_v V.
\end{aligned}
\tag{3.1}
$$

3.3 Methodology on the impact of imperfect vaccine on infectious disease dynamics

The aims is to use mathematical modelling to evaluate the effectiveness of various vaccination strategies in eradicating diseases within a heterogeneous community according to the population turnover level. Specifically, we want to find out whether a vaccine that solely reduces the infection rate is more efficient in achieving disease eradication compared to vaccines that both reduce infection and enhance recovery, or those that made by the trade-off of these properties. Additionally, we seek to explore how these outcomes are influenced by population turnover, with the goal of generalizing our findings to animal populations. To do that, we formulate the mathematical model, detailing the parameters and assumptions that underpin our analysis. Then, we explore the basic properties of the model's steady state solutions and examines the conditions for global stability of the equilibria. Following this, we conduct a global sensitivity analysis using the Latin Hypercube Sampling (LHS) technique and partial rank correlation coefficients (PRCCs) at different time points regarding the level of efficiency of the vaccine and the population turnover. Finally, we present numerical simulations for varying parameter values to illustrate the interaction between population turnover and vaccine trade-offs on disease dynamics. And we conclude by discussing the implications of our findings for vaccination strategies, not only in human populations but also in domesticated and wild animal species, where population turnover rates differ, representing different points along a continuum of epidemiological outcomes.

- **Model Formulation**

The formulation of the model is based on compartmental modelling [9], which consists of creating virtual reservoirs called compartments. A compartment is a kinetically homogeneous structure. This means that any individual who enters a compartment is identical, from the epidemiological point of view to any other already present in that compartment. A mathematical model, therefore, consists of describing the flow of individuals between the various compartments.

To study the dynamics of an infectious disease during and after a vaccination campaign, we extend the model formulated in [48] by incorporating a recovered compartment, and considering a frequency-dependent disease transmission (incidence rate). The model accounts solely for host-to-host disease transmission. Since many vaccines do not confer perfect immunity, we consider a heterogeneous host community/population comprising two

types of hosts: those fully susceptible to the disease and those partially resistant to infection due to imperfect vaccination. The fully susceptible hosts are categorise into uninfected (S_1) and infected (I_1) individuals. Similarly, the partially resistant hosts, include uninfected (S_2) and infected (I_2) individuals. All infected individuals regardless of susceptibility status can recovered (R), and all recovered individuals are fully immune to reinfection [45]. Thus, the total population at time t, $N(t)$ is given by

$$N(t) = S_1(t) + S_2(t) + I_1(t) + I_2(t) + R(t). \tag{3.2}$$

We assume the parasite population is monomorphic that is it consists of only one type or genotype [42]. In addition, we assume that new uninfected hosts enter the population through birth and immigration at a constant rate, $\theta \geq 0$. Among these arrival, a proportion, $0 \leq p \leq 1$, is partially immune due to vaccination, while the remaining proportion, $1 - p$, is susceptible (completely vulnerable to the parasite). Uninfected, infected and recovered hosts experience natural mortality at a rate $\mu \geq 0$, with infected hosts incurring additional mortality due to parasite virulence. To reflect that vaccination induced resistance may reduce the parasite impact on within-host growth [48], we assume the virulence of the parasite on fully susceptible hosts, $d_1 \geq 0$, is greater than on partially resistant hosts, $d_2 \geq 0$. Uninfected hosts become infected through the forces of infection $\lambda_1(t) = \beta_{11}\frac{I_1(t)}{N(t)} + \beta_{12}\frac{I_2(t)}{N(t)}$ and $\lambda_2(t) = \beta_{21}\frac{I_1(t)}{N(t)} + \beta_{22}\frac{I_2(t)}{N(t)}$ depending on whether they are fully susceptible or partially resistant, respectively. The transmission rates are $\beta_{11} \geq 0$ (resp. $\beta_{21} \geq 0$) for transmission from I_1 to S_1 (resp. S_2) and $\beta_{12} \geq 0$ (resp. $\beta_{22} \geq 0$) for transmission I_2 to S_1 (resp. S_2). Since resistance may lower the probability of infection [48], we generally assume $\beta_{21} \leq \beta_{11}$ and $\beta_{22} \leq \beta_{12}$. Recovery rates are denoted by $\gamma_1 \geq 0$ for fully susceptible hosts and $\gamma_2 \geq 0$ for partially resistant hosts. A schematic diagram of the model is shown in Figure 2.

Mathematically, the model is as follows:

$$\begin{cases} \dfrac{dS_1}{dt} &= \theta(1-p) - \lambda_1(t)S_1(t) - \mu S_1(t), \\ \dfrac{dS_2}{dt} &= \theta p - \lambda_2(t)S_2(t) - \mu S_2(t), \\ \dfrac{dI_1}{dt} &= \lambda_1(t)S_1(t) - (\mu + \gamma_1 + d_1)I_1(t), \\ \dfrac{dI_2}{dt} &= \lambda_2(t)S_2(t) - (\mu + \gamma_2 + d_2)I_2(t), \\ \dfrac{dR}{dt} &= \gamma_1 I_1(t) + \gamma_2 I_2(t) - \mu R(t). \end{cases} \tag{3.3}$$

A summary of the biological significance of the model parameters (3.3) is given in Table 2.

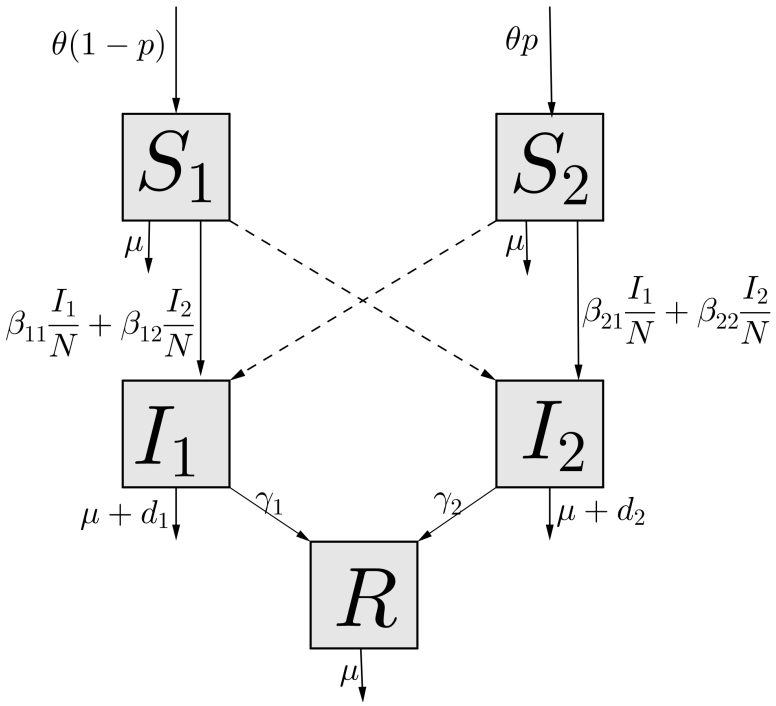

Figure 2: Schematic diagram of the epidemiological model with imperfect vaccination.

Table 2: Description and value of the model parameters.

Parameter	Description	Units	Value	Source
θ	Recruitment rate	person.day^{-1}	variable	Assumed
μ	Natural mortality rate	day^{-1}	variable	Assumed
p	Proportion of new hosts vaccinated	-	variable	Assumed
β_{11}	Transmission rate from I_1 to S_1	day^{-1}	variable	Assumed
β_{12}	Transmission rate from I_2 to S_1	day^{-1}	variable	Assumed
β_{21}	Transmission rate from I_1 to S_2	day^{-1}	variable	Assumed
β_{22}	Transmission rate from I_2 to S_2	day^{-1}	variable	Assumed
d_1	Mortality rate due to infection of S_1	day^{-1}	0.0008	[72]
d_2	Mortality rate due to infection of S_2	day^{-1}	0.0001	[72]
γ_1	Recovery rate of I_1	day^{-1}	0.1	[72]
γ_2	Recovery rate of I_2	day^{-1}	0.13	[72]

3.4 Methodology on the stochastic heterogeneous epidemiological model

The goal is to study the variability associated with individual dynamics such as births, deaths, immigration, emigration, or transitions between states. These types of variations are often referred to as demographic variations. For that purpose, we propose a stochastic epidemic model as a counterpart to the imperfect vaccination model described in [89] by using the recent methodology outlined in [5]. Here, we consider all different independent random changes that occur in the system. Then, The derived stochastic differential equation (SDE) model incorporates diffusion coefficients which depend on the square roots of population sizes. This characteristic introduces challenges, as the coefficients fail to meet the Lipschitz condition when population sizes approach zero. To address this, we rigorously prove the existence and uniqueness of a non-negative weak solution for the derived SDE. Furthermore, we demonstrate that the model exhibits stochastic ultimate boundedness, ensuring that the population sizes remain confined within certain limits despite the randomness inherent in the system. We also explore the conditions under which disease extinction or persistence in mean occurs. Finally, the analytical findings are validated through numerical simulations.

- **Model Formulation**

To derive the SDE model using the approach outlined in [5], we follow the methodology described in [4, 6]. For simplicity, we retain the same notation as in the deterministic model (3.3). We consider the process $X(t) = \{(S_1(t), S_2(t), I_1(t), I_2(t), R(t)) : t \in [0, +\infty)\}$, where t is the time parameter of the process, $S_1(t)$, $S_2(t)$, $I_1(t)$, $I_2(t)$ and $R(t)$ are continuous random variables at time t.

Possible state transitions in the stochastic process are modeled on the deterministic framework in (3.3). We assume that the transition probabilities of the process are within the interval $[0, 1]$ and the time interval Δt, is sufficiently small to ensure that only one change can occur within that period. Thus, in the interval $(t, t + \Delta t)$, one of the eleven possible changes occurs, excluding the case where no change takes place in (Table 3).

Table 3: Possible state changes during Δt.

Description	**Transition at** Δt	**Probability of change** $r_i(t, X)\Delta t$
Recruitment in S_1	$(1, 0, 0, 0, 0)$	$r_1(t, X)\Delta t = \theta(1 - p)\Delta t$
Recruitment in S_2	$(0, 1, 0, 0, 0)$	$r_2(t, X)\Delta t = \theta p \Delta t$
Death of S_1	$(-1, 0, 0, 0, 0)$	$r_3(t, X)\Delta t = \mu S_1 \Delta t$
Death of S_2	$(0, -1, 0, 0, 0)$	$r_4(t, X)\Delta t = \mu S_2 \Delta t$
Death of I_1	$(0, 0, -1, 0, 0)$	$r_5(t, X)\Delta t = (\mu + d_1) I_1 \Delta t$
Death of I_2	$(0, 0, 0, -1, 0)$	$r_6(t, X)\Delta t = (\mu + d_2) I_2 \Delta t$
Death of R	$(0, 0, 0, 0, -1)$	$r_7(t, X)\Delta t = \mu R \Delta t$
Infection of S_1	$(-1, 0, 1, 0, 0)$	$r_8(t, X)\Delta t = \left(\beta_{11}\frac{I_1}{N} + \beta_{12}\frac{I_2}{N}\right) S_1 \Delta t$
Infection of S_2	$(0, -1, 0, 1, 0)$	$r_9(t, X)\Delta t = \left(\beta_{21}\frac{I_1}{N} + \beta_{22}\frac{I_2}{N}\right) S_2 \Delta t$
Recovery of I_1	$(0, 0, -1, 0, 1)$	$r_{10}(t, X)\Delta t = \gamma_1 I_1 \Delta t$
Recovery of I_2	$(0, 0, 0, -1, 1)$	$r_{11}(t, X)\Delta t = \gamma_2 I_2 \Delta t$
No change	$(0, 0, 0, 0, 0)$	$1 - \sum_{i=1}^{11} r_i(t, X)\Delta t$

Using the state changes and their corresponding probabilities, we compute the expectation $E(\Delta X(t))$ and the covariance $E(\Delta X(t)(\Delta X(t))^T)$ to the order Δt. Then

$$E(\Delta X(t)) = f(t, X(t))\Delta t + o(\Delta t) \tag{3.4}$$

and

$$E(\Delta X(t)(\Delta X(t))^T) = \begin{bmatrix} V_{11} & 0 & V_{13} & 0 & 0 \\ 0 & V_{22} & 0 & V_{24} & 0 \\ V_{31} & 0 & V_{33} & 0 & V_{35} \\ 0 & V_{42} & 0 & V_{44} & V_{45} \\ 0 & 0 & V_{53} & V_{54} & V_{55} \end{bmatrix} \Delta t + o(\Delta t) = V(t, X(t))\Delta t + o(\Delta t), \tag{3.5}$$

where $V_{11} = \theta(1-p) + \beta_{11}\frac{S_1 I_1}{N} + \beta_{12}\frac{S_1 I_2}{N} + \mu S_1$, $V_{13} = V_{31} = -\beta_{11}\frac{S_1 I_1}{N} - \beta_{12}\frac{S_1 I_2}{N}$,
$V_{22} = \theta p + \beta_{21}\frac{S_2 I_1}{N} + \beta_{22}\frac{S_2 I_2}{N} + \mu S_2$, $V_{24} = V_{42} = -\beta_{21}\frac{S_2 I_1}{N} - \beta_{22}\frac{S_2 I_2}{N}$,
$V_{33} = \beta_{11}\frac{S_1 I_1}{N} + \beta_{12}\frac{S_1 I_2}{N} + (\mu + \gamma_1 + d_1)I_1$, $V_{35} = V_{53} = -\gamma_1 I_1$,
$V_{44} = \beta_{21}\frac{S_2 I_1}{N} + \beta_{22}\frac{S_2 I_2}{N} + (\mu + \gamma_2 + d_2)I_2$, $V_{45} = V_{54} = -\gamma_2 I_2$ $V_{55} = \gamma_1 I_1 + \gamma_2 I_2 + \mu R$.

As in [4], we can write the dynamic of X as SDEs as follows:

$$dX(t) = f(t, X(t))dt + g(t, X(t))dW^*(t), \tag{3.6}$$
$$dX(t) = f(t, X(t))dt + G(t, X(t))dW(t), \tag{3.7}$$

where g is a 5×5 matrix, G is a 5×11 matrix, $W^*(t)$ is a 5×1 vector and $W(t)$ is a 11×1 vector of independent Wienner processes. In addition $GG^T = V = g^2$ and

$$G(t, X(t)) = \begin{bmatrix} G_{11} & 0 & G_{13} & 0 & 0 & 0 & 0 & G_{18} & 0 & 0 & 0 \\ 0 & G_{22} & 0 & G_{24} & 0 & 0 & 0 & 0 & G_{29} & 0 & 0 \\ 0 & 0 & 0 & 0 & G_{35} & 0 & 0 & G_{38} & 0 & G_{310} & 0 \\ 0 & 0 & 0 & 0 & 0 & G_{46} & 0 & 0 & G_{49} & 0 & G_{411} \\ 0 & 0 & 0 & 0 & 0 & 0 & G_{57} & 0 & 0 & G_{510} & G_{511} \end{bmatrix},$$

where
$G_{11} = \sqrt{\theta(1-p)}$, $G_{13} = -\sqrt{\mu S_1}$, $G_{18} = -\sqrt{\beta_{11}\frac{S_1 I_1}{N} + \beta_{12}\frac{S_1 I_2}{N}}$, $G_{22} = \sqrt{\theta p}$,
$G_{24} = -\sqrt{\mu S_2}$, $G_{29} = -\sqrt{\beta_{21}\frac{S_2 I_1}{N} + \beta_{22}\frac{S_2 I_2}{N}}$, $G_{35} = -\sqrt{(\mu + d_1)I_1}$,
$G_{38} = \sqrt{\beta_{11}\frac{S_1 I_1}{N} + \beta_{12}\frac{S_1 I_2}{N}}$, $G_{310} = -\sqrt{\gamma_1 I_1}$, $G_{46} = -\sqrt{(\mu + d_2)I_2}$,
$G_{49} = \sqrt{\beta_{21}\frac{S_2 I_1}{N} + \beta_{22}\frac{S_2 I_2}{N}}$, $G_{411} = -\sqrt{\gamma_2 I_2}$, $G_{57} = -\sqrt{\mu R}$, $G_{510} = \sqrt{\gamma_1 I_1}$ and
$G_{511} = \sqrt{\gamma_2 I_2}$.

According to [4, Theorem 2.1], the probability density function of the solution to the SDEs (3.6) and (3.7) satisfies the same Kolmogorov partial differential equations. In addition, a solution of one equation is also a solution of the second equation. Consequently, the well posedness of one system implies the well posedness of the other, and vice versa.

As highlighted in [5, 32], the solutions of equations (3.6) and (3.7) may take negative values. To address this, we use a modification similar to that suggested in [5], to derive the

following nonnegative valued SDE models:

$$dX(t) = \hat{f}(X(t))dt + \hat{g}(X(t))dW^*(t), \tag{3.8}$$

$$dX(t) = \hat{f}(X(t))dt + \hat{G}(X(t))dW(t), \tag{3.9}$$

where $\hat{G}\hat{G}^T = \hat{V} = \hat{g}^2$. $\hat{V}$ is a matrix 5×5 with

$\hat{V}_{11} = \hat{r}_1^\delta(X(t)) + \varphi(r_3(X(t))) + \hat{r}_8^\delta(X(t))$, $\hat{V}_{13} = \hat{V}_{31} = -\hat{r}_8^\delta(X(t))$,
$\hat{V}_{22} = \hat{r}_2^\delta(X(t)) + \varphi(r_4(X(t))) + \hat{r}_9^\delta(X(t))$, $\hat{V}_{24} = \hat{V}_{42} = -\hat{r}_9^\delta(X(t))$,
$\hat{V}_{33} = \varphi(r_5(X(t))) + \hat{r}_8^\delta(X(t)) + \hat{r}_{10}^\delta(X(t))$, $\hat{V}_{35} = \hat{V}_{53} = -\hat{r}_{10}^\delta(X(t))$,
$\hat{V}_{44} = \varphi(r_6(X(t))) + \hat{r}_9^\delta(X(t)) + \hat{r}_{11}^\delta(X(t))$, $\hat{V}_{45} = \hat{V}_{54} = -\hat{r}_{11}^\delta(X(t))$,
$\hat{V}_{55} = \varphi(r_7(X(t))) + \hat{r}_{10}^\delta(X(t)) + \hat{r}_{11}^\delta(X(t))$,
$\hat{V}_{12} = \hat{V}_{14} = \hat{V}_{15} = \hat{V}_{21} = \hat{V}_{23} = \hat{V}_{25} = \hat{V}_{32} = \hat{V}_{34} = \hat{V}_{41} = \hat{V}_{43} = \hat{V}_{51} = \hat{V}_{52} = 0$,

$$\varphi(r(t)) = r(t) \vee 0 = \begin{cases} r(t) & \text{if } \ r(t) \geq 0, \\ 0 & \text{if } \ r(t) < 0. \end{cases} \tag{3.10}$$

$$\hat{r}_1^\delta(X(t)) = \begin{cases} \theta(1-p) & \text{for } \ S_1(t) \geq \delta, \\ \theta(1-p)S_1(t)/\delta & \text{for } \ 0 \leq S_1(t) < \delta. \end{cases} \tag{3.11}$$

$$\hat{r}_2^\delta(X(t)) = \begin{cases} \theta p & \text{for } \ S_2(t) \geq \delta, \\ \theta p S_2(t)/\delta & \text{for } \ 0 \leq S_2(t) < \delta. \end{cases} \tag{3.12}$$

$$\hat{r}_8^\delta(X(t)) = \begin{cases} \varphi\Big(\beta_{11}\dfrac{S_1(t)I_1(t)}{N(t)} + \beta_{12}\dfrac{S_1(t)I_2(t)}{N(t)}\Big) & \text{for } \ I_1(t) \geq \delta, \\ \varphi\Big(\beta_{11}\dfrac{S_1(t)I_1(t)}{N(t)} + \beta_{12}\dfrac{S_1(t)I_2(t)}{N(t)}\Big)I_1(t)/\delta & \text{for } \ 0 \leq I_1(t) < \delta. \end{cases} \tag{3.13}$$

$$\hat{r}_9^\delta(X(t)) = \begin{cases} \varphi\Big(\beta_{21}\dfrac{S_2(t)I_1(t)}{N(t)} + \beta_{22}\dfrac{S_2(t)I_2(t)}{N(t)}\Big) & \text{for } \ I_2(t) \geq \delta, \\ \varphi\Big(\beta_{21}\dfrac{S_2(t)I_1(t)}{N(t)} + \beta_{22}\dfrac{S_2(t)I_2(t)}{N(t)}\Big)I_2(t)/\delta & \text{for } \ 0 \leq I_2(t) < \delta. \end{cases} \tag{3.14}$$

$$\hat{r}_{10}^\delta(X(t)) = \begin{cases} \varphi(\gamma_1 I_1(t)) & \text{for } \ R(t) \geq \delta, \\ \varphi(\gamma_1 I_1(t))R(t)/\delta & \text{for } \ 0 \leq R(t) < \delta. \end{cases} \tag{3.15}$$

$$\hat{r}_{11}^\delta(X(t)) = \begin{cases} \varphi(\gamma_2 I_2(t)) & \text{for } \ R(t) \geq \delta, \\ \varphi(\gamma_2 I_2(t))R(t)/\delta & \text{for } \ 0 \leq R(t) < \delta. \end{cases} \tag{3.16}$$

$$\hat{f}(X(t)) = \begin{bmatrix} \hat{f}_1(X(t)) \\ \hat{f}_2(X(t)) \\ \hat{f}_3(X(t)) \\ \hat{f}_4(X(t)) \\ \hat{f}_5(X(t)) \end{bmatrix} = \begin{bmatrix} \varphi(r_1(X(t))) - \varphi(r_8(X(t))) - \varphi(r_3(X(t))) \\ \varphi(r_2(X(t))) - \varphi(r_9(X(t))) - \varphi(r_4(X(t))) \\ \varphi(r_8(X(t))) - \varphi(r_5(X(t))) - \varphi(r_{10}(X(t))) \\ \varphi(r_9(X(t))) - \varphi(r_6(X(t))) - \varphi(r_{11}(X(t))) \\ \varphi(r_{10}(X(t))) + \varphi(r_{11}(X(t))) - \varphi(r_7(X(t))) \end{bmatrix}$$

and

$$0 < \delta < 1.$$

The SDE (3.9) can be written in terms of square roots as follows

$$\begin{cases} \mathrm{d}S_1(t) = \hat{f}_1(X(t))\mathrm{d}t + \sqrt{\hat{r}_1^{\delta}(X(t))}\mathrm{d}W_1(t) - \sqrt{\varphi(r_3(X(t)))}\mathrm{d}W_3(t) - \sqrt{\hat{r}_8^{\delta}(X(t))}\mathrm{d}W_8(t), \\ \mathrm{d}S_2(t) = \hat{f}_2(X(t))\mathrm{d}t + \sqrt{\hat{r}_2^{\delta}(X(t))}\mathrm{d}W_2(t) - \sqrt{\varphi(r_4(X(t)))}\mathrm{d}W_4(t) - \sqrt{\hat{r}_9^{\delta}(X(t))}\mathrm{d}W_9(t), \\ \mathrm{d}I_1(t) = \hat{f}_3(X(t))\mathrm{d}t - \sqrt{\varphi(r_5(X(t)))}\mathrm{d}W_5(t) + \sqrt{\hat{r}_8^{\delta}(X(t))}\mathrm{d}W_8(t) - \sqrt{\hat{r}_{10}^{\delta}(X(t))}\mathrm{d}W_{10}(t), \\ \mathrm{d}I_2(t) = \hat{f}_4(X(t))\mathrm{d}t - \sqrt{\varphi(r_6(X(t)))}\mathrm{d}W_6(t) + \sqrt{\hat{r}_9^{\delta}(X(t))}\mathrm{d}W_9(t) - \sqrt{\hat{r}_{11}^{\delta}(X(t))}\mathrm{d}W_{11}(t), \\ \mathrm{d}R(t) = \hat{f}_5(X(t))\mathrm{d}t - \sqrt{\varphi(r_7(X(t)))}\mathrm{d}W_7(t) + \sqrt{\hat{r}_{10}^{\delta}(X(t))}\mathrm{d}W_{10}(t) + \sqrt{\hat{r}_{11}^{\delta}(X(t))}\mathrm{d}W_{11}(t). \end{cases} \tag{3.17}$$

Vaccination is one of the most effective public health policies for protecting humans and animals from infectious diseases. Global vaccination campaigns have helped eradicate diseases such as smallpox, measles, poliomyelitis and rinderpest in most parts of the world, ultimately saving the lives of millions of humans and animals. By definition, a perfect vaccine would keep vaccinated individuals from becoming infected when exposed to the pathogen. An imperfect vaccine, however, does not prevent vaccinated individuals

from becoming infected upon pathogen exposure but may still be beneficial in various ways [12]. For example, imperfect vaccines may provide benefits such as preventing infection, limiting parasite within-host growth and thus reducing the damage done to the host [110] or preventing transmission by infected hosts [48]. As we have seen recently with the epidemic of COVID-19, imperfect vaccines can be used to reduce the number of infected individuals and also to protect individuals at risk of developing a more lethal form of the infection. The use of imperfect vaccines may be advantageous when the vaccination efficiency is volatile and decreases due to the appearance of new variants of the virus [33, 54, 56].

The effectiveness of a given vaccine is determined not only by its biochemical and immunological properties but also by how the vaccine is deployed and what other health management (biosecurity) measures are in place. Maintaining herd immunity during a disease outbreak, for example, has been promoted as a highly effective disease control strategy [22, 35, 72]. However, a continuous influx of new susceptible, possibly unvaccinated individuals contributes to the long-term persistence of the disease in the population [98, 101]. The frequent introduction of pathogens into a partially immune population (with an intermediate level of population immunity) can lead to longer-lasting epidemics and/or a higher total number of infectious individuals than the introduction into a naive population [98]. This phenomenon is named "epidemic enhancement" [98]. More generally, the population turnover rate, that is, the rate at which individuals can enter and exit the considered population, may affect the effectiveness of control strategies [27, 63, 88]. In humans and also domesticated animals, population turnover takes the form of immigration and emigration in and out of the population, as well as the birth and death of individuals. The turnover is an often neglected factor in epidemiology when generalising predictions of disease modelling from human to domesticated and wild animal populations.

Moreover, a second parameter of importance in studying the efficiency of vaccination strategies is the existence of biological trade-offs in the epidemiology of infectious diseases. The prime example is the trade-off between parasite virulence and transmission rate, which raises challenges for vaccine manufacturing. Indeed, in the seminal paper by [48], vaccines affecting disease transmission are predicted to possibly lead to a decrease in parasite virulence, while other types of vaccines (reducing within-host growth rate) may lead to an increase in parasite virulence and thus the counter-effect of a worst epidemiological outcome. Interestingly, much work has been devoted to generating precise predictions for virulence evolution in known parasite species by incorporating empirical characterisations of vaccine effects into models capturing the epidemiological details of a given system [2, 31, 46]. In contrast, the biochemical and immunological trade-offs of the

vaccine itself have received little attention. We specifically mean here that vaccination can affect several aspects of the disease dynamics, such as within-host growth and transmission, with possible trade-offs between these characteristics. For example, a vaccine reducing within-host growth may be more or less effective in reducing disease transmission. We, therefore, consider the definition of imperfect vaccines as i) providing partial protection (non-maximal efficiency) against infection (decreasing transmission) and ii) partially enhancing the recovery of infected individuals. We are interested in the possible trade-off between these two properties. There has been remarkably little work performed to generally assess how the interplay between different vaccine properties, trade-offs and vaccination strategies influences the burden of the epidemic in a heterogeneous community/population with imperfect vaccination.

The aim of this study is, therefore, to assess, through mathematical modelling, whether the use of vaccines decreasing the infection rate is more efficient to eradicate the disease in a heterogeneous community than a vaccine that both reduces the infection and favours recovery or a vaccine reducing the infection rate but favouring recovery. We also want to assess whether these results depend on the effect of population turnover in order to generalise our results to animal populations.

Chapter 4

Presentation of findings

4.1 Global stability dynamics and sensitivity assessment of COVID-19 with timely-delayed diagnosis in Ghana

Section 4.1.1 concerns the existence and uniqueness as well as the positivity and boundedness of the solution. We present the analysis of disease-free equilibrium in Section 4.1.2 and the endemic equilibrium in Section 4.1.3. The numerical results using data from Ghana and corresponding parameters are presented in Section 4.1.4. A local and global sensibility analysis are presented in section 4.1.5. Finally, the concluding remarks and recommendations are presented in Section 4.1.6. The study was conducted between March 2020 and June 2020, when Ghana experienced spark cases and undergoing delay in diagnosis (therefore, everything that follows should be seen as such).

> These results are published in *Computational and Mathematical Biophysics* [79].

4.1.1 Analysis of the model problem

The model (3.1) is described by a system of first order autonomous nonlinear differential equations. It can be rewritten in the matrix form as

$$X'(t) = F(X(t)), \tag{4.1}$$

where $X(t) := (S, S_q, E, I_1, I_2, H, R, V)^T$ and F is a smooth function defined from $\mathbb{R}^8$ by

$$F(X) := \begin{pmatrix} \Lambda - (\beta_e E + \beta_{i_1} I_1 + \beta_{i_2} I_2 + \beta_v V)S + q_1 S_q - (\mu + q)S \\ qS - q_1 S_q - \mu S_q \\ (\beta_e E + \beta_{i_1} I_1 + \beta_{i_2} I_2 + \beta_v V)S - \omega E - \mu E \\ \phi\omega E - \gamma_1 I_1 - \mu I_1 - dI_1 \\ (1-\phi)\omega E - \gamma_2 I_2 - \mu I_2 - dI_2 \\ \gamma_1 I_1 + \gamma_2 I_2 - mH - \mu H - dH \\ mH - \mu R \\ f_1 E + f_2 I_1 + f_3 I_2 - d_v V \end{pmatrix},$$

where $X := (S, S_q, E, I_1, I_2, H, R, V) \in \mathbb{R}^8$. Since F is a smooth function, then F is locally lipschitz on $\mathbb{R}^8$. And we deduce the existence and uniqueness of the maximal solution to the Cauchy problem associated with the differential system (3.1) relating to the initial condition $(t_0, X_0) \in \mathbb{R} \times \mathbb{R}^8$.

Next, we consider the positivity of the solution. Here, we investigate the asymptotic behavior of orbits starting in the non-negative cone $\mathbb{R}^8_+$.

Theorem 5 *For any initial condition* $\big(t_0 = 0, X_0 = (S(0), S_q(0), E(0), I_1(0), I_2(0), H(0), R(0), V(0)) \in \mathbb{R}^8_+\big)$, *the maximal solution* $\big([0, T[|X(t) = (S(t), S_q(t), E(t), I_1(t), I_2(t), H(t), R(t), V(t))\big)$ *of the Cauchy problem related with system* (3.1) *is non-negative.*

Proof: We define the set $\Delta := \big\{\widetilde{t} \in [0, T[\mid X(t) > 0,\ \forall t \in]0, \widetilde{t}[\big\}$. Since $(S, S_q, E, I_1, I_2, H, R, V)$ are continuous functions, then $\Delta \neq 0$. Also, let $\widetilde{T} := \sup \Delta$ and show that $\widetilde{T} = T$. Assume $\widetilde{T} < T$, then $S, S_q, E, I_1, I_2, H, R$ and V are simultaneously positive on $]0, \widetilde{T}[$.

At least one of the following conditions is satisfied at time $\widetilde{T}$: $S(\widetilde{T}) = 0$, $S_q(\widetilde{T}) = 0$, $E(\widetilde{T}) = 0$, $I_1(\widetilde{T}) = 0$, $I_2(\widetilde{T}) = 0$, $H(\widetilde{T}) = 0$, $R(\widetilde{T}) = 0$ or $V(\widetilde{T}) = 0$.

Assume $S(\widetilde{T}) = 0$, then we deduce from the first equation of system (3.1)

$$\frac{d}{dt}\left(Se^{\int_0^t (\lambda(s)+\mu+q)ds}\right) = (\Lambda + q_1 S_q)e^{\int_0^t (\lambda(s)+\mu+q)ds}. \tag{4.2}$$

The integration of equation (4.2) from 0 to $\widetilde{T}$ yields

$$S(\widetilde{T}) = e^{-\int_0^{\widetilde{T}} (\lambda(s)+\mu+q)ds}\left(S(0) + \int_0^{\widetilde{T}} (\Lambda + q_1 S_q(t))e^{\int_0^t (\lambda(s)+\mu+q)ds} dt\right) > 0.$$

Similarly, we can prove that $S(\widetilde{T}) > 0$, $S_q(\widetilde{T}) > 0$, $E(\widetilde{T}) > 0$, $I_1(\widetilde{T}) > 0$, $I_2(\widetilde{T}) > 0$, $H(\widetilde{T}) > 0$, $R(\widetilde{T}) > 0$ and $V(\widetilde{T}) > 0$.This is a contradiction to the previous claim that $S(\widetilde{T}) = 0$, $S_q(\widetilde{T}) = 0$, $E(\widetilde{T}) = 0$, $I_1(\widetilde{T}) = 0$, $I_2(\widetilde{T}) = 0$, $H(\widetilde{T}) = 0$, $R(\widetilde{T}) = 0$ or $V(\widetilde{T}) = 0$, if $\widetilde{T} < T$. Then, $\widetilde{T} = T$ and consequently the maximal solution $(S(t), S_q(t), E(t), I_1(t), I_2(t), H(t), R(t), V(t))$ of the Cauchy problem related with system (3.1) is positive. □

Therefore, the variables of the system (3.1) are positive for all time $t > 0$. In other terms, solutions of the system (3.1) with nonnegative initial conditions will stay positive for all $t > 0$.

Next, we consider the invariant region of the model problem (3.1).

Theorem 6 *The model problem* (3.1) *has solutions in the invariant region*

$$\Omega := \left\{(S, S_q, E, I_1, I_2, H, R, V) \in \mathbb{R}^8_+, \quad N(t) \leq \frac{\Lambda}{\mu} \quad \textit{and} \quad V(t) \leq (f_1 + f_2 + f_3)\frac{\Lambda}{\mu d_v}\right\}.$$

Proof : We first split model system (3.1) into two parts i.e. the human population $(S, S_q, E, I_1, I_2, H, R)$ and the viral spread in the environment V. Then, using model system (3.1), the dynamics of the total human population satisfy

$$\frac{dN}{dt} = \Lambda - \mu N - d(I_1 + I_2 + H) \leq \Lambda - \mu N. \tag{4.3}$$

Integrating the expression above, we deduce that

$$N(t) \leq \frac{\Lambda}{\mu} + \left(N(0) - \frac{\Lambda}{\mu}\right)e^{-\mu t}, \quad \forall t \geq 0,$$

where $N(0)$ is the value of $N(t)$ at the beginning. We deduce that if $N(0) \leq \frac{\Lambda}{\mu}$, then $0 \leq N(t) \leq \frac{\Lambda}{\mu}$, $\forall t \geq 0$. Now using the fact that $I_1(t) \leq \Lambda/\mu$, $I_2(t) \leq \Lambda/\mu$, $E(t) \leq \Lambda/\mu$, the dynamics of the viral spread in the environment satisfy

$$\frac{dV}{dt} \leq (f_1 + f_2 + f_3)\frac{\Lambda}{\mu} - d_v V.$$

Integrating the expression above, we deduce that

$$V(t) \leq (f_1 + f_2 + f_3)\frac{\Lambda}{\mu d_v} + \left(V(0) - (f_1 + f_2 + f_3)\frac{\Lambda}{\mu d_v}\right)e^{-d_v t}, \quad \forall t \geq 0,$$

where $V(0)$ is the initial condition of V(t). Thus, as $t \longrightarrow +\infty$ we have

$$V(t) \leq (f_1 + f_2 + f_3)\frac{\Lambda}{\mu d_v}.$$

Thus the region Ω is positively invariant and attracting for the system (3.1). It is therefore sufficient to consider the dynamics of the flow generated by the system (3.1). Since each maximal solution of the Cauchy problem associated with (3.1) remains positive and bounded overtime, each solution of the model problem (3.1) is global [50]. □

4.1.2 Disease-free equilibrium and its stability

In analysing the spread of an infection, the disease-free equilibrium (DFE) stands for a state where the disease is entirely absent from the population. This equilibrium is key as it gives a measure for understanding the conditions under which the disease can invade or be eradicated. The disease-free equilibrium is deduced from the resolution of the system of equations in (3.1) by taking $E = 0$, $I_1 = 0$, $I_2 = 0$, $H = 0$ and $V = 0$. Thus, the disease-free equilibrium for model (3.1) satisfies the system following of equations:

$$\begin{cases} (\mu + q)S^0 - q_1 S_q^0 = \Lambda, \\ \\ qS^0 - (\mu + q_1)S_q^0 = 0. \end{cases} \tag{4.4}$$

Solving the system of equations in 4.4 yields the disease-free equilibrium point:

$$Q^0 = (S^0, S_q^0, 0, 0, 0, 0, 0),$$

where $S^0 = \dfrac{\Lambda(\mu + q_1)}{\mu(\mu + q + q_1)}$, $S_q^0 = \dfrac{\Lambda q}{\mu(\mu + q + q_1)}$ and $S^0 + S_q^0 = \dfrac{\Lambda}{\mu}$.

The linear stability of Q^0 depends on the basic reproductive number $\mathcal{R}_0$. The latter is defined as the average number of secondary cases caused by an infected individual during his/her infectivity period when he/she is introduced to a population of susceptible individuals without any intervention. We study the stability of the equilibrium through the next generation operator [58, 36]. Recalling the notations in [36] for model (3.1), the matrices

$\mathcal{F}$ of the new infection and $\mathcal{W}$ of the remaining transfer terms are given by

$$\mathcal{F} = \begin{bmatrix} (\beta_e E + \beta_{i_1} I_1 + \beta_{i_2} I_2 + \beta_v V)S \\ 0 \\ 0 \\ 0 \\ 0 \end{bmatrix} \quad \text{and} \quad \mathcal{W} = \begin{bmatrix} \omega E + \mu E \\ -\phi\omega E + \gamma_1 I_1 + \mu I_1 + dI_1 \\ -(1-\phi)\omega E + \gamma_2 I_2 + \mu I_2 + dI_2 \\ -\gamma_1 I_1 - \gamma_2 I_2 + mH + \mu H + dH \\ -f_1 E - f_2 I_1 - f_3 I_2 + d_v V \end{bmatrix}.$$

The Jacobian matrices of $\mathcal{F}$ and $\mathcal{W}$ at Q^0 are respectively,

$$F = \begin{bmatrix} \beta_e S^0 & \beta_{i_1} S^0 & \beta_{i_2} S^0 & 0 & \beta_v S^0 \\ 0 & 0 & 0 & 0 & 0 \\ 0 & 0 & 0 & 0 & 0 \\ 0 & 0 & 0 & 0 & 0 \\ 0 & 0 & 0 & 0 & 0 \end{bmatrix} \tag{4.5}$$

and

$$W = \begin{bmatrix} \mu+\omega & 0 & 0 & 0 & 0 \\ -\phi\omega & \mu+\gamma_1+d & 0 & 0 & 0 \\ -(1-\phi)\omega & 0 & \mu+\gamma_2+d & 0 & 0 \\ 0 & -\gamma_1 & -\gamma_2 & \mu+m+d & 0 \\ -f_1 & -f_2 & -f_3 & 0 & d_v \end{bmatrix} \tag{4.6}$$

Then, the basic reproduction number of model system (3.1) is

$$\mathcal{R}_0 = \rho(FW^{-1}) = \mathcal{R}_{0e} + \mathcal{R}_{0i_1} + \mathcal{R}_{0i_2} + \mathcal{R}_{0v}, \tag{4.7}$$

where $\mathcal{R}_{0e} = \dfrac{\beta_e S^0}{\mu+\omega}$, $\mathcal{R}_{0i_1} = \dfrac{\beta_{i_1}\phi\omega S^0}{(\mu+\omega)(\mu+\gamma_1+d)}$, $\mathcal{R}_{0i_2} = \dfrac{\beta_{i_2}(1-\phi)\omega S^0}{(\mu+\omega)(\mu+\gamma_2+d)}$,

$\mathcal{R}_{0v} = \dfrac{\beta_v f_3(1-\phi)\omega(\mu+\gamma_1+d)S^0 + \beta_v(\mu+\gamma_2+d)[f_1(\mu+\gamma_1+d)+f_2\phi\omega]S^0}{d_v(\mu+\omega)(\mu+\gamma_1+d)(\mu+\gamma_2+d)}$ and $\rho(FW^{-1})$ is the spectral radius of FW^{-1}.

The term $\mathcal{R}_{0e}$ represents the average number of secondary cases caused by an exposed individual during their infectious period. Similarly, $\mathcal{R}_{0i_1}$ (respectively $\mathcal{R}_{0i_2}$) represents the

average number of secondary cases caused by an infectious timely diagnosis (respectively, delayed diagnosis) during their infectious period. Moreover, the term $\mathcal{R}_{0v}$ represents the average number of secondary cases assigned to a single virus particle in the environment over its infectious period.

The importance of the basic reproduction number comes from the result outlined in the next Lemma, which is obtained from Theorem 2 in [36].

Lemma 1 *The DFE Q^0 of the system (3.1) is locally asymptotically stable (LAS) whenever $\mathcal{R}_0 \leq 1$ and unstable whenever $\mathcal{R}_0 > 1$.*

The biological meaning of Lemma 1 is that a sufficiently small number of infected hosts will not cause an epidemic unless $\mathcal{R}_0 > 1$. Global asymptotic stability (GAS) of the DFE is required for better disease control. In addition, expanding the basin of attraction of Q^0 presents a more challenging task for the model under consideration. This leads to the following new result. For this purpose, we will use Theorems 2.1 and 2.2 of [104].

Theorem 7 *If $\mathcal{R}_0 \leq 1$, the DFE Q^0 of the system (3.1) is GAS in Ω. If $\mathcal{R}_0 > 1$, Q^0 is unstable, the system (3.1) is uniformly persistent and there exists at least one endemic equilibrium in the interior of Ω.*

Proof : The system (3.1) can be written as

$$\begin{aligned} \frac{dx}{dt} &= (F - W)x - f(x, y), \\ \frac{dy}{dt} &= g(x, y), \end{aligned} \tag{4.8}$$

where $x = (E, I_1, I_2, H, V)^T$ is the vector representing the infected classes, $y = (S, S_q, R)^T$ is the vector representing the uninfected classes, the matrices F and W are given as in (4.5) and (4.6) respectively, and

$$f(x, y) = \begin{bmatrix} \beta_e E(S^0 - S) + \beta_{i_1} I_1(S^0 - S) + \beta_{i_2} I_2(S^0 - S) + \beta_v V(S^0 - S) \\ 0 \\ 0 \\ 0 \\ 0 \end{bmatrix}$$

and

$$g(x,y) = \begin{bmatrix} \Lambda - (\beta_e E + \beta_{i_1} I_1 + \beta_{i_2} I_2 + \beta_v V)S + q_1 S_q - (\mu + q)S \\ qS - q_1 S_q - \mu S_q \\ (\beta_e E + \beta_{i_1} I_1 + \beta_{i_2} I_2 + \beta_v V)S - \omega E - \mu E \end{bmatrix}.$$

Then,

$$W^{-1}F = \begin{bmatrix} A\beta_e S^0 & A\beta_{i_1} S^0 & A\beta_{i_2} S^0 & 0 & A\beta_v S^0 \\ B\beta_e S^0 & B\beta_{i_1} S^0 & B\beta_{i_2} S^0 & 0 & B\beta_v S^0 \\ C\beta_e S^0 & C\beta_{i_1} S^0 & C\beta_{i_2} S^0 & 0 & C\beta_v S^0 \\ D\beta_e S^0 & D\beta_{i_1} S^0 & D\beta_{i_2} S^0 & 0 & D\beta_v S^0 \\ E\beta_e S^0 & E\beta_{i_1} S^0 & E\beta_{i_2} S^0 & 0 & E\beta_v S^0 \end{bmatrix},$$

where

$$A = \frac{1}{\mu + \omega}, \quad B = \frac{\phi\omega}{(\mu + \omega)(\mu + \gamma_1 + d)} \quad C = \frac{(1-\phi)\omega}{(\mu + \omega)(\mu + \gamma_2 + d)},$$
$$D = \frac{\omega[\gamma_1\phi(\mu + \gamma_2 + d) + \gamma_2(1-\phi)(\mu + \gamma_1 + d)]}{(\mu + \omega)(\mu + \gamma_1 + d)(\mu + \gamma_2 + d)(\mu + m + d)}, \quad \text{and}$$
$$E = \frac{f_3(1-\phi)\omega(\mu + \gamma_1 + d) + (\mu + \gamma_2 + d)[f_1(\mu + \gamma_1 + d) + f_2\phi\omega]}{d_v(\mu + \omega)(\mu + \gamma_1 + d)(\mu + \gamma_2 + d)}.$$

Let $(\omega_1, \omega_2, \omega_3, \omega_4, \omega_5)$ be the left eigenvalue of $W^{-1}F$ and be given by

$$\omega_1 = \frac{\beta_e}{\beta_{i_1}}, \quad \omega_2 = 1, \quad \omega_3 = \frac{\beta_{i_1}}{\beta_v}, \quad \omega_4 = 0 \quad \text{and} \quad \omega_5 = 1, \tag{4.9}$$

since $(\omega_1, \omega_2, \omega_3, \omega_4, \omega_5)W^{-1}F = \mathcal{R}_0(\omega_1, \omega_2, \omega_3, \omega_4, \omega_5)$. We consider the following Lyapunov function

$$Q = (\omega_1, \omega_2, \omega_3, \omega_4, \omega_5)W^{-1}(E, I_1, I_2, H, V)^T = \mathcal{A}E + \mathcal{B}I_1 + CI_2 + \mathcal{D}V, \tag{4.10}$$

where $\mathcal{A} = \frac{\mathcal{R}_{0e}}{\beta_{i_1} S^0} + \frac{\mathcal{R}_{0i_1}}{\beta_{i_1} S^0} + \frac{\mathcal{R}_{0i_2}}{\beta_v S^0} + \frac{\mathcal{R}_{0v}}{\beta_v S^0}, \mathcal{B} = \frac{d_v + f_2}{d_v(\mu + \gamma_1 + d)}, C = \frac{\beta_{i_2} d_v + f_3\beta_v}{\beta_v d_v(\mu + \gamma_2 + d)}$ and

$\mathcal{D} = \dfrac{1}{d_v}$. Then the derivative of the Lyapunov function Q yields,

$$Q^{'} = (\mathcal{R}_0 - 1)(\omega_1, \omega_2, \omega_3, \omega_4, \omega_5)^T x - (\omega_1, \omega_2, \omega_3, \omega_4, \omega_5)^T W^{-1} f(x, y).$$

Since $(\omega_1, \omega_2, \omega_3, \omega_4, \omega_5) \geq 0, W^{-1} \geq 0$ and $f(x, y) \geq 0$ in Ω, then $(\omega_1, \omega_2)^T W^{-1} f(x, y) \geq 0$. Therefore, $Q^{'} \leq 0$ in Ω if $\mathcal{R}_0 \leq 1$ and Q is a Lyapunov function for the system (3.1). By LaSalle's invariance principle [65, 66], Q^0 is GAS in Ω [21].

If $\mathcal{R}_0 > 1$, then $Q^{'} = (\mathcal{R}_0 - 1)(\omega_1, \omega_2, \omega_3, \omega_4, \omega_5)^T x > 0$ provided that $x > 0$ and $y = (S^0, S_q^0, 0)$. By continuity, $Q^{'} > 0$ in the neighborhood of Q^0. Solutions in positive cone sufficiently close to Q^0 move away from Q^0, implying that Q^0 is unstable. Thus, the model system (3.1) is uniformly persistent [43, 69]. Uniform persistence and the positively invariance of Ω imply the existence of an endemic equilibrium. □

As a consequence of the above result, we can confidently conclude that COVID-19 can be eradicated from the host community if the value of $\mathcal{R}_0$ is reduced and constantly maintained below one. Figure 3 shows the validation of the global stability analysis for the disease-free equilibrium point.

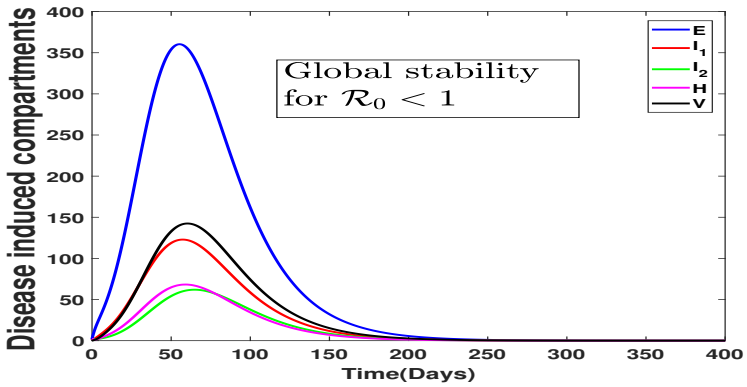

Figure 3: Global stability when $\mathcal{R}_0 < 1$, in accordance with Theorem 7. Parameter values used are as given in Table 4, except $\gamma_2 = 1/10$, so that $\mathcal{R}_0 = 0.77 < 1$.

4.1.3 Endemic equilibrium and its stability

Let $Q^* = (S^*, S_q^*, I_1^*, I_2^*, H^*, R^*, V^*)$ be the positive endemic equilibrium (EE) of model system (3.1). Then, the positive endemic equilibrium can be obtained by setting the right hand side of all equations in model system (3.1) to zero, giving:

$$\begin{cases} \Lambda - \lambda^* S^* + q_1 S_q^* - (\mu + q) S^* & = 0, \\ q S^* - q_1 S_q^* - \mu S_q^* & = 0, \\ \lambda^* S^* - \omega E^* - \mu E^* & = 0, \\ \phi\omega E^* - \gamma_1 I_1^* - \mu I_1^* - d I_1^* & = 0, \\ (1-\phi)\omega E^* - \gamma_2 I_2^* - \mu I_2^* - d I_2^* & = 0, \\ \gamma_1 I_1^* + \gamma_2 I_2^* - m H^* - \mu H^* - d H^* & = 0, \\ m H^* - \mu R^* & = 0, \\ f_1 E^* + f_2 I_1^* + f_3 I_2^* - d_v V^* & = 0, \end{cases} \tag{4.11}$$

where $\lambda^* = \beta_e E^* + \beta_{i_1} I_1^* + \beta_{i_2} I_2^* + \beta_v V^*$. Given the complexity of the system (4.11), we are going to try to determine an explicit formula for the endemic equilibrium point Q^*. To do this, we will solve the system (4.11). After algebraic manipulations of this system, we obtain:

$$R^* = \frac{m}{\mu} H^*, E^* = \frac{\mu + \gamma_1 + d}{\phi\omega} I_1^*, I_2^* = \frac{(1-\phi)(\mu + \gamma_1 + d)}{\phi(\mu + \gamma_2 + d)} I_1^*, S_q^* = \frac{q_1 + \mu}{q} S^*,$$

$$H^* = \frac{\gamma_1\phi(\mu + \gamma_2 + d) + \gamma_2(1-\phi)(\mu + \gamma_1 + d)}{\phi(\mu + \gamma_2 + d)(\mu + m + d)} I_1^*,$$

$$V^* = \frac{f_1(\mu + \gamma_1 + d)(\mu + \gamma_2 + d) + f_2\phi\omega(\mu + \gamma_2 + d) + f_3(1-\phi)\omega(\mu + \gamma_1 + d)}{\phi\omega d_v(\mu + \gamma_2 + d)} I_1^*,$$

$$S^* = \frac{d_v(\mu + \omega)(\mu + \gamma_1 + d)(\mu + \gamma_2 + d)}{\beta_e d_v(\mu + \gamma_1 + d)(\mu + \gamma_2 + d) + \beta_{i_1}\phi\omega d_v(\mu + \gamma_2 + d) + \beta_{i_2}(1-\phi)\omega d_v(\mu + \gamma_1 + d)}$$
$$+ \frac{d_v(\mu + \omega)(\mu + \gamma_1 + d)(\mu + \gamma_2 + d)}{\beta_v f_1(\mu + \gamma_1 + d)(\mu + \gamma_2 + d) + \beta_v f_2\phi\omega(\mu + \gamma_2 + d) + \beta_v f_3(1-\phi)\omega(\mu + \gamma_1 + d)},$$

and

$$I_1^* = \frac{\phi\omega[(q + \mu)(q_1 + \mu) - q q_1]}{(q_1 + \mu)(\mu + \omega)(\mu + \gamma_1 + d)} S^*(\mathcal{R}_0 - 1).$$

Lemma 2 *Model* (3.1) *has exactly one endemic equilibrium whenever* $\mathcal{R}_0 > 1$.

We establish the following result to analyze the stability of Q^*.

Theorem 8 *If* $\mathcal{R}_0 > 1$, *the endemic equilibrium* Q^* *is GAS in* Ω.

Proof : Consider the following Lyapunov function candidate [1, 109]:

$$L = \left(S - S^* - S^* \ln \frac{S}{S^*}\right) + h_1\left(S_q - S_q^* - S_q^* \ln \frac{S_q}{S_q^*}\right) + h_2\left(E - E^* - E^* \ln \frac{E}{E^*}\right) + h_3\left(I_1 - I_1^* - I_1^* \ln \frac{I_1}{I_1^*}\right) + h_4\left(I_2 - I_2^* - I_2^* \ln \frac{I_2}{I_2^*}\right) + h_5\left(V - V^* - V^* \ln \frac{V}{V^*}\right), \quad (4.12)$$

where h_1, h_2, h_3, h_4 and h_5 are positive constants to be determined later. Differentiating the function (4.12) with respect to time yields

$$\dot{L} = \left(1 - \frac{S^*}{S}\right)\dot{S} + h_1\left(1 - \frac{S_q^*}{S_q}\right)\dot{S}_q + h_2\left(1 - \frac{E^*}{E}\right)\dot{E} + h_3\left(1 - \frac{I_1^*}{I_1}\right)\dot{I}_1 + h_4\left(1 - \frac{I_2^*}{I_2}\right)\dot{I}_2 + h_5\left(1 - \frac{V^*}{V}\right)\dot{V}. \quad (4.13)$$

Substituting equation (3.1) into equation (4.13) and using Equation (4.11) at the positive endemic equilibrium with further simplification yields

$$\begin{aligned}\dot{L} =& -(q+\mu)\left(1 - \frac{1}{x_1}\right)^2 S + \beta_e S^* E^*\left(1 - \frac{1}{x_1} + x_3 - x_1 x_3\right) + \beta_{i_1} S^* I_1^*\left(1 - \frac{1}{x_1} + x_4 - x_1 x_4\right) \\ &+ \beta_{i_2} S^* I_2^*\left(1 - \frac{1}{x_1} + x_5 - x_1 x_5\right) + \beta_v S^* V^*\left(1 - \frac{1}{x_1} + x_6 - x_1 x_6\right) + q_1 S_q^*\left(x_2 + \frac{1}{x_1} - \frac{x_2}{x_1} - 1\right) \\ &+ h_1 q S^*\left(x_1 - x_2 - \frac{x_1}{x_2} + 1\right) + h_2 \beta_e S^* E^*\left(1 - x_1 - x_3 + x_1 x_3\right) + h_2 \beta_{i_1} S^* I_1^*\left(1 - x_3 + x_1 x_4 - \frac{x_1 x_4}{x_3}\right) \\ &+ h_2 \beta_{i_2} S^* I_2^*\left(1 - x_3 + x_1 x_5 - \frac{x_1 x_5}{x_3}\right) + h_2 \beta_v S^* V^*\left(1 - x_3 + x_1 x_6 - \frac{x_1 x_6}{x_3}\right) \\ &+ h_3 \phi \omega E^*\left(1 + x_3 - x_4 - \frac{x_3}{x_4}\right) + h_4(1-\phi)\omega E^*\left(1 + x_3 - x_5 - \frac{x_3}{x_5}\right) + h_5 f_1 E^*\left(1 + x_3 - x_6 - \frac{x_3}{x_6}\right) \\ &+ h_5 f_2 I_1^*\left(1 + x_4 - x_6 - \frac{x_4}{x_6}\right) + h_5 f_3 I_2^*\left(1 + x_5 - x_6 - \frac{x_5}{x_6}\right), \end{aligned} \quad (4.14)$$

where $x_1 = \frac{S}{S^*}$, $x_2 = \frac{S_q}{S_q^*}$, $x_3 = \frac{E}{E^*}$, $x_4 = \frac{I_1}{I_1^*}$, $x_5 = \frac{I_2}{I_2^*}$ and $x_6 = \frac{V}{V^*}$. Then equation (4.14)

becomes

$$\begin{aligned}\dot{L} =& -(q+\mu)\left(1-\frac{1}{x_1}\right)^2 S + \beta_e S^* E^* + \beta_{i_1} S^* I_1^* + \beta_{i_2} S^* I_2^* + \beta_v S^* V^* - q_1 S_q^* + h_1 q S^* \\ &+ h_2\beta_e S^* E^* + h_2\beta_{i_1} S^* I_1^* + h_2\beta_{i_2} S^* I_2^* + h_2\beta_v S^* V^* + h_3\phi\omega E^* + h_4(1-\phi)\omega E^* + h_5 f_1 E^* \\ &+ h_5 f_2 I_1^* + h_5 f_3 I_2^* + \left(-\beta_e S^* E^* - \beta_{i_1} S^* I_1^* - \beta_{i_2} S^* I_2^* - \beta_v S^* V^* + q_1 S_q^*\right)\frac{1}{x_1} \\ &+ (h_1 q S^* - h_2\beta_e S^* E^*)x_1 + (q_1 S_q^* - h_1 q S^*)x_2 + (\beta_e S^* E^* - h_2\beta_e S^* E^* - h_2\beta_{i_1} S^* I_1^* \\ &- h_2\beta_{i_2} S^* I_2^* - h_2\beta_v S^* V^* + h_3\phi\omega E^* + h_4(1-\phi)\omega E^* + h_5 f_1 E^*)x_3 \\ &+ (\beta_{i_1} S^* I_1^* - h_3\phi\omega E^* + h_5 f_2 I_1^*)x_4 + (\beta_{i_2} S^* I_2^* + h_4(1-\phi)\omega E^* + h_5 f_3 I_2^*)x_5 \\ &+ (\beta_v S^* V^* - h_5 f_1 E^* - h_5 f_2 I_1^* - h_5 f_3 I_2^*)x_6 + (-\beta_e S^* E^* + h_2\beta_e S^* E^*)x_1 x_3 \\ &+ (-\beta_{i_1} S^* I_1^* + h_2\beta_{i_1} S^* I_1^*)x_1 x_4 + (-\beta_{i_2} S^* I_2^* + h_2\beta_{i_2} S^* I_2^*)x_1 x_5 \\ &+ (-\beta_v S^* V^* + h_2\beta_v S^* V^*)x_1 x_6 - q_1 S_q^* \frac{x_2}{x_1} + h_1 q S^* \frac{x_1}{x_2} - h_3\phi\omega E^* \frac{x_3}{x_4} - h_4(1-\phi)\omega E^* \frac{x_3}{x_5} \\ &- h_5 f_1 E^* \frac{x_3}{x_6} - h_5 f_2 I_1^* \frac{x_4}{x_6} - h_5 f_3 I_2^* \frac{x_5}{x_6} - h_2\beta_{i_1} S^* I_1^* \frac{x_1 x_4}{x_3} - h_2\beta_{i_2} S^* I_2^* \frac{x_1 x_5}{x_3} - h_2\beta_v S^* V^* \frac{x_1 x_6}{x_3}.\end{aligned} \tag{4.15}$$

Considering the expressions

$$h_2\beta_e S^* E^* = \beta_e S^* E^*,\ h_2\beta_{i_1} S^* I_1^* = \beta_{i_1} S^* I_1^*, h_2\beta_{i_2} S^* I_2^* = \beta_{i_2} S^* I_2^*,\ \text{and}\ h_2\beta_v S^* V^* = \beta_v S^* V^*,$$

we have $h_2 = 1$, thus the coefficients of x_1x_3, x_1x_4, x_1x_5 and x_1x_6 are all 0. By setting the coefficients of x_2, x_4, x_5, and x_6 to 0 and solving for h_1, h_3, h_4 and h_5 yields

$$\begin{aligned}h_1 =& \frac{q_1 S_q^*}{q S^*}, \quad h_3 = \frac{\beta_{i_1} S^* I_1^* (f_1 E^* + f_2 I_1^* + f_3 I_2^*) + \beta_v f_2 S^* V^* I_1^*}{\phi\omega E^* (f_1 E^* + f_2 I_1^* + f_3 I_2^*)}, \\ h_4 =& \frac{\beta_{i_2} S^* I_2^* (f_1 E^* + f_2 I_1^* + f_3 I_2^*) + \beta_v f_3 S^* V^* I_1^*}{(1-\phi)\omega E^* (f_1 E^* + f_2 I_1^* + f_3 I_2^*)} \quad \text{and} \quad h_5 = \frac{\beta_v S^* V^*}{f_1 E^* + f_2 I_1^* + f_3 I_2^*}.\end{aligned}$$

Therefore, $\dot{L}$ can be rewritten as

$$\begin{aligned}\dot{L} =& -(q+\mu)\left(1-\frac{1}{x_1}\right)^2 S - \beta_e S^* E^*\left(x_1+\frac{1}{x_1}-2\right)\\
&-\beta_{i_1} S^* I_1^*\left(x_3-x_4+\frac{1}{x_1}+\frac{x_1x_4}{x_3}-2\right)-\beta_{i_2} S^* I_2^*\left(x_3-x_5+\frac{1}{x_1}+\frac{x_1x_5}{x_3}-2\right)\\
&-\beta_v S^* V^*\left(x_3-x_6+\frac{1}{x_1}+\frac{x_1x_6}{x_3}-2\right)-q_1 S_q^*\left(\frac{x_1}{x_2}+\frac{x_2}{x_1}-x_1-\frac{1}{x_1}\right)\\
&-h_3\phi\omega E^*\left(x_4-x_3-1+\frac{x_3}{x_4}\right)-h_4(1-\phi)\omega E^*\left(x_5-x_3-1+\frac{x_3}{x_5}\right)\\
&-h_5 f_1 E^*\left(x_6-x_3-1+\frac{x_3}{x_6}\right)-h_5 f_2 I_1^*\left(x_6-x_4-1+\frac{x_4}{x_6}\right)-h_5 f_3 I_2^*\left(x_6-x_5-1+\frac{x_5}{x_6}\right).\end{aligned}$$

Thus, using the arithmetic-geometric means inequality, we can see that $\dot{L}$ is less or equal to zero with equality only if $x_1 = 1$, $x_2 = 1$, $x_2 = 1$, $x_3 = 1$, $x_4 = 1$, $x_5 = 1$ and $x_6 = 1$. By LaSalle's invariance principle the largest invariant set in Ω, contained in

$$\{(S, S_q, E, I_1, I_2, H, R, V) \in \Omega \quad | \quad \dot{L} = 0\}$$

is reduced to the endemic equilibrium Q^*. Then, we conclude that the endemic equilibrium is globally asymptotically stable in Ω [29, 109]. □

Figure 4 shows the validation of the global stability analysis for the endemic equilibrium point.

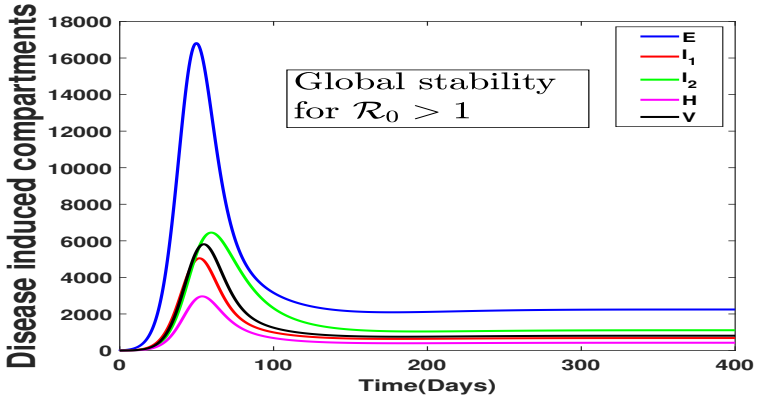

Figure 4: Global stability when $\mathcal{R}_0 > 1$, in accordance with Theorem 8. Parameter values used are as given in Table 4, except $\phi = 0.8$, so that $\mathcal{R}_0 = 2.06 > 1$.

4.1.4 Numerical results

In this section, we present numerical simulations of the proposed model (3.1), using parameters estimated from COVID-19 data for Ghana [111]. The estimation was performed using the least squares approach, which consists of minimizing the sum of the squared differences between the observed cumulative cases data point and the corresponding model(3.1) predicted points. In Figure 5, we present the fitted model, along with the cumulative cases and residual plot for Ghana using 100 data points. The initial conditions are set based on the first confirmed cases, dated 12th March, 2020. The incubation periods of COVID-19 is known to range from 2 to 14 days. On 12th March, 2020, Ghana reported its first two COVID-19 cases, so we assume an initial number of hospitalized to be two i.e. $H(0) = 2$. The total population of Ghana at the time was $30,417,856$. It is assumed that, there were no recoveries at the start, and the number of exposed, timely diagnosed, and delayed individual was equal to the initial number of detected cases. Therefore, the initial values for Ghana are given by $S(0) = 30,417,848$ $S_q(0) = 0$ $E(0) = 2$ $I_1(0) = 2$ $I_2(0) = 2$ $H(0) = 2$ $R(0) = 0$ $V(0) = 0$. From the data fitting, as shown in Figure 5 and Table 4, the computed reproduction number, $\mathcal{R}_0$, for the 100 data points is given as $\mathcal{R}_c = 1.0410$. In what follows, we present the results of the sensitivity analysis and other numerical outputs of the model using the obtained parameters in Table 4.

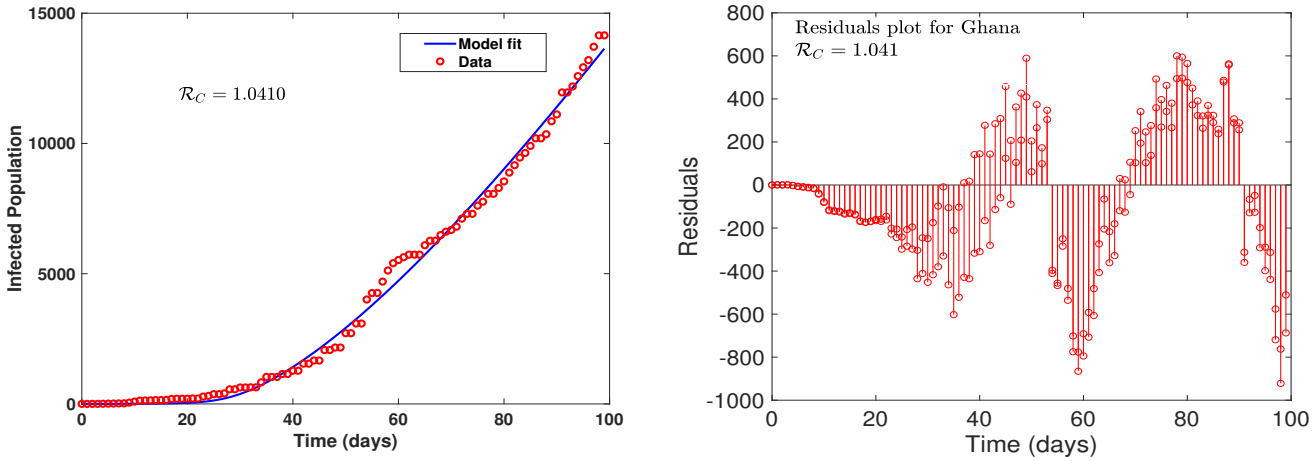

(a) Model fit

(b) Residual plot.

Figure 5: Model fit for Ghana during the time window 12 March, 2020 to 19 June, 2020 .

4.1.5 Sensitivity analysis

In this section, we utilized two sensitivity analysis approaches to find the factors that contribute the most to the transmission: the forward sensitivity index normalised and LHS

Table 4: Estimated parameters

Parameters	Value/day	Source	Parameters	Value/day	Source
Λ	1319.294	[94]	γ_1	0.5000	Fitted
q	0.0333	Fitted	γ_2	0.0714	Fitted
q_1	1.6945×10^{-5}	Estimated	μ	4.2578×10^{-5}	[103]
β_e	6.0380×10^{-8}	Fitted	d	0.006139	Estimated
β_{i_1}	3.8196×10^{-8}	Fitted	f_1	0.0178	Fitted
β_{i_2}	1.4286×10^{-5}	Fitted	f_2	0.3115	Fitted
β_v	4.00199×10^{-8}	[21]	f_3	4.6131×10^{-5}	Fitted
ω	1/5.2	[103]	m	0.9815	Fitted
ϕ	0.9000 unitless	Fitted	d_v	0.3117	[97]

as seen in [20, 55, 17, 76, 16]. From [76, 19], the normalized forward-sensitivity index of $\mathcal{R}_0$, is defined as:

$$\Delta_{\mathcal{R}_0}^{\rho^*} = \frac{\partial \mathcal{R}_0}{\partial \rho^*} \frac{\rho^*}{\mathcal{R}_0}. \tag{4.16}$$

where ρ^* represent the various parameters in $\mathcal{R}_0$. Using the parameter values in Table 4, the calculated (local) sensitivity indexes are given in Table 5. LHS is known to be a Monte Carlo sampling method. It divides the various parameters into equal intervals and indiscriminately draws one sample from each equal interval. LHS is usually carried out with PRCC to estimate the nonlinearity between the parameters and also the unmodulated relationship between model parameters [18, 112]. Using the LHS with 2500 samples from a uniform distribution, the parameters in the basic reproduction number $\mathcal{R}_0$ were employed to obtain the global sensitivity of the various parameters in $\mathcal{R}_0$. Using the PRCC plot in Figure 6, we noticed further that the parameters contributing to the growth of the basic reproduction number are $\beta_v, \beta_e, f_1, q_1, f_2, \Lambda, \beta_{i_1}, \phi, f_3$, and β_{i_2} (ordered in order of magnitude). While, $\mu, q, d_v, \omega, d, \gamma_1, \gamma_2$, contribute to the decline of the basic reproduction number, $\mathcal{R}_0$ (ordered in order of magnitude). Among the positive parameters from the PRCC analysis, β_v and β_e are the most dominant. This suggests that a reducing interaction of susceptible individuals with exposed individuals and virus in the environment, will significantly slow the spread of virus in the community, in turn decrease the basic reproduction number more rapidly. Among the negative parameters, q and d_v are the most dominant. This suggests that increasing these parameters would reduce the virus spread and leads to a quicker decline of the basic reproduction number. Although μ (natural death rate) has the longest bar in the analysis, it is not a viable control parameter. Therefore, in Figures 7 and 8 we show the graphical trajectories of some parameters on the infected classes.

Table 5: Local sensitivity analysis.

Parameters	Sensitivity index	Parameters	Sensitivity index
Λ	1	ϕ	-8.7710
q	-0.9982	γ_1	-0.0073
β_e	0.0166	γ_2	-0.8977
q_1	0.2842	μ	-0.2867
d_v	0.0110	d	-0.0773
β_{i_1}	0.0036	f_1	0.0006
β_{i_2}	0.9754	f_2	0.0110
β_v	0.0044	f_3	1.6314×10^{-6}
ω	-0.0170		

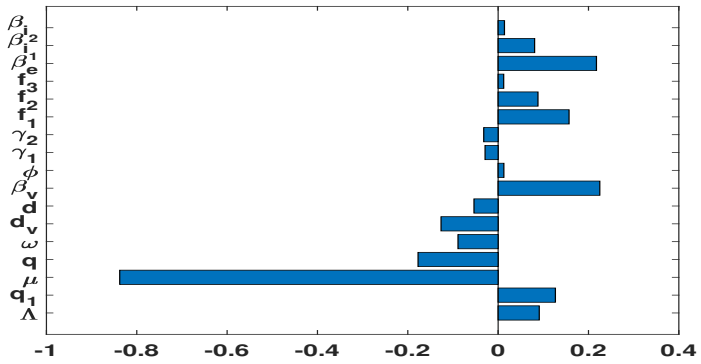

Figure 6: PRCC plot for the parameters in the basic reproduction number, $\mathcal{R}_0$.

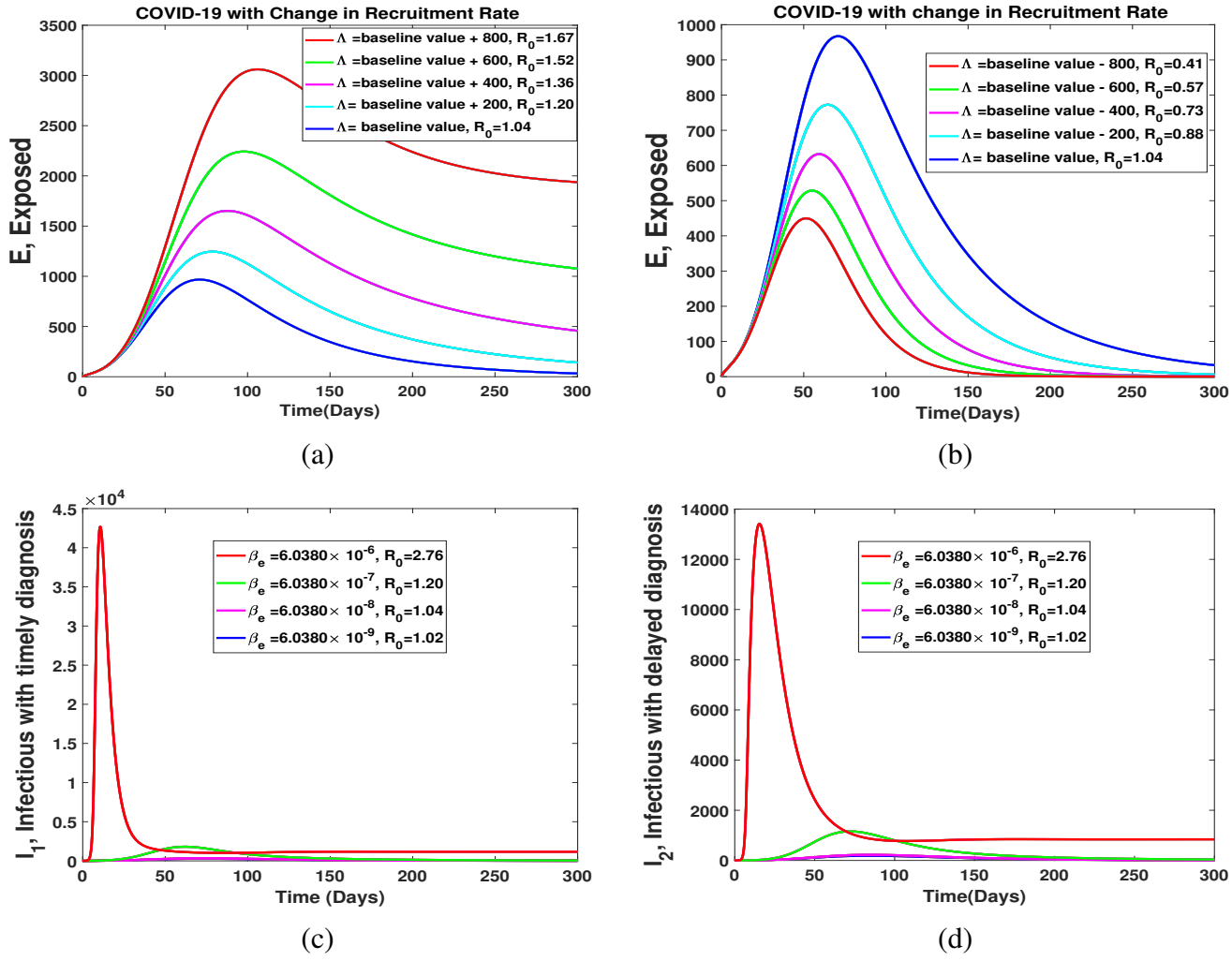

Figure 7: Sensitivity analysis plot for COVID-19 model with timely-delayed diagnosis, using Λ, and β_e.

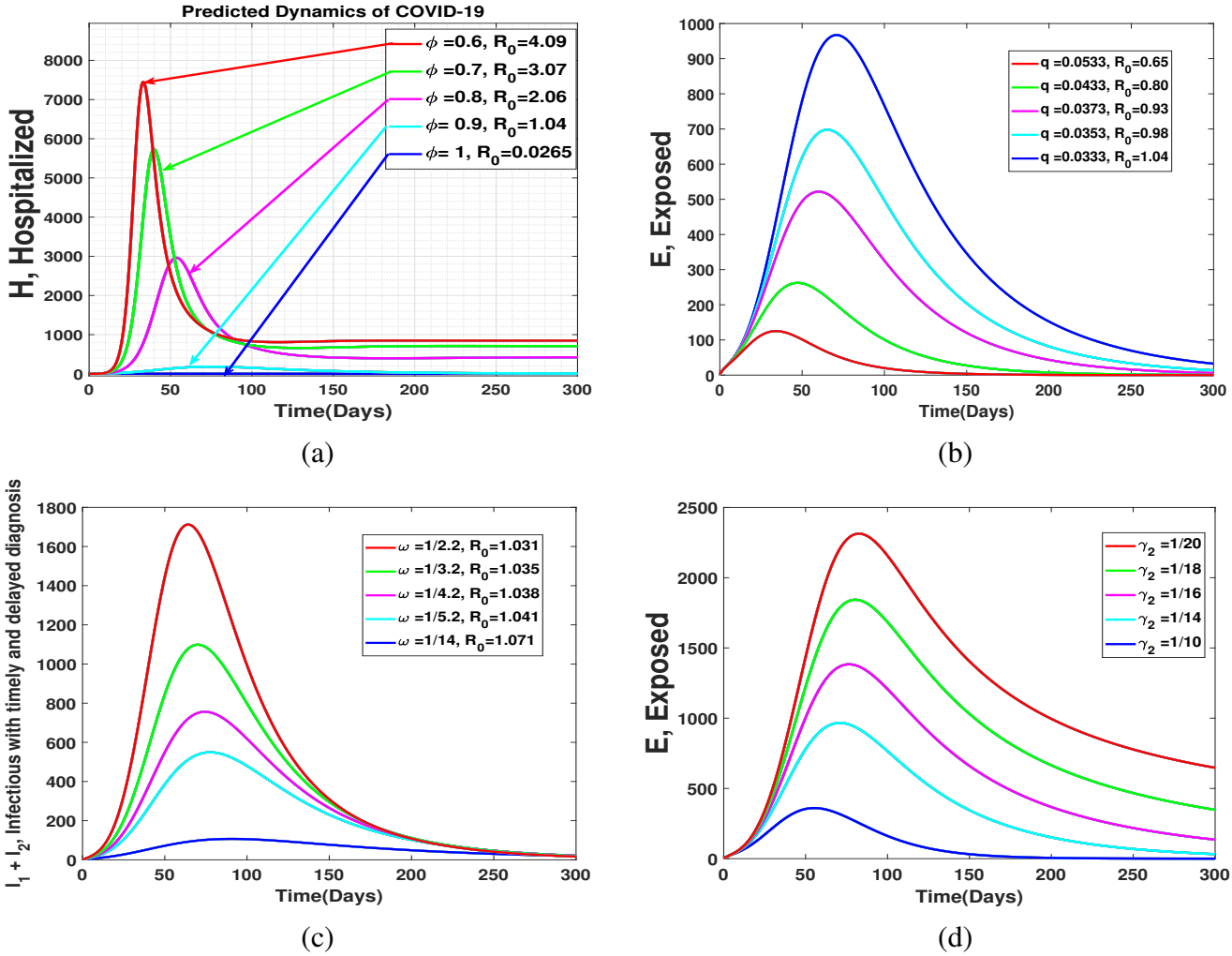

Figure 8: Sensitivity analysis plot for COVID-19 model with timely-delayed diagnosis, using ϕ, q, ω and γ_2.

In Figures 7(a)-7(d), we show the impact of the rate of recruitment Λ, and the rate of relative transmissibility of exposed individuals β_e, on the model. We noticed in Figure 7(a) that an increase in Λ would have an immediate increase in the number of new infections, whiles Figure 7(b) shows that a decline in Λ will help eradicate the disease in Ghana. In Figures 7(c) and 7(d), we notice that an increase in the relative transmissibility of exposed individuals will have exponential growth in the number of secondary infections. Hence, we suggest that all persons keep to the regular washing of hands with soap and alcohol-based sanitiser whenever they use public facilities since this will help reduce the spread of the virus by exposed individuals.

Figures 8(a) and Figure 8(b) illustrate the dynamical effects of varying the proportion of individual with timely diagnosis and self-quarantined rate among susceptible individuals. Figure 8(a) indicates that an increase in the proportion of infectious individual promptly diagnosis leads to a reduction in the basic reproduction number. Notably that a 100% timely detection of infected individuals reduces the basic reproduction number to 0.025, resulting in complete eradication of the disease within 100 days. In Figure 8(b), we noticed that the willingness of individuals to practice self-quarantine has a major role in reducing the spread of disease in Ghana. Figure 8(c) demonstrates the effect of the incubation period of the disease on the number of individuals timely-delayed diagnosis. We noticed that an increase in the number of incubation periods reduces the number of timely-delayed diagnosis individuals. Figure 8(d) shows the dynamic effects of delayed diagnosis on the number of exposed individuals. A reduction in the delay time decreases the number of exposed individuals. Based on these findings, we suggest that the government enhance their diagnostic efforts to reduce the number of infected individuals in each community.

4.1.6 Summary

In this section, we presented the results of the analysis of a COVID-19 model that considers self-quarantined individuals, delay in diagnosis and environmental transmission and analysed the transmission dynamics of the pandemic in Ghana. The proposed model was shown to be globally asymptotically stable when $\mathcal{R}_0 \leq 1$ and when $\mathcal{R}_0 > 1$. Then we suggest that all persons should keep to the regular washing of hands with soap and alcohol based sensitizer whenever they use public facilities, since this will help reduce the spread of the virus by exposed individuals. In addition to reduce the risk of infection from exposed individuals, we advise to improve air quality by increasing airflow, cleaning the air, or opting to gather outdoors. And the government should increase their efforts in diagnoses

so to reduce the number of infected individuals in each community.

4.2 Impact of imperfect vaccine, vaccine trade-off and population turnover on infectious disease dynamics

In this section, we compute the basic properties of the steady-state solutions as well as the existence of local and global stability of the equilibria of the model (Section **??**). We then perform a numerical sensitivity analysis of the model and study examples of numerical analyses for different parameter values to describe the interaction between population turnover and vaccine trade-offs on the epidemiological outcome. We conclude by providing predictions on the applicability of these results to vaccination strategies in human populations, but also domesticated (and wild) animal species for which turnover rates represent a different end of a continuum.

These results are published in *Mathematics* [89].

4.2.1 Basic properties

First, we study the basic characteristics of the system solutions: the existence, non-negativity and boundedness of solutions. These are (1) essential to make sure that the model (3.3) is well defined mathematically and epidemiologically and (2) useful for the proofs of the stability results.

4.2.1.1 Positive invariance of the non-negative orthant

For any associated Cauchy problem, system (3.3), which is a C^∞-differentiable system, has a unique maximal solution.

Lemma 3 *The following result corresponds to Proposition B.7, Appendix B in [106]. Let D be an open subset of $\mathbb{R}^n$, $f : \mathbb{R}\times D \to \mathbb{R}^n$, be a vector-valued function, $f = (f_1, f_2, \cdots, f_n)$. Consider a system of ODEs of the form*

$$x' = f(t, x). \tag{4.17}$$

Suppose that f in Equation (4.17) has the property that solutions of initial value problems $x(t_0) = x_0 \geq 0$ are unique and for all i $f_i(t, x) \geq 0$ whenever $x \geq 0$ satisfies $x_i = 0$. Then $x(t) \geq 0$ for all $t \geq t_0$ for which it is defined, provided $x(t_0) \geq 0$.

Theorem 9 *If the initial conditions of system (3.3) are such that* $S_1(0) \geq 0$, $S_2(0) \geq 0$, $I_1(0) \geq 0$, $I_2(0) \geq 0$ *and* $R(0) \geq 0$, *then the solution* $(S_1(t), S_2(t), I_1(t), I_2(t), R(t))$ *of the system equation is non-negative for all* $t \geq 0$.

Proof : Considering model (3.3). We have

$$\left.\frac{dS_1}{dt}\right|_{S_1=0} = \theta(1-p) \geq 0,$$

$$\left.\frac{dS_2}{dt}\right|_{S_2=0} = \theta p \geq 0,$$

$$\left.\frac{dI_1}{dt}\right|_{I_1=0} = \beta_{11}\frac{I_1(t)}{N(t)}S_1(t) \geq 0,$$

$$\left.\frac{dI_2}{dt}\right|_{I_2=0} = \beta_{21}\frac{I_1(t)}{N(t)}S_2(t) \geq 0,$$

$$\left.\frac{dR}{dt}\right|_{R=0} = \gamma_1 I_1(t) + \gamma_2 I_2(t) \geq 0,$$

for all $S_1, S_2, I_1, I_2, R \geq 0$. By using Lemma 3, we conclude that the solution $(S_1(t), S_2(t), I_1(t), I_2(t), R(t))$ of the system equation is non-negative for all $t \geq 0$.

Thus, solutions of system (3.3) with non-negative initial conditions will be non-negative for all $t \geq 0$.

4.2.1.2 Boundedness of solutions

Since the variables of model (3.3) are non-negative, and we are dealing with the dynamic of a number of individuals, it is important and biologically realistic that the total number of individuals does not explode (that is, it is bounded).

Lemma 4 *The closed set*

$$\Omega = \left\{(S_1(t), S_2(t), I_1(t), I_2(t), R(t)) \in \mathbb{R}^5 : S_1(t) \geq 0, S_2(t) \geq 0, I_1(t) \geq 0, I_2(t) \geq 0, R(t) \geq 0,\right.$$

is positively invariant and attracting for system (3.3).

Proof : Using system (3.3), the dynamics of the total human population satisfies:

$$\frac{\mathrm{d}N}{\mathrm{d}t} = \theta - \mu N - d_1 I_1 - d_2 I_2 \leqslant \theta - \mu N.$$

Integrating both sides of the expression above, we deduce that

$$N(t) \leqslant \frac{\theta}{\mu} + \left(N(0) - \frac{\theta}{\mu}\right) e^{-\mu t}, \quad \forall t \geqslant 0, \tag{4.18}$$

where $N(0)$ is the value of $N(t)$ at time zero. We deduce that if $N(0) \leqslant \dfrac{\theta}{\mu}$, then $0 \leqslant N(t) \leqslant \dfrac{\theta}{\mu}$, $\forall t \geqslant 0$ and Ω is positively invariant. If $N(0) \geqslant \dfrac{\theta}{\mu}$, then from Equation (4.18) the total population decreases, and the solutions of system (3.3) enter Ω. Hence $N(t)$ is bounded as $t \longrightarrow \infty$, which means that Ω is attracting.

Remark 2 *We know from Theorem 13 in [68] that every maximal solution of the Cauchy problem (4.17) that is bounded is global; that is, it exists for all $t \geq 0$. Then, every maximal solution of system (3.3) is well-defined for all $t \geq 0$.*

System (3.3) is epidemiologically and mathematically well-posed in Ω since its state variables are non-negative, and the size of the total population is bounded. The maximum value of N represents the size of the total population under the ideal situation without infection.

4.2.2 Disease-free equilibrium and its stability

For the analysis of the spread of an infection, we define the DFE, which is the state of the population without infection. The disease-free equilibrium is deduced from the resolution of system (3.3) by taking $I_1 = 0$ and $I_2 = 0$. Thus, the disease-free equilibrium satisfies the following system of equations:

$$\begin{cases} \theta(1-p) - \mu S_1^0 = 0, \\ \theta p - \mu S_2^0 = 0. \end{cases} \tag{4.19}$$

Solving the system of equations (4.19) yields the disease-free equilibrium point:

$$Q^0 = (S_1^0, S_2^0, 0, 0, 0),$$

where $S_1^0 = \dfrac{\theta(1-p)}{\mu}$, $S_2^0 = \dfrac{\theta p}{\mu}$ and $N^0 = S_1^0 + S_2^0 = \dfrac{\theta}{\mu}$.

The linear stability of Q^0 depends on the well-known reproduction number $\mathcal{R}_0$, which is defined as the average number of secondary cases caused by an infected individual during its infectious period when introduced into a population of susceptible individuals. We study the stability of the equilibrium through the next-generation operator [36, 59]. Recalling the notations in [36] for system (3.3), the matrices $\mathcal{F}$ of the new infection and $\mathcal{V}$ of the remaining transfer terms are, respectively, given by

$$\mathcal{F} = \begin{bmatrix} \beta_{11}\dfrac{S_1 I_1}{N} + \beta_{12}\dfrac{S_1 I_2}{N} \\ \\ \beta_{21}\dfrac{S_2 I_1}{N} + \beta_{22}\dfrac{S_2 I_2}{N} \end{bmatrix} \text{ and } \mathcal{V} = \begin{bmatrix} (\mu+\gamma_1+d_1)I_1 \\ \\ (\mu+\gamma_2+d_2)I_2 \end{bmatrix}.$$

The Jacobian matrices of $\mathcal{F}$ and $\mathcal{V}$ at Q^0 are, respectively,

$$F = \begin{bmatrix} \beta_{11}\dfrac{S_1^0}{N^0} & \beta_{12}\dfrac{S_1^0}{N^0} \\ \\ \beta_{21}\dfrac{S_2^0}{N^0} & \beta_{22}\dfrac{S_2^0}{N^0} \end{bmatrix} \text{ and } V = \begin{bmatrix} \mu+\gamma_1+d_1 & 0 \\ \\ 0 & \mu+\gamma_2+d_2 \end{bmatrix}. \tag{4.20}$$

Then,

$$FV^{-1} = \begin{bmatrix} \dfrac{\beta_{11}S_1^0}{N^0(\mu+\gamma_1+d_1)} & \dfrac{\beta_{12}S_1^0}{N^0(\mu+\gamma_2+d_2)} \\ \\ \dfrac{\beta_{21}S_2^0}{N^0(\mu+\gamma_1+d_1)} & \dfrac{\beta_{22}S_2^0}{N^0(\mu+\gamma_2+d_2)} \end{bmatrix},$$

and the reproduction number of model system (3.3) is

$$\begin{aligned} \mathcal{R}_0 = \rho(FV^{-1}) =& \frac{1}{2}\left[\frac{S_1^0}{N^0}\mathcal{R}_{0,11} + \frac{S_2^0}{N^0}\mathcal{R}_{0,22} + \sqrt{\left(\frac{S_1^0}{N^0}\mathcal{R}_{0,11} - \frac{S_2^0}{N^0}\mathcal{R}_{0,22}\right)^2 + 4\frac{S_1^0}{N^0}\frac{S_2^0}{N^0}\mathcal{R}_{0,12}\mathcal{R}_{0,21}}\right], \\ \mathcal{R}_0 =& \frac{1}{2}\left[(1-p)\mathcal{R}_{0,11} + p\mathcal{R}_{0,22} + \sqrt{\left((1-p)\mathcal{R}_{0,11} - p\mathcal{R}_{0,22}\right)^2 + 4p(1-p)\mathcal{R}_{0,12}\mathcal{R}_{0,21}}\right], \end{aligned} \tag{4.21}$$

where $\dfrac{S_1^0}{N^0} = 1-p$ ($\dfrac{S_2^0}{N^0} = p$) is the proportion of susceptible individuals that have not been vaccinated (have been vaccinated) at the DFE Q^0. Similarly, we define $\mathcal{R}_{0,11} = \dfrac{\beta_{11}}{\mu+\gamma_1+d_1}$ which represents the average number of secondary cases generated by an unvaccinated

infected individual during its infectious period through interaction within the unvaccinated population. Furthermore, $\mathcal{R}_{0,12} = \dfrac{\beta_{12}}{\mu + \gamma_1 + d_1}$ represents the average number of secondary cases generated by a vaccinated infected individual in the unvaccinated segment of the population. For the vaccinated population $\mathcal{R}_{0,21} = \dfrac{\beta_{21}}{\mu + \gamma_2 + d_2}$ represents the average number of secondary cases generated by an unvaccinated infected individual, while $\mathcal{R}_{0,22} = \dfrac{\beta_{22}}{\mu + \gamma_2 + d_2}$ represents the average number of secondary cases generated by a vaccinated infected individual. Further, $\rho(FV^{-1})$ is the spectral radius of FV^{-1}.

Remark 3 *From the expression of the reproduction number $\mathcal{R}_0$ in Equation 4.21, we deduce that*
$\mathcal{R}_0 \geq \max\{(1-p)\mathcal{R}_{0,11}; p\mathcal{R}_{0,22}\}$. *Moreover, using (4.21) for $p = 0$ (all new hosts are unvaccinated), $\mathcal{R}_0 = \mathcal{R}_{0,11}$. Further, if $p = 1$ (all new hosts are vaccinated), then $\mathcal{R}_0 = \mathcal{R}_{0,22}$.*

The importance of the reproduction number is due to the result given in the next lemma derived from Theorem 2 in [36].

Lemma 5 *The disease-free equilibrium Q^0 of system (3.3) is locally asymptotically stable in Ω if $\mathcal{R}_0 < 1$, and unstable if $\mathcal{R}_0 > 1$.*

The biological meaning of Lemma 5 is that a sufficiently small number of infected hosts does not induce an epidemic unless the reproduction number $\mathcal{R}_0$ is greater than unity. That is, the disease rapidly dies out (when $\mathcal{R}_0 < 1$) if the initial number of infected hosts is in the basin of attraction of the DFE, Q^0. Global asymptotic stability of the DFE is required to better control the disease. In addition, analysing the expansion of the basin of attraction of Q^0 is a more challenging task for the model under consideration, involving a fairly new result. For this purpose, we use Theorems 2.1 and 2.2 in [104].

Theorem 10 *If $\mathcal{R}_0 \leqslant 1$, the disease-free equilibrium Q^0 of system (3.3) is globally asymptotic stable in Ω. If $\mathcal{R}_0 > 1$, Q^0 is unstable, system (3.3) is uniformly persistent, and there exists at least one endemic equilibrium in the interior of Ω.*

Proof : See Appendix 4.A.

As a consequence of the meaning of Theorem 10 and Remark 3, we can confidently deduce that the disease can be eradicated from the host community if the value of $\mathcal{R}_0$ is reduced to less than unity, independently of whether individuals introduced to the population are all vaccinated or not.

4.2.3 Endemic equilibrium and its stability

Let $Q^* = (S_1^*, S_2^*, I_1^*, I_2^*, R^*)$ be the positive EE of model system (3.3). Then, the positive endemic equilibrium can be obtained by setting the right-hand side of all equations in model system (3.3) to zero, giving:

$$\begin{cases} \theta(1-p) - \beta_{11}\dfrac{S_1^* I_1^*}{N^*} - \beta_{12}\dfrac{S_1^* I_2^*}{N^*} - \mu S_1^* = 0, \\ \theta p - \beta_{21}\dfrac{S_2^* I_1^*}{N^*} - \beta_{22}\dfrac{S_2^* I_2^*}{N^*} - \mu S_2^* = 0, \\ \beta_{11}\dfrac{S_1^* I_1^*}{N^*} + \beta_{12}\dfrac{S_1^* I_2^*}{N^*} - (\mu + \gamma_1 + d_1) I_1^* = 0, \\ \beta_{21}\dfrac{S_2^* I_1^*}{N^*} + \beta_{22}\dfrac{S_2^* I_2^*}{N^*} - (\mu + \gamma_2 + d_2) I_2^* = 0, \\ \gamma_1 I_1^* + \gamma_2 I_2^* - \mu R^* = 0. \end{cases} \tag{4.22}$$

Given the complexity of system (4.22), we are not determining an explicit formula for the endemic equilibrium point Q^*. Note that determining Q^* is often very difficult to be carried out when the system is complex and has a large size. However, to prove the existence of Q^*, we can rewrite system (4.22) as a fixed point problem and use Theorem 2.1 in [53]. To do this, we solve system (4.22). After algebraic manipulations, we obtain:

$$R^* = \frac{\gamma_1 I_1^* + \gamma_2 I_2^*}{\mu}, \; S_1^* = \frac{\theta(1-p)N^*}{\beta_{11} I_1^* + \beta_{12} I_2^* + \mu N^*}, \quad S_2^* = \frac{\theta p N^*}{\beta_{21} I_1^* + \beta_{22} I_2^* - d_1 I_1^* - d_2 I_2^* + \theta},$$

$$I_1^* = \frac{\theta(1-p)(\beta_{11} I_1^* + \beta_{12} I_2^*)}{(\mu + \gamma_1 + d_1)(\beta_{11} I_1^* + \beta_{12} I_2^* - d_1 I_1^* - d_2 I_2^* + \theta)} = H_1(I^*) \text{ and}$$

$$I_2^* = \frac{\theta p(\beta_{21} I_1^* + \beta_{22} I_2^*)}{(\mu + \gamma_2 + d_2)(\beta_{21} I_1^* + \beta_{22} I_2^* - d_1 I_1^* - d_2 I_2^* + \theta)} = H_2(I^*) \text{ with } I^* = (I_1^*, I_2^*).$$

Then, the endemic equilibrium is the fixed points of H given by $I = H(I)$ where $I = (I_1, I_2)$. By definition, H is continuous, monotonously non-decreasing and strictly sublinear. H is also a bounded function that maps the non-negative orthant Ω into itself. Moreover, $H(0) = 0$ by definition and the jacobian of H at the zero, $H'(0)$, exists and is irreducible since

$$H'(0) = \begin{bmatrix} \beta_{11} a_1 & \beta_{12} a_1 \\ \beta_{21} a_2 & \beta_{22} a_2 \end{bmatrix} = FV^{-1},$$

where $a_1 = \dfrac{1-p}{\mu+\gamma_1+d_1}$ and $a_2 = \dfrac{p}{\mu+\gamma_2+d_2}$.

We deduce that the spectral radius $\rho(H^{'}(0))$ of the matrix $H^{'}(0)$ is $\mathcal{R}_0$. Then, the existence and the uniqueness of a non-negative fixed point occur if and only if $\mathcal{R}_0 > 1$.

Proposition 2 *System (3.3) has only one endemic equilibrium whenever* $\mathcal{R}_0 > 1$.

We establish the following result to analyse the stability of Q^*.

Theorem 11 *If* $\mathcal{R}_0 > 1$, *the endemic equilibrium* Q^* *is globally asymptotic stable in* Ω.

Proof : Consider the following Lyapunov candidate function:

$$L = L_1 + L_2 + L_3 + L_4,$$

where $L_1 = S_1 - S_1^* - S_1^* \log\left(\dfrac{S_1}{S_1^*}\right)$, $L_2 = S_2 - S_2^* - S_2^* \log\left(\dfrac{S_2}{S_2^*}\right)$, $L_3 = I_1 - I_1^* - I_1^* \log\left(\dfrac{I_1}{I_1^*}\right)$ and $L_4 = I_2 - I_2^* - I_2^* \log\left(\dfrac{I_2}{I_2^*}\right)$.

Using the inequality $1 - z + \log(z) \leqslant 0$ for $z > 0$ with equality if and only if $z = 1$, differentiation and using the EE values give

$$L^{'} = L_1^{'} + L_2^{'} + L_3^{'} + L_4^{'},$$

where

$$
\begin{aligned}
L_1^{'} &= \left(1 - \frac{S_1^*}{S_1}\right)\frac{\mathrm{d}S_1}{\mathrm{d}t} \\
&= \left(1 - \frac{S_1^*}{S_1}\right)\left[\beta_{11}\frac{S_1^*I_1^*}{N^*} - \beta_{11}\frac{S_1I_1}{N} + \beta_{12}\frac{S_1^*I_2^*}{N^*} - \beta_{12}\frac{S_1I_2}{N} - \mu S_1 + \mu S_1^*\right] \\
&= -\frac{\mu(S_1 - S_1^*)^2}{S_1} + \beta_{11}\frac{S_1^*I_1^*}{N^*}\left[1 - \frac{S_1^*}{S_1} - \frac{S_1I_1N^*}{S_1^*I_1^*N} + \frac{I_1N^*}{I_1^*N}\right] + \beta_{12}\frac{S_1^*I_2^*}{N^*}\left[1 - \frac{S_1^*}{S_1} - \frac{S_1I_2N^*}{S_1^*I_2^*N} + \right.
\end{aligned}
$$

Then
$$
\begin{aligned}
L_1^{'} \leqslant\ & \beta_{11}\frac{S_1^*I_1^*}{N^*}\left[\frac{I_1N^*}{I_1^*N} - \log\left(\frac{I_1N^*}{I_1^*N}\right) - \frac{S_1I_1N^*}{S_1^*I_1^*N} + \log\left(\frac{S_1I_1N^*}{S_1^*I_1^*N}\right)\right] \\
&+\beta_{12}\frac{S_1^*I_2^*}{N^*}\left[\frac{I_2N^*}{I_2^*N} - \log\left(\frac{I_2N^*}{I_2^*N}\right) - \frac{S_1I_2N^*}{S_1^*I_2^*N} + \log\left(\frac{S_1I_2N^*}{S_1^*I_2^*N}\right)\right].
\end{aligned} \tag{4.23}
$$

We can also deduce in an analogous way:

$$
\begin{aligned}
L_2^{'} \leqslant\ & \beta_{22}\frac{S_2^*I_2^*}{N^*}\left[\frac{I_2N^*}{I_2^*N} - \log\left(\frac{I_2N^*}{I_2^*N}\right) - \frac{S_2I_2N^*}{S_2^*I_2^*N} + \log\left(\frac{S_2I_2N^*}{S_2^*I_2^*N}\right)\right] \\
&+\beta_{21}\frac{S_2^*I_1^*}{N^*}\left[\frac{I_1N^*}{I_1^*N} - \log\left(\frac{I_1N^*}{I_1^*N}\right) - \frac{S_2I_1N^*}{S_2^*I_1^*N} + \log\left(\frac{S_2I_1N^*}{S_2^*I_1^*N}\right)\right].
\end{aligned} \tag{4.24}
$$

We also have

$$
\begin{aligned}
L_3^{'} &= \left(1-\frac{I_1^*}{I_1}\right)\frac{\mathrm{d}I_1}{\mathrm{d}t} \\
&= \left(1-\frac{I_1^*}{I_1}\right)\left[\beta_{11}\frac{S_1I_1}{N}+\beta_{12}\frac{S_1I_2}{N}-(\mu+\gamma_1+d_1)I_1\right] \\
&= \left(1-\frac{I_1^*}{I_1}\right)\left[\beta_{11}\frac{S_1I_1}{N}+\beta_{12}\frac{S_1I_2}{N}-\beta_{11}\frac{S_1^*I_1}{N^*}+\beta_{12}\frac{S_1^*I_2^*I_1}{N^*I_1^*}\right] \\
&= \beta_{11}\frac{S_1^*I_1^*}{N^*}\left[\frac{S_1I_1N^*}{S_1^*I_1^*N}-\frac{S_1N^*}{S_1^*N}-\frac{I_1}{I_1^*}+1\right]+\beta_{12}\frac{S_1^*I_2^*}{N^*}\left[\frac{S_1I_2N^*}{S_1^*I_2^*N}-\frac{S_1I_1^*I_2N^*}{S_1^*I_1I_2^*N}-\frac{I_1}{I_1^*}+1\right], \\
L_3^{'} &\leqslant \beta_{11}\frac{S_1^*I_1^*}{N^*}\left[\frac{S_1I_1N^*}{S_1^*I_1^*N}-\log\left(\frac{S_1I_1N^*}{S_1^*I_1^*N}\right)-\frac{I_1}{I_1^*}+\log\left(\frac{I_1}{I_1^*}\right)\right] \\
&\quad +\beta_{12}\frac{S_1^*I_2^*}{N^*}\left[\frac{S_1I_2N^*}{S_1^*I_2^*N}-\log\left(\frac{S_1I_2N^*}{S_1^*I_2^*N}\right)-\frac{I_1}{I_1^*}+\log\left(\frac{I_1}{I_1^*}\right)\right].
\end{aligned}
\tag{4.25}
$$

Similarly, we obtain

$$
\begin{aligned}
L_4^{'} &\leqslant \beta_{22}\frac{S_2^*I_2^*}{N^*}\left[\frac{S_2I_2N^*}{S_2^*I_2^*N}-\log\left(\frac{S_2I_2N^*}{S_2^*I_2^*N}\right)-\frac{I_2}{I_2^*}+\log\left(\frac{I_2}{I_2^*}\right)\right] \\
&\quad +\beta_{21}\frac{S_2^*I_1^*}{N^*}\left[\frac{S_2I_1N^*}{S_2^*I_1^*N}-\log\left(\frac{S_2I_1N^*}{S_2^*I_1^*N}\right)-\frac{I_2}{I_2^*}+\log\left(\frac{I_2}{I_2^*}\right)\right].
\end{aligned}
\tag{4.26}
$$

Therefore, by adding (4.23), (4.24), (4.25) and (4.26), we deduce

$$\begin{aligned} L^{'} \leqslant & \left(-\frac{I_1 N^*}{I_1^* N} + \log\left(\frac{I_1 N^*}{I_1^* N}\right)\right)\left(-\beta_{11}\frac{S_1^* I_1^*}{N^*} - \beta_{21}\frac{S_2^* I_1^*}{N^*}\right) \\ & + \left(-\frac{I_2 N^*}{I_2^* N} + \log\left(\frac{I_2 N^*}{I_2^* N}\right)\right)\left(-\beta_{12}\frac{S_1^* I_2^*}{N^*} - \beta_{22}\frac{S_2^* I_2^*}{N^*}\right) \\ & + \left(-\frac{I_1}{I_1^*} + \log\left(\frac{I_1}{I_1^*}\right)\right)\left(\beta_{11}\frac{S_1^* I_1^*}{N^*} + \beta_{12}\frac{S_1^* I_2^*}{N^*}\right) \\ & + \left(-\frac{I_2}{I_2^*} + \log\left(\frac{I_2}{I_2^*}\right)\right)\left(\beta_{22}\frac{S_2^* I_2^*}{N^*} + \beta_{21}\frac{S_2^* I_1^*}{N^*}\right). \end{aligned}$$

Then $L^{'} \leqslant 0$, since $-z + \log(z) \leqslant -1, \ \forall z > 0.$

Since $\{Q^*\}$ is the only invariant subset in Ω where $L = 0$, therefore, by La Salle's invariance principle [66], Q^* is globally global asymptotic stable in Ω.

The epidemiological consequence of this theorem is that the disease persists as endemic in the host population as soon as $\mathcal{R}_0 > 1$.

4.2.4 Herd immunity threshold

Herd immunity is a form of indirect protection against infectious disease that occurs when a sufficient percentage of a population has become immune, either through previous infections or vaccination. This notably reduce the likelihood of infection for individuals lacking immunity, as immune individuals are less likely to contribute to disease transmission, thereby disrupting chains of infection, and slowing or halting disease spread. To compute the herd immunity threshold associated with system (3.3), we set the basic reproduction number, $\mathcal{R}_0$, to one and solve for $p = \dfrac{S_2^0}{N^0}$, which is the proportion of susceptible individuals that have been vaccinated at the DFE, Q^0 [35, 22]. Thus we have,

$$\begin{aligned} \mathcal{R}_0 = 1 \Longleftrightarrow & \left[2 - \mathcal{R}_{0,11} + (\mathcal{R}_{0,11} - \mathcal{R}_{0,22})p\right]^2 = \left[\mathcal{R}_{0,11} - (\mathcal{R}_{0,11} + \mathcal{R}_{0,11})p\right]^2 + 4p(1-p)\mathcal{R}_{0,12}\mathcal{R}_{0,21} \\ \Longleftrightarrow & \left[(\mathcal{R}_{0,11} - \mathcal{R}_{0,22})^2 - (\mathcal{R}_{0,11} + \mathcal{R}_{0,22})^2 + 4\mathcal{R}_{0,12}\mathcal{R}_{0,21}\right]p^2 + \left[2(2 - \mathcal{R}_{0,11})(\mathcal{R}_{0,11} - \mathcal{R}_{0,22})\right. \\ & \left. + 2\mathcal{R}_{0,11}(\mathcal{R}_{0,11} + \mathcal{R}_{0,22}) - 4\mathcal{R}_{0,12}\mathcal{R}_{0,21}\right]p + (2 - \mathcal{R}_{0,11})^2 - \mathcal{R}_{0,11}^2 = 0. \end{aligned}$$

Thus, solving $\mathcal{R}_0 = 1$ is equivalent to finding the roots of polynomial $Q(p)$ given by:

$$Q(p) = Ap^2 + Bp + C, \tag{4.27}$$

where $A = 4\mathcal{R}_{0,12}\mathcal{R}_{0,21} - 4\mathcal{R}_{0,11}\mathcal{R}_{0,22}$, $B = 4\mathcal{R}_{0,11}(1 + \mathcal{R}_{0,22}) - 4(\mathcal{R}_{0,22} + \mathcal{R}_{0,12}\mathcal{R}_{0,21})$ and $C = 4(1 - \mathcal{R}_{0,11})$.

Since negative thresholds are biologically meaningless in this context, the conditions under which $Q(p)$ has positive real roots are determined below. To achieve this, we perform a case-by-case analysis to determine the positive real zeros of Q.

Let $\Delta = B^2 - 4AC$ be the discriminant of the equation $Q(p) = 0$.

Case 1 Suppose $A = 0$. Then

$$p_c = -\frac{C}{B}$$

is the only real root of Q. In addition, $p_c > 0$ if and only if B and C have opposite signs and $B \neq 0$.

Case 2 Suppose $A \neq 0$ and $\Delta = 0$. Then

$$p_{c_0} = -\frac{B}{2A}$$

is the only real root of Q. Further $p_{c_0} > 0$ if and only if A and B have opposite signs.

Case 3 Suppose $A \neq 0$ and $\Delta > 0$. Then

$$p_{c_1} = \frac{-B - \sqrt{\Delta}}{2A} \text{ and } p_{c_2} = \frac{-B + \sqrt{\Delta}}{2A}$$

are the real roots of Q.

Moreover, if $A > 0$, then

$$\begin{cases} p_{c_1} > 0 \text{ if and only if } \sqrt{\Delta} < -B, \\ p_{c_2} > 0 \text{ if and only if } \sqrt{\Delta} > B. \end{cases}$$

Therefore, $Q(p)$ has two positive real roots if $A > 0$, $B < 0$, $C > 0$ and $\Delta > 0$. In addition, it has one positive real root if ($A > 0$, $B < 0$, $C < 0$ and $\Delta > 0$) or ($A > 0$, $B > 0$ and $C < 0$ and $\Delta > 0$).

Finally, if $A < 0$, then

$$\begin{cases} p_{c_1} > 0 \text{ if and only if } \sqrt{\Delta} > -B, \\ p_{c_2} > 0 \text{ if and only if } \sqrt{\Delta} < B. \end{cases}$$

Therefore, $Q(p)$ has two positive real roots if $A < 0$, $B > 0$, $C < 0$ and $\Delta > 0$. It has one positive real root if ($A < 0$, $B > 0$, $C > 0$ and $\Delta > 0$) or ($A < 0$, $B < 0$, $C > 0$ and $\Delta > 0$).

Theorems 10 and 11 can be combined to give the following result:

Corollary 1 *An imperfect vaccine can lead to the elimination of the disease if* $Q(p) > 0$ *(i.e.,* $\mathcal{R}_0 < 1$*). If* $Q(p) < 0$ *(i.e.,* $\mathcal{R}_0 > 1$*), then the disease persists in the population.*

Corollary 1 implies that using an imperfect vaccine can lead still to the elimination of the disease within the host population, provided the proportion of vaccinated individuals satisfies one of the following conditions:

1. $p > p_c$, if $A = 0$, $B > 0$ and $C < 0$;
2. $p \in [0, p_c[$, if $A = 0$, $B > 0$ and $C > 0$;
3. $p \neq p_{c_0}$, if $A > 0$, $\Delta = 0$ and $B < 0$;
4. $p \in [0, p_{c_1}[$ or $p > p_{c_2}$, if $A > 0$, $\Delta > 0$, $B < 0$ and $C > 0$;
5. $p > p_{c_1}$ or $p > p_{c_2}$, if ($A > 0$, $\Delta > 0$, $B < 0$ and $C < 0$) or ($A > 0$, $\Delta > 0$, $B > 0$ and $C < 0$);
6. $p \in]p_{c_2}, p_{c_1}[$, if $A < 0$, $\Delta > 0$, $B > 0$ and $C < 0$;
7. $p \in [0, p_{c_1}[$ or $p \in [0, p_{c_2}[$, if ($A < 0$, $\Delta > 0$, $B > 0$ and $C > 0$) or ($A < 0$, $\Delta > 0$, $B < 0$ and $C > 0$).

Conversely, the disease persists within the population if the proportion of vaccinated individuals satisfies one of the following conditions:

1. $p \in [0, p_c[$, if $A = 0$, $B > 0$ and $C < 0$;
2. $p > p_c$, if $A = 0$, $B > 0$ and $C > 0$;
3. $p \neq p_{c_0}$, if $A < 0$, $\Delta = 0$ and $B > 0$;

4. $p \in]p_{c_1}, p_{c_2}[$, if $A > 0$, $\Delta > 0$, $B < 0$ and $C > 0$;

5. $p \in [0, p_{c_1}[$ or $p \in [0, p_{c_2}[$, if ($A > 0$, $\Delta > 0$, $B < 0$ and $C < 0$) or ($A > 0$, $\Delta > 0$, $B > 0$ and $C < 0$);

6. $p \in [0, p_{c_2}[$ or $p > p_{c_1}$, if $A < 0$, $\Delta > 0$, $B > 0$ and $C < 0$;

7. $p > p_{c_1}$ or $p > p_{c_2}$, if ($A < 0$, $\Delta > 0$, $B > 0$ and $C > 0$) or ($A < 0$, $\Delta > 0$, $B < 0$ and $C > 0$).

We conclude the analytical portion of our study by stating that disease eradication depends on achieving a critical vaccination threshold represented by p_c. In some cases, a single critical threshold determines whether the basic reproduction number,$\mathcal{R}_0$, is less than one (disease elimination) or greater than one (persistence). In other cases, two critical proportions emerged, defining three potential dynamics: disease eradication when $\mathcal{R}_0 < 1$, persistence dynamics when $\mathcal{R}_0 > 1$, and persistence with or without epidemiological oscillations in the number of infected individuals. For scenarios involving two thresholds, the analytical results derived above do not provide predictions for the epidemiological dynamics or optimal vaccination proportions. To add on this, we supplement our analysis with some numerical simulations.

4.2.5 Numerical simulations

We refine the above analytical results by numerical simulations to assess the influence of the various model parameters and the impact of population turnover and trade-offs in vaccination efficiency on the epidemiological dynamics (i.e., the number of infected individuals and $\mathcal{R}_0$). To illustrate the behaviour of model (3.3), we use parameter values for the mortality rates, d_1 and d_2, and the recovery rates, γ_1, γ_2, measured for COVID-19 as an example of a highly transmissible disease (based on data from the United States [72]). In order to assess the influence of the various parameters of the model on the epidemiological outcome, we vary their values as described in Table 2. Note that we do not attempt here to precisely model the COVID-19 epidemic, but we focus on highly transmissible diseases relevant to public health. We indeed aim to go beyond applicability to a particular diseases (COVID-19) and to provide a generalised overview of the influence of vaccination trade-offs on epidemics.

4.2.5.1 Global sensitivity analysis

Uncertainty/sensitivity analyses are first used to determine which model input parameters have the greatest impact on the epidemiological outcome [75]. The sensitivity analysis of the model parameters is carried out to measure the correlation between the model parameters and 1) the total number of infected individuals ($I_1 + I_2$) and 2) the threshold parameter $\mathcal{R}_0$. The analysis is performed using the LHS technique and PRCCs [75]. In our analysis, 1,000 model simulations are performed by running the model for 200 time steps (equivalent to 200 days), and the number of infected is recorded at time points 50, 100 and 200. To perform the sensitivity analysis, each parameter has a parameter range defined by the maximum (the minimum), being 50% greater (less) than its baseline (values in Table 7, 8, 9, 10). We then divide each parameter range into 1000 equally large sub-intervals, and draw a value per parameter within that interval using a Uniform draw. By this means, we obtain a uniform distribution of 1000 parameter values for each parameter. The parameter space (or LHS matrix) has dimensions of length 11, with each dimension specifying an uncertain parameter vector of length 1,000. The base parameter values are chosen to define several scenarios of interest regarding the intensity of the turnover (weak and strong) and the efficiency of the vaccine (weak and strong). In PRCC analysis, the parameters with larger positive or negative PRCC values (> 0.5 or < -0.5) and with correspondingly small p-values (< 0.05) are deemed the most influential in determining the outcome of the model. A positive (negative) correlation coefficient corresponds to an increasing (decreasing) monotonic trend between the chosen response function and the parameter under consideration. The results of the PRCC analyses are found in Tables 7, 8, 9, 10 in Appendix 4.B .

Based on the results in Tables 7, 8, 9, 10, we provide, in Table 6, a summary of the parameters that significantly affect the number of infected individuals. Overall, it appears that the recruitment rate, θ, and the recovery rate of the infected who have not been vaccinated, γ_1, are the two main parameters driving the number of infected individuals. This suggests that an effective control strategy should aim to significantly limit the immigration of new hosts in the population (to decrease θ) and improve the treatment of infected individuals (to increase γ_1). We then proceed to a similar analysis with $\mathcal{R}_0$ and summarise the sensitivity analysis of the LHS and PRCC techniques in Figure 9. We find, perhaps unsurprisingly, that the proportion of new hosts vaccinated, p, is the most significant parameter explaining the change in $\mathcal{R}_0$, along with the transmission rate from unvaccinated infected to unvaccinated susceptibles, β_{11}, and the recovery rate of the infected who have

not been vaccinated, γ_1 (Table 6).

Table 6: Summary of the influence of parameters on the total numbers of infected at different time points.

Scenarios	**Total Infected: $I_1 + I_2$**		
	t = 50 days	**t = 100 days**	**t = 200**
Strong turnover and weak efficiency	$\theta(+), \beta_{11}(+), \mu(-), \gamma_1(-)$	$\theta(+), \beta_{11}(+), \mu(-), \gamma_1(-)$	$\theta(+), \beta_{11}(+),$
Strong turnover and strong efficiency	$\theta(+), \beta_{11}(+), \mu(-), \gamma_1(-)$	$\theta(+), \beta_{11}(+), \mu(-), \gamma_1(-)$	$\theta(+), \beta_{11}(+),$
Weak turnover and weak efficiency	$\beta_{11}(-), \beta_{21}(-), \beta_{22}(-)$	$\beta_{21}(-), \beta_{22}(-), \gamma_1(+), \gamma_2(+)$	$\theta(+), \beta_{21}(-$
Weak turnover and strong efficiency	$\theta(+), \beta_{11}(-), \beta_{21}(-), \gamma_1(-)$	$\beta_{21}(-), \mu(-), \gamma_1(+)$	$\theta(+), \beta_{21}(-),$

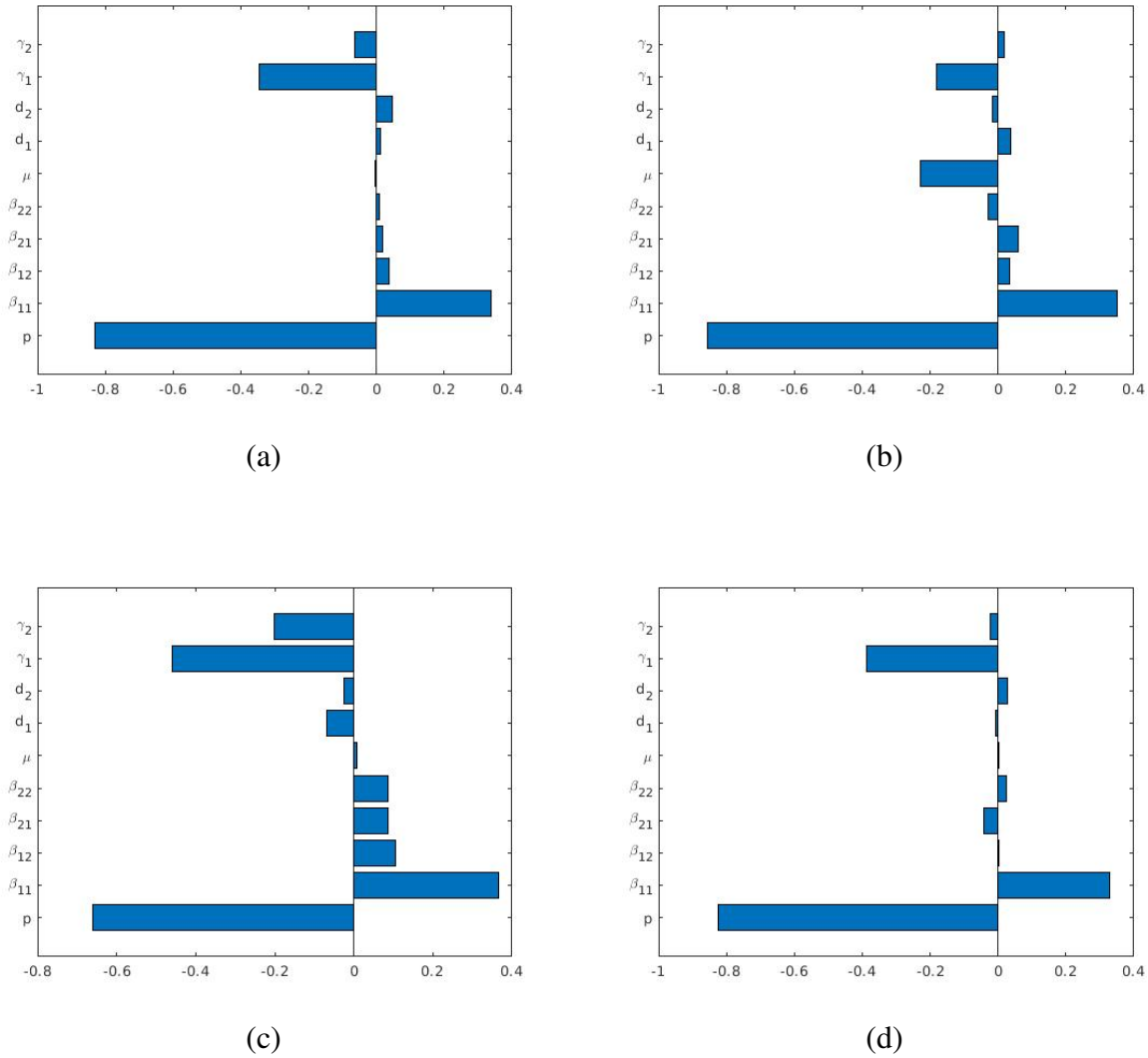

(a) (b)

(c) (d)

Figure 9: PRCCs describing the impact of model parameters on $\mathcal{R}_0$ of model (3.3) with respect to some scenarios: (**a**) strong turnover and weak efficiency, (**b**) strong turnover and strong efficiency, (**c**) weak turnover and weak efficiency and (**d**) weak turnover and strong efficiency. The range of parameters in (**a**), (**b**), (**c**) and (**d**) is the same as given in Tables 7, 8, 9 and 10.

4.2.5.2 Interplay between vaccine efficiency and population turnover

We now study the impact of population turnover and vaccine efficiency on the epidemiological dynamics. Specifically, we conduct numerical simulations to determine the vaccination coverage required to eradicate the disease in the community (as described Corollary 1), under two population turnover rates. To control the turnover, we fix θ/μ defining strong turnover scenario with $\theta = 1000$ and $\mu = 0.09$, and weak turnover scenario with $\theta = 10$ and $\mu = 0.0009$. In both cases, we assume that the vaccine can only reduce transmission. We examine two levels of vaccine efficiency: weak efficiency (50%) where $\beta_{21} = (1 - 0.5)\beta_{11}$ and $\beta_{22} = (1 - 0.5)\beta_{12}$ and strong efficiency (90%), where ($\beta_{21} = (1 - 0.9)\beta_{11}$ and $\beta_{22} = (1 - 0.9)\beta_{12}$.

Strong population turnover

The epidemiological dynamics in Figure 10(b) under strong turnover and weak vaccine efficiency ($\mathcal{R}_0 = 1.2352$) show that the dynamics reach the endemic disease equilibrium. Furthermore, if p takes a value between 0 and p_1 (with $p_1 \approx 0.696$), the basic reproduction number is greater than 1, but if p is between p_1 and 1, the basic reproduction number is less than 1 (as predicted in the analytical results in Corollary 1). Therefore, to eradicate the disease under strong population turnover and weak efficiency of the vaccine, a minimum vaccination rate is needed and is defined by p_1. Under strong turnover and strong efficiency (Figure 10(d), with $\mathcal{R}_0 = 0.9808$) the disease becomes extinct. Furthermore, if parameter p is between 0 and p_2 with $p_2 \approx 0.489$, the basic reproduction number is greater than 1, while for p between p_2 and 1, the basic reproduction number is less than 1. Therefore, to eradicate the disease in this context of strong turnover and strong efficiency of the vaccine, there is a need to vaccinate more than 48.9% of the new host individuals.

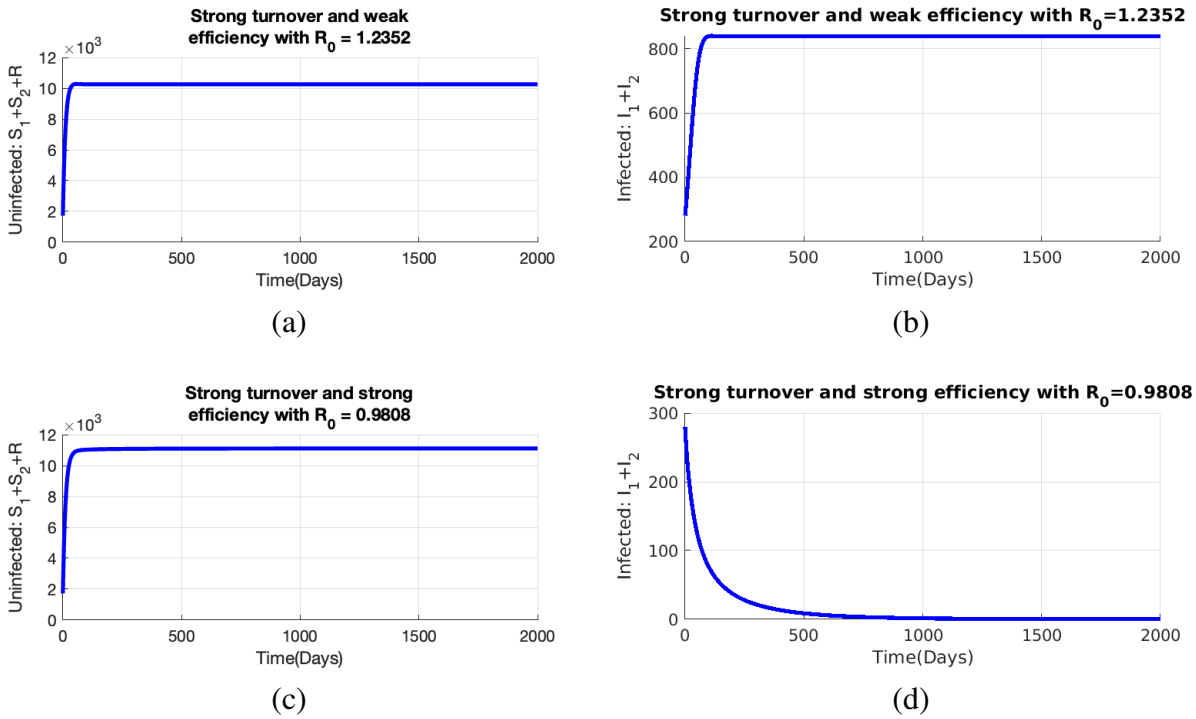

Figure 10: Epidemiological dynamics with initial conditions $S_1(0) = 1000$, $S_2(0) = 700$, $I_1(0) = 200$, $I_2(0) = 80$ and $R(0) = 20$, for various scenarios assuming the parameters $\beta_{11} = 0.35$, $\beta_{12} = 0.28$, $p = 0.5$ and strong population turnover ($\theta = 1000$, $\mu = 0.09$). We present, under weak vaccine efficiency ($\beta_{21} = 0.175, \beta_{22} = 0.14$), the number of (**a**) uninfected and (**b**) infected individuals. We present, under strong vaccine efficiency ($\beta_{21} = 0.035, \beta_{22} = 0.028$) the number of (**c**) uninfected and (**d**) infected individuals. Others parameter values are as in Table 2.

Weak population turnover

To illustrate a weak population turnover, we consider the values $\theta = 10$ and $\mu = 0.0009$, noting that the ratio of θ/μ is the same as for the strong turnover investigated above. Under weak turnover, the epidemiological dynamics exhibit damped oscillations (recurring outbreaks) before stabilising at the endemic state with disease persistence (Figure 11(b) with $\mathcal{R}_0 = 2.2551$, Figure 11(d) with $\mathcal{R}_0 = 1.8276$). These oscillations are due to the fact that individuals migrate rapidly in the recovered compartment, and a new outbreak only occurs when a sufficient number of susceptible individuals are available for new recruitment into the population and recovered individuals lose their immunity (so-called waning immunity). This phenomenon was also described in [22, 51, 98, 101], and the effect of turnover and waning immunity is specifically described in [22, 98].

With respect to the control of the disease, under weak vaccine efficiency, p can take any value between 0 and 1, and the basic reproduction number is always greater than 1 (Figure 11(b) with $\mathcal{R}_0 = 2.2551$). In contrast, when vaccine efficiency is strong, three

cases occur, Figure 11(d) (with $\mathcal{R}_0 = 1.8276$). When p has a value between 0 and p_3, with $p_3 \approx 0.753$, the basic reproduction number is greater than 1, and we observe a damped periodicity of the number of infected individuals converging towards a stable endemic state. When p takes a value between p_3 and p_4 (with $p_4 \approx 0.756$), the basic reproduction number, $\mathcal{R}_0$, is greater than 1, but no oscillations are observed. For $p \in [p_4, 1]$, the basic reproduction number, $\mathcal{R}_0$, is less than 1, and the disease becomes extinct. Note that between p_3 and p_4, the behaviour can change very finely, but the resolution of our simulations does not allow us to decide on a very precise bound when oscillations occur or not. Therefore, to eradicate the disease in this context of weak population turnover and strong efficiency of the vaccine, high vaccination coverage (more than 75.6% of the new host individuals) is needed. Our results extend those in [87], showing that it is feasible to control the disease by a weakly efficient vaccine acting on disease transmission but that the required vaccination coverage depends on the population turnover. We note that the persistence of an endemic equilibrium is predicted by the condition $\mathcal{R}_0 > 1$, even if damped oscillations in the number of infected individuals occur. In other words, while the population turnover does not factor directly in the analytical expression of $\mathcal{R}_0$, it enters only indirectly by affecting the proportion of susceptible individuals available (Equation 4.21). The simulation results provide examples of the analytical expressions obtained in eq. 4.27 following Corollary 1.

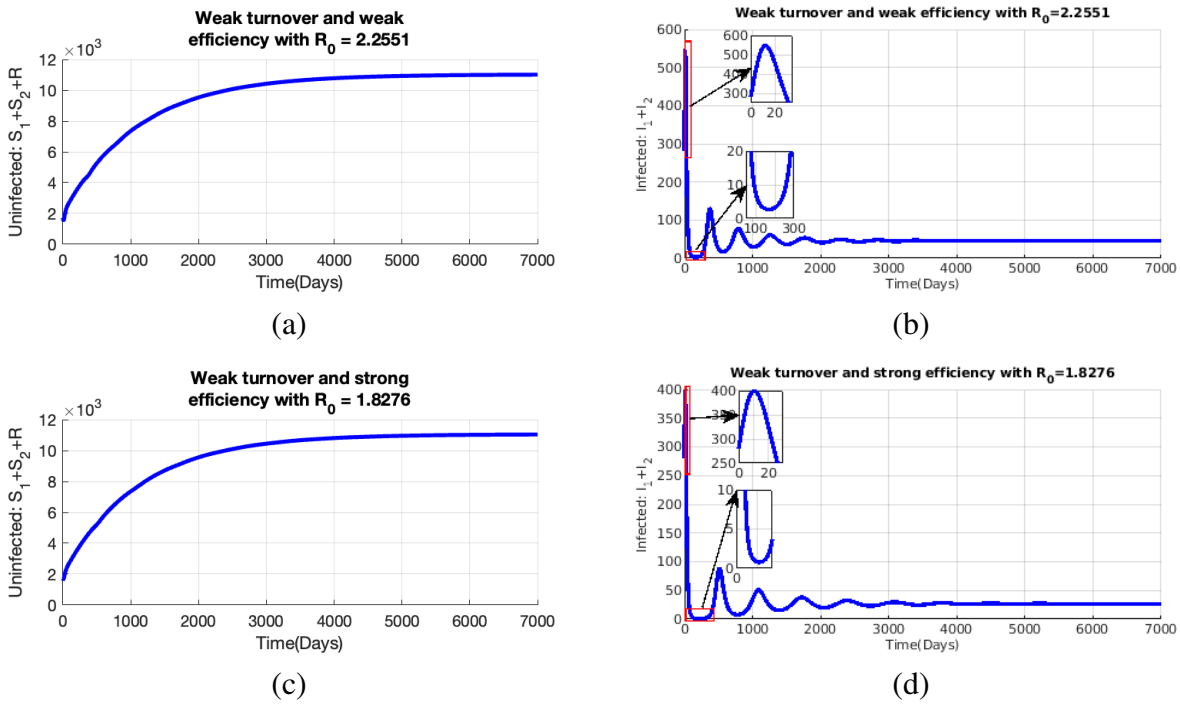

Figure 11: Simulation of model (3.3) at the initial conditions $S_1(0) = 1000$, $S_2(0) = 700$, $I_1(0) = 200$, $I_2(0) = 80$ and $R(0) = 20$, when $\theta = 10$, $\beta_{11} = 0.35$, $\beta_{12} = 0.28$, $\beta_{21} = 0.175, \beta_{22} = 0.14$, $\mu = 0.0009$, $p = 0.5$, (**a**) uninfected individuals with a weak turnover and weak efficiency scenario and (**b**) infected individuals with a weak turnover and weak efficiency scenario. When $\theta = 10$, $\beta_{11} = 0.35$, $\beta_{12} = 0.28$, $\beta_{21} = 0.035, \beta_{22} = 0.028$, $\mu = 0.0009$ and $p = 0.5$, (**c**) uninfected individuals with a weak turnover and strong efficiency scenario and (**d**) infected individuals with a weak turnover and strong efficiency scenario. Others parameter values are as in Table 2.

4.2.5.3 Interplay between types of vaccines and population turnover

We now assume that a vaccine can act on two ways: namely blocking transmission and/or favouring the recovery in infected individuals. We investigate the effect of these vaccines on the disease dynamics based on the population turnover. Specifically, we modify model (3.3) to account for the impact of the vaccine on the probability of infection and the recovery rate. This is achieved by simply rescaling the parameters as follows:

$$\beta_{21} = (1-\varepsilon)\beta_{11}, \beta_{22} = (1-\varepsilon)\beta_{12}, \text{ and } \gamma_1 = (1-\nu)\gamma_2, \tag{4.28}$$

where $0 \leq \varepsilon \leq 1$ represents the effect of the vaccine on disease transmission, and $0 \leq \nu \leq 1$ represents its effect on recovery. Substituting the rescaled expressions into model (3.3) gives the following new expression of the basic reproduction number

$$\mathcal{R}_0 = \frac{1}{2}\left[(1-p)\mathcal{R}_{0,11} + p\mathcal{R}_{0,22} + \sqrt{\left((1-p)\mathcal{R}_{0,11} - p\mathcal{R}_{0,22}\right)^2 + 4p(1-p)\mathcal{R}_{0,12}\mathcal{R}_{0,21}}\right], \tag{4.29}$$

with $\mathcal{R}_{0,11} = \dfrac{\beta_{11}}{\mu + (1-\nu)\gamma_2 + d_1}$, $\mathcal{R}_{0,12} = \dfrac{\beta_{12}}{\mu + (1-\nu)\gamma_2 + d_1}$, $\mathcal{R}_{0,21} = \dfrac{(1-\varepsilon)\beta_{11}}{\mu + \gamma_2 + d_2}$ and $\mathcal{R}_{0,22} = \dfrac{(1-\varepsilon)\beta_{12}}{\mu + \gamma_2 + d_2}$. Simulations are carried out to assess the interplay of the type of vaccine and the population turnover.

Under a strong population turnover, as expected, the reproduction number decreases as vaccine coverage and efficiency in reducing transmission increase (Figure 12(a)). In particular, if the vaccine is designed to reduce the transmission by 80% (i.e., $\varepsilon = 0.8$), the disease can be eradicated in the host population (i.e., $\mathcal{R}_0 < 1$) if at least 70% of the population is vaccinated (Figure 12(a)). On the other hand, when the vaccine is designed to primary enhance recovery, the reproduction number decreases as vaccine coverage increases and as vaccines efficiency in promoting recovery decreases (Figure 12(b)). With a vaccine that imposed recovery by 20% (i.e., $\nu = 0.2$), the eradication of the disease can be achieved ($\mathcal{R}_0 < 1$) if at least 68% of the population is vaccinated (Figure 12(b)). In Figure 12(c), we present the combined effect of the vaccine's efficiency in both reducing transmission and enhancing recovery on the reproduction number, with $p = 0.5$. In this situation, disease eradication is possible ($\mathcal{R}_0 < 1$) if the vaccine achieves at least 85% efficiency in reducing infection (and thus transmission) and at least 20% efficiency in enhancing recovery for the given vaccination coverage of $p = 0.5$.

These figures represent subsets of the general results presented in Figure 14, in which $\mathcal{R}_0$ is a function of ε, ν and p. The use of a vaccine with a combined efficiency (decreasing transmission and favouring recovery) can be associated with vaccination coverage in order to achieve the elimination of the disease. For example, with vaccination coverage of 20% ($p = 0.2$), it is not possible to eliminate the disease no matter the combined efficiency of the vaccine (Figure 15), while at 80% coverage ($p = 0.8$), there are several combinations of vaccine types, decreasing transmission and favouring recovery, that can promote disease control (Figure 15).

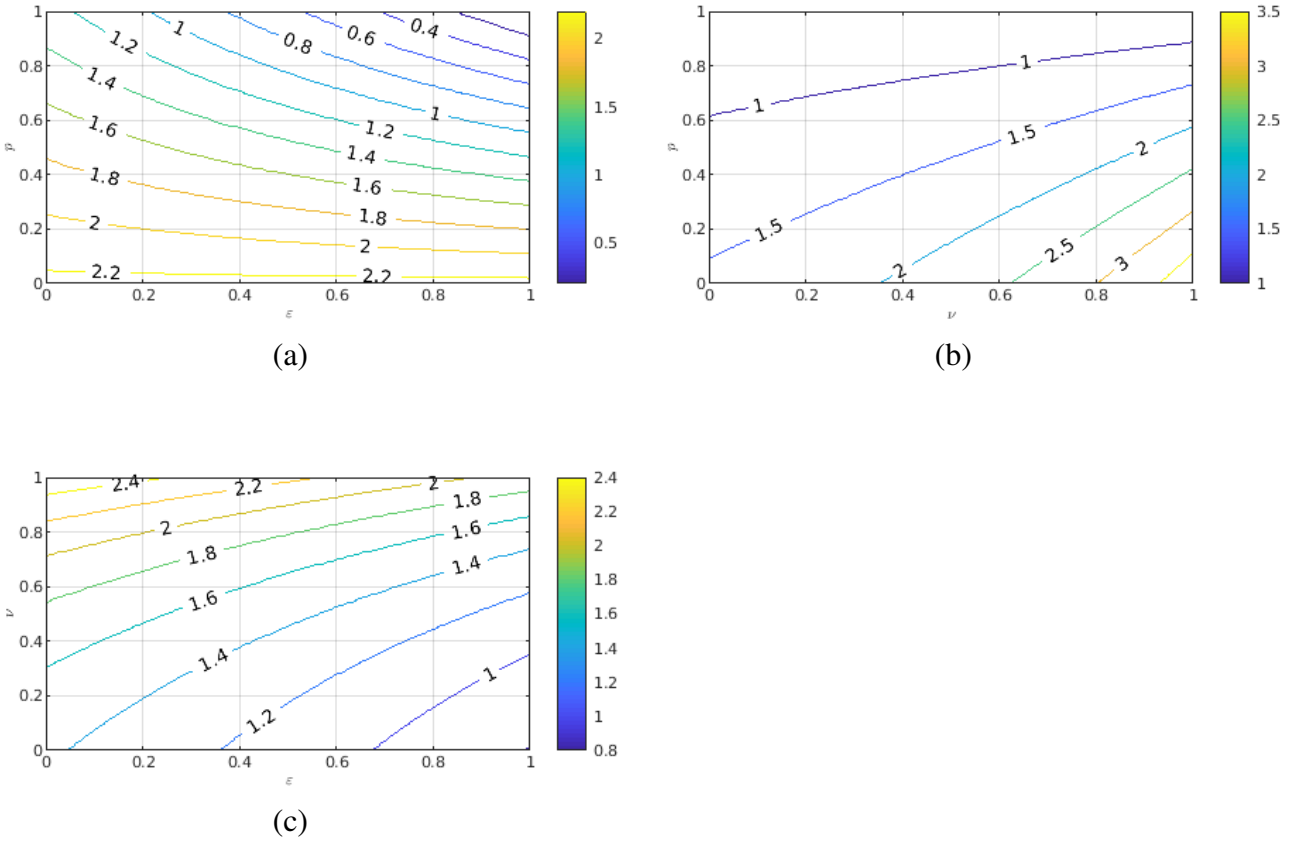

Figure 12: Contour plots of the basic reproduction number ($\mathcal{R}_0$) of model (3.3) with a strong population turnover as a function of (**a**) vaccination coverage, p, and vaccine efficiency on disease transmission, ε (with fixed $\nu = 0.5$); (**b**) vaccination coverage, p, and vaccine efficiency on recovery, ν (with fixed $\varepsilon = 0.5$); and (**c**) vaccine efficiency on recovery, ν, and vaccine efficiency on transmission, ε (with fixed $p = 0.5$). The parameters are $\theta = 1000$, $\beta_{11} = 0.35$, $\beta_{12} = 0.28$, $\beta_{21} = 0.175$, $\beta_{22} = 0.14$, $\mu = 0.09$, $d_1 = 0.0008$, $d_2 = 0.0001$, $\gamma_1 = 0.065$ and $\gamma_2 = 0.13$.

The above results dramatically change under a weak population turnover. As expected, the value of the reproduction number decreases as coverage and efficiency of the vaccine on the transmission increase (Figure 16(a)), but higher vaccination coverage is needed compared to the strong population turnover to achieve $\mathcal{R}_0 < 1$. Moreover, it is not possible to eradicate the disease if 1) the vaccine is only efficient in enhancing recovery, no matter the vaccination coverage (Figure 16(b)), or 2) if the efficiency of the vaccine is combined, but vaccination coverage is $p = 0.5$ (Figure 17). The general results of $\mathcal{R}_0$ as a function of ε, ν and p demonstrate that under weak population turnover, disease eradication requires a very strong efficiency of the vaccine and high coverage (Figure 18).

4.2.5.4 Interplay between vaccine efficiency trade-off and population turnover

Thus far, we assumed that the efficiency parameters of the vaccine can be independently selected. We now study, the epidemiological dynamics assuming that there exists a realistic trade-off between the vaccine's efficiency in reducing transmission and its efficiency in enhancing recovery. We consider three possible trade-off curves: convex ($\nu = \varepsilon^2$), concave ($\nu = \sqrt{\varepsilon}$) or linear ($\nu = \varepsilon$). Under a strong population turnover and assuming a vaccine of at least 60% efficiency, disease eradication ($\mathcal{R}_0 < 1$) can be achieved with the following vaccination coverage:

(i) At least 65% coverage under a convex trade-off (Figure 13(a))

(ii) At least 80% coverage under a concave trade-off (Figure 13(b))

(iii) At least 75% under a linear trade-off (Figure 13(c)).

Imposing vaccine trade-off, therefore, affects the shape of the $\mathcal{R}_0$ curves in Figure 13(a)–(c) compared to Figure 12(a)–(b), and may be important to predict the minimum vaccination coverage to be achieved. However, under a weak population turnover, the disease persists no matter the vaccination coverage and whatever trade-off are assumed in the vaccine (Figure 19(a)–(c)).

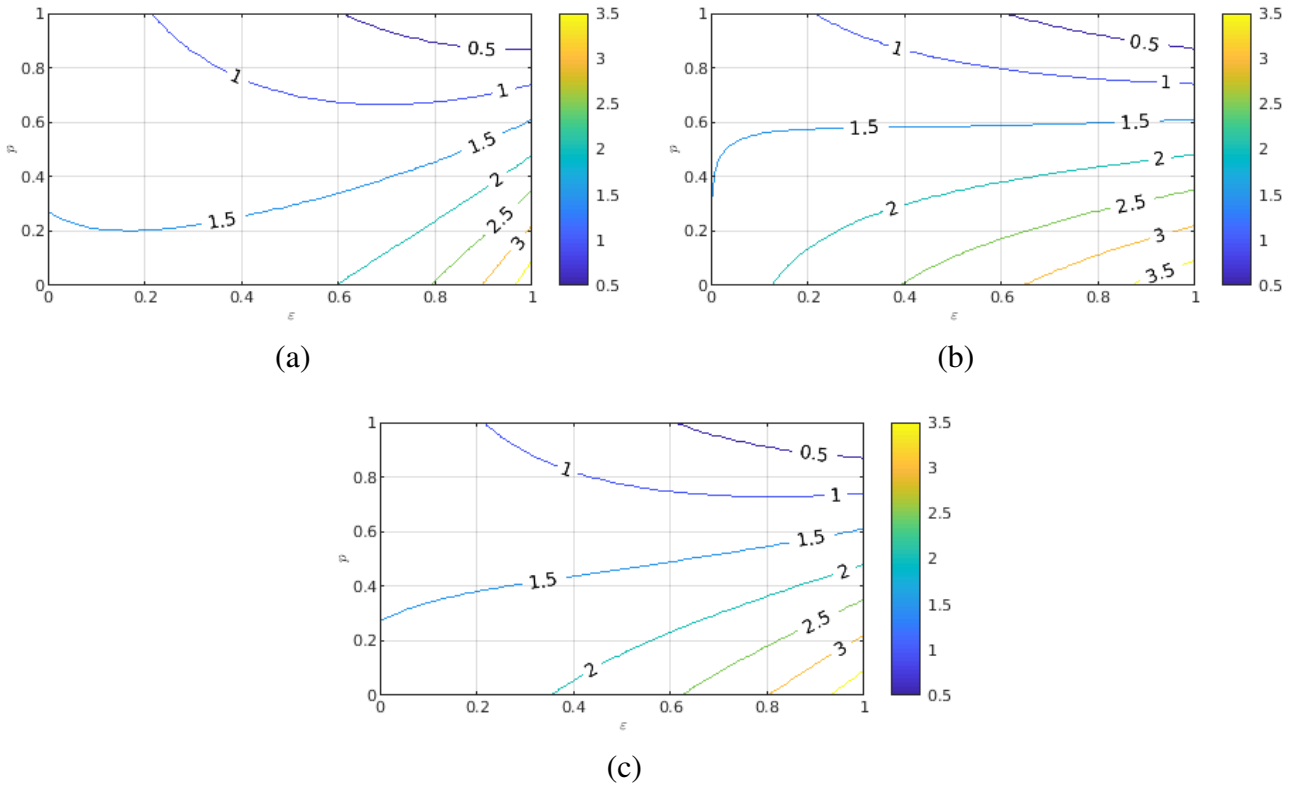

Figure 13: Contour plots of the basic reproduction number ($\mathcal{R}_0$) of model (3.3) with a strong population turnover as a function of vaccine coverage, p, and vaccine efficiency on the transmission, ε when: (**a**) $\nu = \varepsilon^2$ (convex relationship); (**b**) $\nu = \sqrt{\varepsilon}$ (concave relationship); (**c**)$\nu = \varepsilon$ (linear relationship). The parameters are $\theta = 1000$, $\beta_{11} = 0.35$, $\beta_{12} = 0.28$, $\beta_{21} = 0.175$, $\beta_{22} = 0.14$, $\mu = 0.09$, $d_1 = 0.0008$, $d_2 = 0.0001$, $\gamma_1 = 0.065$ and $\gamma_2 = 0.13$.

4.2.6 Summary

In this session, we used mathematical modelling approaches (analysis and numerical simulations) to assess the potential population level impact of using different types of imperfect vaccines to control the burden of a disease in a community. In the first part, we provide a theoretical analysis of the model, including the basic reproduction number $\mathcal{R}_0$ and conditions for the stability of the equilibria. We derive the condition to be satisfied regarding the proportion of vaccinated individuals at a steady state in order to attain herd immunity. We express this condition as the critical coverage to be achieved for $\mathcal{R}_0 < 1$. Our results show that we can use a weak imperfect vaccine designed to reduce transmission to control a disease within a community of strong level of population turnover. And we must undertake a mass vaccination campaign and using a high efficiency vaccine (only targeting transmission) to eradicate a disease within a community of weak level of population turnover. Finally we recommend a vaccine with convex trade-off between the efficiency to

reduce transmission and to enhance recovery along with a high vaccination coverage under a strong migration of hosts to control an epidemic.

4.A Proof of Theorem 3.4

Proof : The system (3.3) can be written as:

$$\begin{aligned} \frac{\mathrm{d}a}{\mathrm{d}t} &= (F-V)a - f(a,b), \\ \frac{\mathrm{d}b}{\mathrm{d}t} &= g(a,b), \end{aligned} \tag{4.30}$$

where $a = (I_1, I_2)^T$ is the vector representing the infected classes, $b = (S_1, S_2, R)^T$ is the vector representing the uninfected classes, the matrices F and V are given as in Equation (4.20) and

$$f(a,b) = \begin{bmatrix} \beta_{11}\left(\frac{S_1^0}{N^0} - \frac{S_1}{N}\right)I_1 + \beta_{12}\left(\frac{S_1^0}{N^0} - \frac{S_1}{N}\right)I_2 \\ \\ \beta_{21}\left(\frac{S_2^0}{N^0} - \frac{S_2}{N}\right)I_1 + \beta_{22}\left(\frac{S_2^0}{N^0} - \frac{S_2}{N}\right)I_2 \end{bmatrix} \text{ and } g(a,b) = \begin{bmatrix} \theta(1-p) + \lambda_1 S_1 - \mu S_1 \\ \\ \theta p + \lambda_2 S_2 - \mu S_2 \\ \\ \gamma_1 I_1 + \gamma_2 I_2 - \mu R \end{bmatrix}.$$

Then,

$$V^{-1}F = \begin{bmatrix} \frac{\beta_{11}S_1^0}{N^0(\mu+\gamma_1+d_1)} & \frac{\beta_{12}S_1^0}{N^0(\mu+\gamma_1+d_1)} \\ \\ \frac{\beta_{21}S_2^0}{N^0(\mu+\gamma_2+d_2)} & \frac{\beta_{22}S_2^0}{N^0(\mu+\gamma_2+d_2)} \end{bmatrix},$$

and the left eigenvector of $V^{-1}F$, (ω_1, ω_2) associated with the eigenvalue $\mathcal{R}_0$ is given by:

$\omega_1 = 1$ and $\omega_2 = \dfrac{N^0(\mu+\gamma_2+d_2)}{\beta_{21}S_2^0}\left(\mathcal{R}_0 - \dfrac{\beta_{11}S_1^0}{N^0(\mu+\gamma_1+d_1)}\right)$ since $(\omega_1, \omega_2)V^{-1}F = \mathcal{R}_0(\omega_1, \omega_2)$.

Let us consider the following Lyapunov function:

$$\begin{aligned} Q =&(\omega_1, \omega_2)V^{-1}(I_1, I_2)^T \\ =&\frac{I_1}{\mu + \gamma_1 + d_1} + \left(\mathcal{R}_0 - \frac{\beta_{11}S_1^0}{N^0(\mu + \gamma_1 + d_1)}\right)\frac{N^0 I_2}{\beta_{21}S_2^0}. \end{aligned} \tag{4.31}$$

Then the derivative of Q with respect to t yields,

$$Q^{'} = (\mathcal{R}_0 - 1)(\omega_1, \omega_2)^T a - (\omega_1, \omega_2)^T V^{-1} f(a, b).$$

Since $(\omega_1, \omega_2) \geqslant 0$, $V^{-1} \geqslant 0$ and $f(a, b) \geqslant 0$ in Ω, then $(\omega_1, \omega_2)^T V^{-1} f(a, b) \geqslant 0$. Therefore, $Q^{'} \leqslant 0$ in Ω if $\mathcal{R}_0 \leqslant 1$ and Q is a Lyapunov function for the system (1). By LaSalle's invariance principle [65, 66], Q^0 is GAS in Ω.

If $\mathcal{R}_0 > 1$, then $Q^{'} = (\mathcal{R}_0 - 1)(\omega_1, \omega_2)^T a > 0$ provided that $a > 0$ and $b = (S_1^0, S_2^0, 0)$. By continuity, $Q^{'} > 0$ in the neighborhood of Q^0. Solutions in positive cone sufficiently close to Q^0 move away from Q^0, implying that Q^0 is unstable. Thus, the model system (1) is uniformly persistent [43, 69]. Uniform persistence and the positively invariance of Ω imply the existence of an endemic equilibrium.

4.B Tables

Table 7: PRCC of model's parameters at time t (days) with strong turnover and weak efficiency of vaccine. The values $\theta = 1000$, $\mu = 0.09$, $\beta_{11} = 0.35$, $\beta_{12} = 0.28$, $\beta_{21} = 0.175$, $\beta_{22} = 0.14$ are used as baseline.

Parameters	Range of parameters			Total Infected: $I_1 + I_2$		
	Min	Baseline	Max	$t = 50$ days	$t = 100$ days	$t = 200$ days
θ	500	1000	1500	0.71395**	0.78511**	0.76166***
p	0	0.5	1	0.020314	0.0029584	0.028397
β_{11}	0.175	0.35	0.525	0.85757***	0.8731***	0.87175***
β_{12}	0.14	0.28	0.42	0.0047432	0.027724	−0.030496
β_{21}	0.0875	0.175	0.2625	0.0090246	−0.012341	0.026579
β_{22}	0.07	0.14	0.21	−0.047262	0.02905	−0.037461
μ	0.045	0.09	0.135	−0.7695**	−0.80652***	−0.79222**
d_1	0.0004	0.0008	0.0012	−0.012188	0.03368	−0.046922
d_2	0.00005	0.0001	0.00015	−0.025215	0.016188	−0.043869
γ_1	0.05	0.1	0.15	−0.78315**	−0.84015***	−0.82903***
γ_2	0.0625	0.13	0.1925	0.010702	0.05007	0.012449

: PRCC values: 0.7 to 0.79 or −0.7 to −0.79; *: PRCC values: 0.8 to 0.99 or −0.8 to −0.99

Table 8: PRCC of model's parameters at time t days with strong turnover and strong efficiency of vaccine, when $\theta = 1000$, $\mu = 0.09$, $\beta_{11} = 0.35$, $\beta_{12} = 0.28$, $\beta_{21} = 0.035$, $\beta_{22} = 0.028$ as baseline.

Parameters	Range of parameters			Total Infected: $I_1 + I_2$		
	Min	Baseline	Max	$t = 50$ days	$t = 100$ days	$t = 200$ days
θ	500	1000	1500	0.7381**	0.76387**	0.78486**
p	0	0.5	1	0.003905	0.0037356	0.027257
β_{11}	0.175	0.35	0.525	0.86469***	0.87427***	0.88181***
β_{12}	0.14	0.28	0.42	0.0079816	0.033516	0.030158
β_{21}	0.0175	0.035	0.0525	0.0012134	0.018087	−0.00058438
β_{22}	0.014	0.028	0.042	0.021841	−0.0038364	0.018881
μ	0.045	0.09	0.135	−0.78849**	−0.80304***	−0.81535***
d_1	0.0004	0.0008	0.0012	−0.054627	0.066816	0.019678
d_2	0.00005	0.0001	0.00015	−0.033227	−0.021472	−0.028882
γ_1	0.05	0.1	0.15	−0.80324***	−0.83346***	−0.84421***
γ_2	0.0625	0.13	0.1925	−0.0099732	−0.02272	0.0020891

: PRCC values: 0.7 to 0.79 or −0.7 to −0.79; *: PRCC values: 0.8 to 0.99 or −0.8 to −0.99

Table 9: PRCC of model's parameters at time t days with weak turnover and weak efficiency of vaccine, when $\theta = 10$, $\mu = 0.0009$, $\beta_{11} = 0.35$, $\beta_{12} = 0.28$, $\beta_{21} = 0.175$, $\beta_{22} = 0.14$ as baseline.

Parameters	Range of parameters			Total Infected: $I_1 + I_2$		
	Min	Baseline	Max	t = 50 days	t = 100 days	t = 200 days
θ	5	10	15	0.45737	0.37556	0.51163*
p	0	0.5	1	−0.041574	0.028378	0.030938
β_{11}	0.175	0.35	0.525	−0.63334*	−0.23892	0.355
β_{12}	0.14	0.28	0.42	−0.23979	−0.24053	−0.13989
β_{21}	0.0875	0.175	0.2625	−0.90072***	−0.90502***	−0.80837***
β_{22}	0.07	0.14	0.21	−0.52059*	−0.50519*	−0.30843
μ	0.00045	0.0009	0.00135	−0.031697	−0.18722	−0.15951
d_1	0.0004	0.0008	0.0012	0.012078	−0.038623	0.01511
d_2	0.00005	0.0001	0.00015	0.028409	0.0088495	0.047733
γ_1	0.05	0.1	0.15	−0.12428	0.81303***	0.59284*
γ_2	0.0625	0.13	0.1925	0.48726	0.62754*	0.48082

*: PRCC values: 0.5 to 0.69 or −0.5 to −0.69; ***: PRCC values: 0.8 to 0.99 or −0.8 to −0.99

Table 10: PRCC of model's parameters at time t days with weak turnover and strong efficiency of vaccine, when $\theta = 10$, $\mu = 0.0009$, $\beta_{11} = 0.35$, $\beta_{12} = 0.28$, $\beta_{21} = 0.035$, $\beta_{22} = 0.028$ as baseline.

Parameters	Range of parameters			Total Infected: $I_1 + I_2$		
	Min	Baseline	Max	$t = 50$ days	$t = 100$ days	$t = 200$ days
θ	5	10	15	0.5751*	0.48818	0.61256*
p	0	0.5	1	0.052835	0.014154	0.050557
β_{11}	0.175	0.35	0.525	−0.70943**	−0.47854	0.44458
β_{12}	0.14	0.28	0.42	−0.16357	−0.16371	−0.03405
β_{21}	0.0175	0.035	0.0525	−0.84854***	−0.90973***	−0.85731***
β_{22}	0.014	0.028	0.042	−0.17909	−0.22613	−0.14446
μ	0.00045	0.0009	0.00135	−0.40329	−0.61646*	−0.72754**
d_1	0.0004	0.0008	0.0012	−0.072168	0.04039	−0.040258
d_2	0.00005	0.0001	0.00015	0.019586	−0.053637	−0.030518
γ_1	0.05	0.1	0.15	−0.81298***	0.76378**	0.69479*
γ_2	0.0625	0.13	0.1925	0.20028	0.31528	0.2891

*: PRCC values: 0.5 to 0.69 or −0.5 to −0.69; **: PRCC values: 0.7 to 0.79 or −0.7 to −0.79; ***: PRCC values: 0.8 to 0.99 or −0.8 to −0.99

4.C Figures

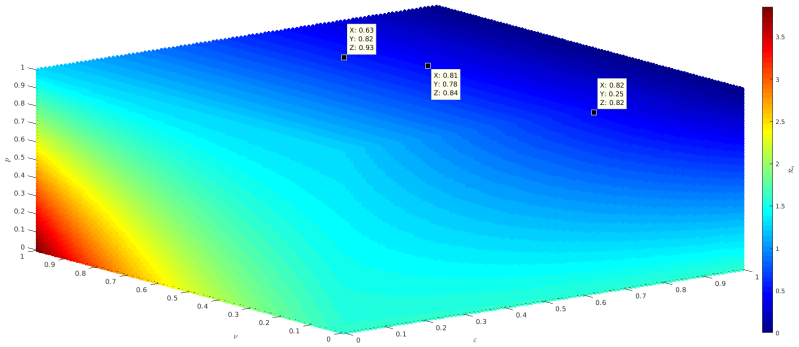

Figure 14: Scatter plots of $\mathcal{R}_0$ with a strong turnover as a function of ε, ν and p .The parameters are $\theta = 1000$, $\beta_{11} = 0.35$, $\beta_{12} = 0.28$, $\beta_{21} = 0.175$, $\beta_{22} = 0.14$, $\mu = 0.09$, $d_1 = 0.0008$, $d_2 = 0.0001$, $\gamma_1 = 0.065$, $\gamma_2 = 0.13$.

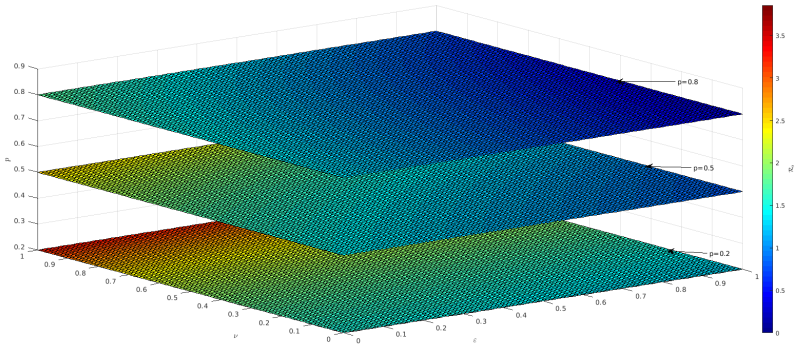

Figure 15: Slice planes of $\mathcal{R}_0$ orthogonal to the p-axis at the values 0.2, 0.5, 0.8 with a strong turnover. The parameters are $\theta = 1000$, $\beta_{11} = 0.35$, $\beta_{12} = 0.28$, $\beta_{21} = 0.175$, $\beta_{22} = 0.14$, $\mu = 0.09$, $d_1 = 0.0008$, $d_2 = 0.0001$, $\gamma_1 = 0.065$, $\gamma_2 = 0.13$.

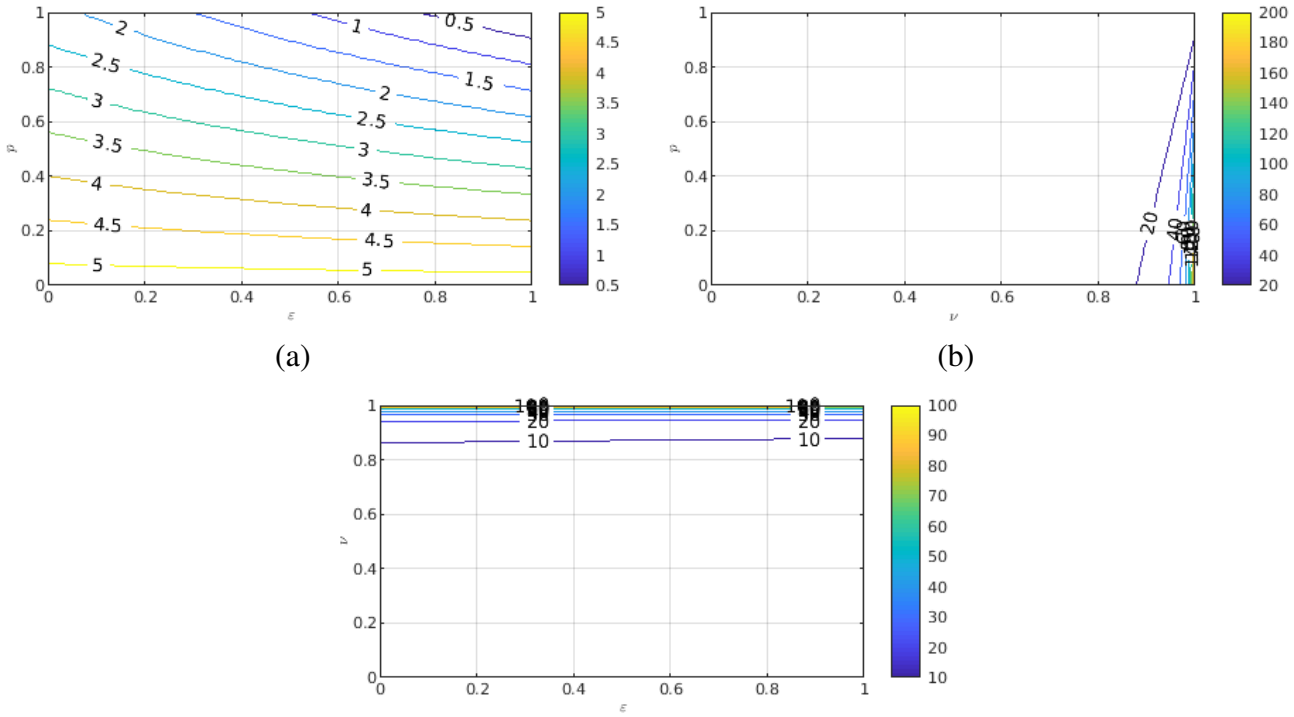

(a)

(b)

(c)

Figure 16: Contour plots of the basic reproduction number ($\mathcal{R}_0$) of the model (3.3) with a weak turnover as a function of: (a) vaccine coverage, p, and vaccine efficiency on the transmission, ε (fixed $\nu = 0.5$); (b) vaccine coverage, p, and vaccine efficiency on the ability to enhance recovery, ν (fixed $\varepsilon = 0.5$); (c) vaccine efficiency on the ability of being recovered, ν, and vaccine efficiency on the transmission, ε (fixed $p = 0.5$). The parameters are $\theta = 10$, $\beta_{11} = 0.35$, $\beta_{12} = 0.28$, $\beta_{21} = 0.175$, $\beta_{22} = 0.14$, $\mu = 0.0009$, $d_1 = 0.0008$, $d_2 = 0.0001$, $\gamma_1 = 0.065$, $\gamma_2 = 0.13$

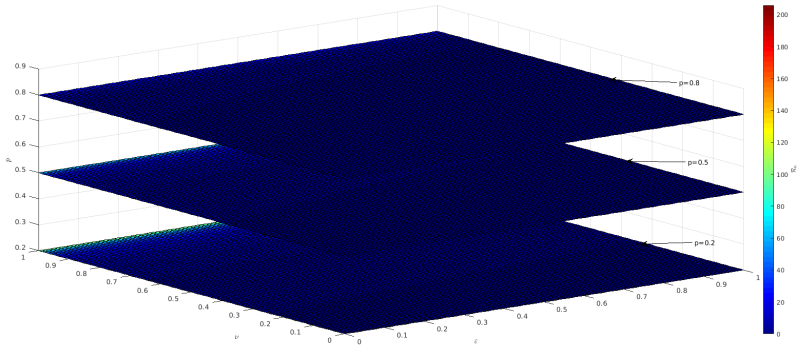

Figure 17: Slice planes of $\mathcal{R}_0$ orthogonal to the p-axis at the values 0.2, 0.5, 0.8 with a weak turnover. The parameters are $\theta = 10$, $\beta_{11} = 0.35$, $\beta_{12} = 0.28$, $\beta_{21} = 0.175$, $\beta_{22} = 0.14$, $\mu = 0.0009$, $d_1 = 0.0008$, $d_2 = 0.0001$, $\gamma_1 = 0.065$, $\gamma_2 = 0.13$.

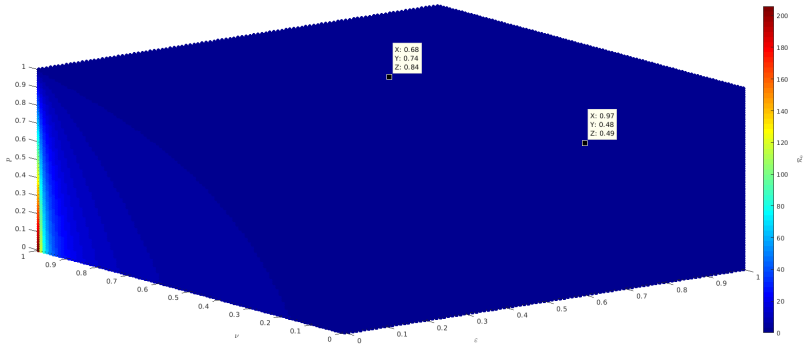

Figure 18: Scatter plots of $\mathcal{R}_0$ with a weak turnover as a function of ε, ν and p .The parameters are $\theta = 10$, $\beta_{11} = 0.35$, $\beta_{12} = 0.28$, $\beta_{21} = 0.175$, $\beta_{22} = 0.14$, $\mu = 0.0009$, $d_1 = 0.0008$, $d_2 = 0.0001$, $\gamma_1 = 0.065$, $\gamma_2 = 0.13$.

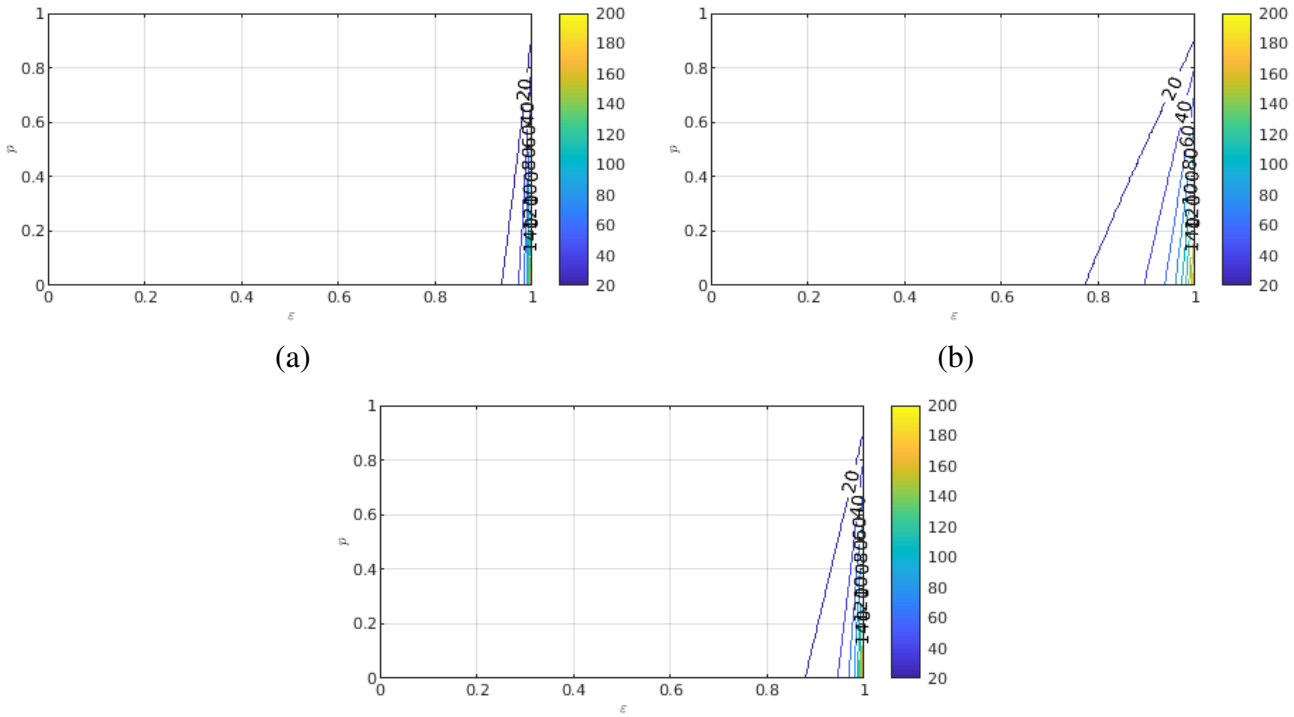

Figure 19: Contour plot of the basic reproduction number ($\mathcal{R}_0$) of the model (3.3) with a weak turnover as a function of vaccine coverage, p, and vaccine efficiency on the transmission, ε when: (a) $\nu = \varepsilon^2$(convex relationship); (b) $\nu = \sqrt{\varepsilon}$(concave relationship); (c)$\nu = \varepsilon$(linear relationship). The parameters are $\theta = 1000$, $\beta_{11} = 0.35$, $\beta_{12} = 0.28$, $\beta_{21} = 0.175, \beta_{22} = 0.14$, $\mu = 0.09$, $p = 0.5$, $d_1 = 0.0008$, $d_2 = 0.0001$, $\gamma_1 = 0.065$, $\gamma_2 = 0.13$.

4.4 Stochastic extinction and persistence of a heterogeneous epidemiological model

In this section, we prove the existence and uniqueness of a non-negative weak solution of the derived SDE (3.17). We show that the derived model is stochastically ultimately bounded. We compute and discuss the conditions for disease extinction and disease persistence in mean. We finally perform numerical simulation to support our analytical results.

These results are published in *Journal of Applied Mathematics and Computing* [90].

4.4.1 Mathematical analysis of the stochastic model

4.4.1.1 Existence and uniqueness of nonnegative weak solution

In this subsection, we investigate the well posedness of the above SDE, focusing on the existence and uniqueness of a global nonnegative weak solution to the SDE (3.17). While the SDE was used for analysis in [5], the author did not establish crucial result. Here, we address the gap and derive the following results

Proposition 3 *The set $\mathbb{R}^5_+$ is invariant for the modified stochastic model* (3.17).

Proof : Since the drift and diffusion coefficients of the modified stochastic model (3.17) satisfy the hypothesis of [32, Corollary A.1] that is

- $f_i(t,x) \geq 0$ for $x \in \mathbb{R}^5_+$ such that $x_i = 0$,
- $g_{i,j}(t,x) = 0$ for $x \in \mathbb{R}^5_+$ such that $x_i = 0$, $j \in \{1,2,\ldots,5\}$,

for all $t \geq 0$ and $i \in \{1,2,\ldots,5\}$, then the result follows. The above result suggests that if there is a unique solution of system (3.17), this solution is necessarily nonnegative.

Theorem 12 *Suppose that $\theta = \mu K$, $(\theta < K)$ where K is the carrying capacity. Then, for any initial condition $X_0 = (S_1(0), S_2(0), I_1(0), I_2(0), R(0)) \in \mathbb{R}^5_+$, there is exactly one weak solution $X(t) = (S_1(t), S_2(t), I_1(t), I_2(t), R(t)) \in \mathbb{R}^5_+$ of system* (3.17) *on $t \geq 0$.*

The proof of the above result is done in four steps and makes use of [24, Theorem 1.2] (see also Appendix 4.A). In particular, we check that the coefficients satisfy the condition of [24, Theorem 1.2]. *Proof :*

Identifying the coefficients of the operator L in (4.50) we have $(b_i)_{i\leq 5} = (\hat{f}_i)_{i\leq 5}$ and the matrix $(\gamma_{i,j})_{i,j\leq 5}$ can be defined from the matrix $(\hat{V}_{i,j})_{i,j\leq 5}$. That is

$$\hat{V}_{i,j} = 2\sqrt{x_i x_j}\gamma_{i,j} \quad \text{for all} \quad i,j = 1,2,\ldots,5. \tag{4.32}$$

Let $\mathcal{S}_5^+$ denote the space of 5×5 symmetric strictly positive definite matrices and $|x|$ denote the Euclidean norm of $x \in \mathbb{R}^5$. We only consider some coefficients in the matrix in checking the conditions, due to their similarities.

Step 1: We verify that $(\gamma_{i,j})_{i,j\leq 5}$ is $\frac{1}{2}$- Hölder continuous on compacts sets. We only consider γ_{11}, γ_{13}, since the bounds for the others can be found in a similar way. Based on the definition of φ, there are several cases. Define $\mathcal{B}(a) := \{x \in \mathbb{R}^5 : \ |$

$x \ |\leq \ a\}$ and $x, \tilde{x} \in \mathcal{B}(a) \bigcap \mathbb{R}^5_+$ such that $x = (s_1, s_2, i_1, i_2, r)^T$, $\tilde{x} = (\tilde{s}_1, \tilde{s}_2, \tilde{i}_1, \tilde{i}_2, \tilde{r})^T$, $n = s_1 + s_2 + i_1 + i_2 + r = \tilde{s}_1 + \tilde{s}_2 + \tilde{i}_1 + \tilde{i}_2 + \tilde{r}$.

Case 1: We consider γ_{11}

- For $0 \leq s_1 < \delta$ and $0 \leq i_1 < \delta$, $\gamma_{11}(x) = \dfrac{\theta(1-p)}{2\delta} + \dfrac{1}{2}\mu + \beta_{11}\dfrac{i_1^2}{2\delta n} + \beta_{12}\dfrac{i_1 i_2}{2\delta n}$,

$$\begin{aligned}
| \ \gamma_{11}(x) - \gamma_{11}(\tilde{x}) \ | &= | \ \beta_{11}\frac{i_1^2}{2\delta n} - \beta_{11}\frac{\tilde{i}_1^2}{2\delta n} + \beta_{12}\frac{i_1 I_2}{2\delta n} - \beta_{12}\frac{\tilde{i}_1\tilde{i}_2}{2\delta n} \ | \\
&\leq \frac{\beta_{11}}{2\delta n} \ | \ i_1^2 - \tilde{i}_1^2 \ | + \frac{\beta_{12}}{2\delta n} \ | \ i_1 i_2 - \tilde{i}_1\tilde{i}_2 \ | \\
&\leq \frac{\beta_{11}}{2\delta n} \ | \ i_1 + \tilde{i}_1 \ || \ i_1 - \tilde{i}_1 \ | + \frac{\beta_{12}}{2\delta n} \ | \ i_1 i_2 - i_1\tilde{i}_2 + i_1\tilde{i}_2 - \tilde{i}_1\tilde{i}_2 \ | \\
&\leq \frac{\beta_{11}}{\delta} \ | \ i_1 - \tilde{i}_1 \ | + \frac{\beta_{12}}{2\delta}\big(\ | \ i_1 - \tilde{i}_1 \ | + | \ i_2 - \tilde{i}_2 \ | \ \big) \\
&\leq \sqrt{a} \max\left\{\left(\frac{\beta_{11}}{\delta} + \frac{\beta_{12}}{2\delta}\right); \frac{\beta_{12}}{2\delta}\right\}(| \ i_1 - \tilde{i}_1 \ |^{1/2} + | \ i_2 - \tilde{i}_2 \ |^{1/2}).
\end{aligned}$$

- For $0 \leq s_1 < \delta$ and $i_1 \geq \delta$, $\gamma_{11}(x) = \dfrac{\theta(1-p)}{2\delta} + \dfrac{1}{2}\mu + \beta_{11}\dfrac{i_1}{2n} + \beta_{12}\dfrac{i_2}{2n}$. In this case, γ_{11} is $\dfrac{1}{2}$- Hölder continuous on compacts sets by definition.

- For $s_1 \geq \delta$ and $0 \leq i_1 < \delta$, $\gamma_{11}(x) = \dfrac{\theta(1-p)}{2s_1} + \dfrac{1}{2}\mu + \beta_{11}\dfrac{i_1^2}{2\delta n} + \beta_{12}\dfrac{i_1 i_2}{2\delta n}$,

$$\begin{aligned}
| \ \gamma_{11}(x) - \gamma_{11}(\tilde{x}) \ | &= | \ \frac{\theta(1-p)}{2s_1} - \frac{\theta(1-p)}{2\tilde{s}_1} + \beta_{11}\frac{i_1^2}{2\delta n} - \beta_{11}\frac{\tilde{i}_1^2}{2\delta n} + \beta_{12}\frac{i_1 i_2}{2\delta n} - \beta_{12}\frac{\tilde{i}_1\tilde{i}_2}{2\delta n} \ | \\
&\leq \sqrt{a} \max\left\{\frac{\theta(1-p)}{2\delta^2}; \left(\frac{\beta_{11}}{\delta} + \frac{\beta_{12}}{2\delta}\right); \frac{\beta_{12}}{2\delta}\right\}(| \ s_1 - \tilde{s}_1 \ |^{1/2} \\
&\quad + | \ i_1 - \tilde{i}_1 \ |^{1/2} + | \ i_2 - \tilde{i}_2 \ |^{1/2}).
\end{aligned}$$

- For $s_1 \geq \delta$ and $i_1 \geq \delta$, $\gamma_{11}(x) = \dfrac{\theta(1-p)}{2s_1} + \dfrac{1}{2}\mu + \beta_{11}\dfrac{i_1}{2n} + \beta_{12}\dfrac{i_2}{2n}$.

  In this case, γ_{11} is $\dfrac{1}{2}$- Hölder continuous on compacts sets by definition.

Case 2: We consider γ_{13}

- For $0 \leq i_1 < \delta$, $\gamma_{13}(x) = -\beta_{11}\dfrac{i_1\sqrt{s_1 i_1}}{2\delta n} - \beta_{12}\dfrac{i_2\sqrt{s_1 i_1}}{2\delta n}$,

$$
\begin{aligned}
\mid \gamma_{13}(x) - \gamma_{13}(\tilde{x}) \mid &= \mid \beta_{11}\frac{i_1\sqrt{s_1 i_1}}{2\delta n} - \beta_{11}\frac{\tilde{i}_1\sqrt{\tilde{s}_1\tilde{i}_1}}{2\delta n} + \beta_{12}\frac{i_2\sqrt{s_1 i_1}}{2\delta n} - \beta_{12}\frac{\tilde{i}_2\sqrt{\tilde{s}_1\tilde{i}_1}}{2\delta n} \mid \\
&\leq \beta_{11}\frac{\sqrt{s_1 i_1}}{2\delta n} \mid i_1 - \tilde{i}_1 \mid + \beta_{11}\frac{\tilde{i}_1\sqrt{i_1}}{2\delta n} \mid s_1 - \tilde{s}_1 \mid^{1/2} + \beta_{11}\frac{\tilde{i}_1\sqrt{\tilde{s}_1}}{2\delta n} \mid i_1 - \tilde{i}_1 \mid^{1/2} \\
&\quad + \beta_{12}\frac{\sqrt{s_1 i_1}}{2\delta n} \mid i_2 - \tilde{i}_2 \mid + \beta_{12}\frac{\tilde{i}_2\sqrt{i_1}}{2\delta n} \mid s_1 - \tilde{s}_1 \mid^{1/2} + \beta_{12}\frac{\tilde{i}_2\sqrt{\tilde{s}_1}}{2\delta n} \mid i_1 - \tilde{i}_1 \mid^{1/2} \\
&\leq \frac{\sqrt{a}}{2\delta}(\beta_{11} + \beta_{12}) \mid s_1 - \tilde{s}_1 \mid^{1/2} + \frac{\sqrt{a}}{2\delta}(\beta_{11} + \beta_{12}) \mid i_1 - \tilde{i}_1 \mid^{1/2} \\
&\quad + \beta_{12}\frac{\sqrt{a}}{2\delta} \mid i_2 - \tilde{i}_2 \mid^{1/2} \\
&\leq \max\left\{\frac{\sqrt{a}}{2\delta}(\beta_{11} + \beta_{12}); \beta_{12}\frac{\sqrt{a}}{2\delta}\right\}(\mid s_1 - \tilde{s}_1 \mid^{1/2} \\
&\quad + \mid i_1 - \tilde{i}_1 \mid^{1/2} + \mid i_2 - \tilde{i}_2 \mid^{1/2}).
\end{aligned}
$$

- For $i_1 \geq \delta$, $\gamma_{13}(x) = -\beta_{11}\dfrac{\sqrt{s_1 i_1}}{2n} - \beta_{12}\dfrac{i_2\sqrt{s_1}}{2n\sqrt{i_1}}$,

$$
\begin{aligned}
\mid \gamma_{13}(x) - \gamma_{13}(\tilde{x}) \mid &= \mid \beta_{11}\frac{\sqrt{s_1 i_1}}{2n} - \beta_{11}\frac{\sqrt{\tilde{s}_1\tilde{i}_1}}{2n} + \beta_{12}\frac{i_2\sqrt{s_1}}{2n\sqrt{i_1}} - \beta_{12}\frac{\tilde{i}_2\sqrt{\tilde{s}_1}}{2n\sqrt{\tilde{i}_1}} \mid \\
&\leq \beta_{11}\frac{\sqrt{i_1}}{2n} \mid s_1 - \tilde{s}_1 \mid^{1/2} + \beta_{11}\frac{\sqrt{\tilde{s}_1}}{2n} \mid i_1 - \tilde{i}_1 \mid^{1/2} + \beta_{12}\frac{\sqrt{s_1}}{2n\sqrt{i_1}} \mid i_2 - \tilde{i}_2 \mid \\
&\quad + \beta_{12}\frac{\tilde{i}_2}{2n\sqrt{i_1}} \mid s_1 - \tilde{s}_1 \mid^{1/2} + \beta_{12}\frac{\tilde{i}_2\sqrt{\tilde{s}_1}}{2n\sqrt{i_1\tilde{i}_1}} \mid i_1 - \tilde{i}_1 \mid^{1/2} \\
&\leq \left(\frac{\beta_{11}\sqrt{a}}{2\delta} + \frac{\beta_{12}}{2\sqrt{\delta}}\right) \mid s_1 - \tilde{s}_1 \mid^{1/2} + \frac{\sqrt{a}}{2\delta}(\beta_{11} + \beta_{12}) \mid i_1 - \tilde{i}_1 \mid^{1/2} + \frac{a\beta_{12}}{2\delta\sqrt{\delta}} \mid i_2 \\
&\leq \max\left\{\frac{\beta_{11}\sqrt{a}}{2\delta} + \frac{\beta_{12}}{2\sqrt{\delta}}; \frac{\sqrt{a}}{2\delta}(\beta_{11} + \beta_{12}); \frac{a\beta_{12}}{2\delta\sqrt{\delta}}\right\}(\mid s_1 - \tilde{s}_1 \mid^{1/2} \\
&\quad + \mid i_1 - \tilde{i}_1 \mid^{1/2} + \mid i_2 - \tilde{i}_2 \mid^{1/2}).
\end{aligned}
$$

Using similar arguments, we can show that the remaining coefficients of $(\gamma_{i,j})_{i,j\leq 5}$ are $\frac{1}{2}$- Hölder continuous on compact sets.

Step 2: Using the definition of the drift vector $(\hat{f}_i)_{i\leq 5}$, it holds that Assumption (H2) in Theorem 16 is satisfied.

Step 3: We claim that the drift $(\hat{f}_i)_{i\leq 5}$ in (3.17) satisfies the linear growth condition.

Let $x \in \mathbb{R}^5_+$ such that $x = (s_1, s_2, i_1, i_2, r)^T$,

$$\begin{aligned} \mid \hat{f}_1(x) \mid &= \mid \theta(1-p) - \beta_{11}\frac{s_1 i_1}{n} - \beta_{12}\frac{s_1 i_2}{n} - \mu s_1 \mid, \\ &\leq \theta(1-p) + (\beta_{11} + \beta_{12} + \mu) \mid s_1 \mid . \\ \mid \hat{f}_3(x) \mid &= \mid \beta_{11}\frac{s_1 i_1}{n} + \beta_{12}\frac{s_1 i_2}{n} - (\mu + \gamma_1 + d_1) i_1 \mid, \\ &\leq (\beta_{11} + \beta_{12}) \mid s_1 \mid + (\mu + \gamma_1 + d_1) \mid i_1 \mid . \end{aligned}$$

One can also easily show that $\hat{f}_2$, $\hat{f}_4$ and $\hat{f}_5$ are also of satisfy the linear growth. Thus Assumption (4.51) of Theorem 16 is fulfilled.

Step 4: We show that $(\gamma_{i,j})_{i,j\leq 5}$ satisfy the condition (4.52) of Theorem 16. To do that, we assume that $\theta = \mu K$ where K is the carrying capacity [102]. Then the total population n may vary in time but should be less than $K \geq 1$. This implies the boundedness of the matrix coefficient $(\gamma_{i,j})_{i,j\leq 5}$. Therefore, set

$$c_{1.1} = \frac{\mathcal{M}}{\mu},$$

where $\mathcal{M} = \beta_{11} + \beta_{22} + (\beta_{12} + \beta_{21} + \gamma_1 + \gamma_2)\sqrt{\frac{K}{\delta}}$. By the definition of the matrix γ,

$$\min_i \gamma_{ii}(x) \geq \mu, \quad \forall x \in \partial\mathbb{R}^5_+.$$

Next, we show that $\sum_{i\neq j} \mid \gamma_{ij}(x) \leq \mathcal{M}$, $\forall x \in \partial\mathbb{R}^5_+$. We consider once more several cases:

- For $s_1 = 0$, $s_2 \geq \delta$, $i_1 \geq \delta$, $i_2 \geq \delta$ and $r \geq \delta$,

$$\begin{aligned} \sum_{i\neq j} \mid \gamma_{ij}(x) \mid &= \beta_{21}\frac{i_1\sqrt{s_2}}{n\sqrt{i_2}} + \beta_{22}\frac{\sqrt{s_2 i_2}}{n} + \gamma_1\sqrt{\frac{i_1}{r}} + \gamma_1\sqrt{\frac{i_2}{r}} \\ &\leq \beta_{22} + (\beta_{21} + \gamma_1 + \gamma_2)\sqrt{\frac{K}{\delta}} \leq \mathcal{M}. \end{aligned}$$

- For $s_1 = 0, 0 \leq s_2 < \delta < 1, 0 \leq i_1 < \delta < 1, 0 \leq i_2 < \delta < 1$ and $0 \leq r < \delta < 1$,

$$\sum_{i \neq j} \mid \gamma_{ij}(x) \mid = \beta_{21} \frac{i_1 \sqrt{s_2 i_2}}{\delta n} + \beta_{22} \frac{i_2 \sqrt{s_2 i_2}}{\delta n} + \gamma_1 \frac{\sqrt{i_1 r}}{\delta} + \gamma_1 \frac{\sqrt{i_2 r}}{\delta}$$
$$\leq \beta_{21} + \beta_{22} + \gamma_1 + \gamma_2 \leq \mathcal{M}.$$

- For $s_1 \geq \delta, s_2 = 0, i_1 \geq \delta, i_2 \geq \delta$ and $r \geq \delta$,

$$\sum_{i \neq j} \mid \gamma_{ij}(x) \mid = \beta_{12} \frac{i_2 \sqrt{s_1}}{n \sqrt{i_1}} + \beta_{11} \frac{\sqrt{s_1 i_1}}{N} + \gamma_1 \sqrt{\frac{i_1}{r}} + \gamma_1 \sqrt{\frac{i_2}{r}}$$
$$\leq \beta_{11} + (\beta_{12} + \gamma_1 + \gamma_2) \sqrt{\frac{K}{\delta}} \leq \mathcal{M}.$$

- For $s_1 \geq \delta, s_2 \geq \delta, i_1 = 0, i_2 \geq \delta$ and $r \geq \delta$,

$$\sum_{i \neq j} \mid \gamma_{ij}(x) \mid = \beta_{22} \frac{\sqrt{s_2 i_2}}{n} + \gamma_1 \sqrt{\frac{i_2}{r}} \leq \beta_{22} + \gamma_2 \sqrt{\frac{K}{\delta}} \leq \mathcal{M}.$$

- For $s_1 \geq \delta, s_2 \geq \delta, i_1 \geq \delta, i_2 = 0$ and $r \geq \delta$,

$$\sum_{i \neq j} \mid \gamma_{ij}(x) \mid = \beta_{11} \frac{\sqrt{s_1 i_1}}{n} + \gamma_1 \sqrt{\frac{i_1}{r}} \leq \beta_{11} + \gamma_1 \sqrt{\frac{K}{\delta}} \leq \mathcal{M}.$$

- For $s_1 \geq \delta, s_2 \geq \delta, i_1 \geq \delta, i_2 \geq \delta$ and $r = 0$,

$$\sum_{i \neq j} \mid \gamma_{ij}(x) \mid = \beta_{11} \frac{\sqrt{s_1 i_1}}{n} + \beta_{12} \frac{i_2 \sqrt{s_1}}{n \sqrt{i_1}} + \beta_{22} \frac{\sqrt{s_2 i_2}}{n} + \beta_{21} \frac{i_1 \sqrt{s_2}}{n \sqrt{i_2}}$$
$$\leq \beta_{11} + \beta_{22} + (\beta_{12} + \beta_{21}) \sqrt{\frac{K}{\delta}} \leq \mathcal{M}.$$

For the remaining cases, we can proceed on the similar way.

4.4.1.2 Stochastically ultimate boundedness

In this section, we examine the ultimate boundedness in probability of solution.

Theorem 13 *For any initial value* $X_0 = (S_1(0), S_2(0), I_1(0), I_2(0), R(0)) \in \mathbb{R}^5_+$, *the solution of the model* (3.17) *is stochastically ultimately bounded.*

Proof : Let $m_0 \geq 1$ be sufficiently large such that each component of the initial value $(S_1(0), S_2(0), I_1(0), I_2(0), R(0))$ lies within the interval $\left[\frac{1}{m_0}, m_0\right]$. For each integer $m \geq m_0$, we define the stopping time

$$\tau_m = \inf\left\{t \in \mathbb{R}_+ : \min\{S_1(t), S_2(t), I_1(t), I_2(t), R(t)\} \leq \frac{1}{m} \text{ or } \max\{S_1(t), S_2(t), I_1(t), I_2(t), R(t)\right. \tag{4.33}$$

Using (3.2) and (3.17) we have that

$$\begin{aligned}
\mathrm{d}N(t) =&[\theta - \mu N(t) - d_1 I_1(t) - d_2 I_2(t)]\mathrm{d}t + \sqrt{\hat{r}_1^{\delta}(X(t))}\mathrm{d}W_1(t) + \sqrt{\hat{r}_2^{\delta}(X(t))}\mathrm{d}W_2(t) \\
&- \sqrt{\varphi(r_3(X(t)))}\mathrm{d}W_3(t) - \sqrt{\varphi(r_4(X(t)))}\mathrm{d}W_4(t) - \sqrt{\varphi(r_5(X(t)))}\mathrm{d}W_5(t) \\
&- \sqrt{\varphi(r_6(X(t)))}\mathrm{d}W_6(t) - \sqrt{\varphi(r_7(X(t)))}\mathrm{d}W_7(t)
\end{aligned}$$

Let $V(t) = (1 + N(t))^{\alpha}$ where $\alpha \in (0, 1)$. From the generalized Itô's formula, we get

$$\begin{aligned}
\mathrm{d}V(t) =&LV(t)\mathrm{d}t + \alpha(1 + N(t))^{\alpha-1}\Big[\sqrt{\hat{r}_1^{\delta}(X(t))}\mathrm{d}W_1(t) + \sqrt{\hat{r}_2^{\delta}(X(t))}\mathrm{d}W_2(t) \\
&- \sqrt{\varphi(r_3(X(t)))}\mathrm{d}W_3(t) - \sqrt{\varphi(r_4(X(t)))}\mathrm{d}W_4(t) - \sqrt{\varphi(r_5(X(t)))}\mathrm{d}W_5(t) \\
&- \sqrt{\varphi(r_6(X(t)))}\mathrm{d}W_6(t) - \sqrt{\varphi(r_7(X(t)))}\mathrm{d}W_7(t)\Big],
\end{aligned} \tag{4.34}$$

where

$$\begin{aligned}
LV(t) =&\alpha(1 + N(t))^{\alpha-1}\Big[\theta - \mu N(t) - d_1 I_1(t) - d_2 I_2(t)\Big] + \frac{\alpha(\alpha-1)}{2}(1 + N(t))^{\alpha-2}\Big[\hat{r}_1^{\delta}(X(t)) \\
&+ \varphi(r_3(X(t))) + \hat{r}_2^{\delta}(X(t)) + \varphi(r_4(X(t))) + \varphi(r_5(X(t))) + \varphi(r_6(X(t))) + \varphi(r_7(X(t)))\Big] \\
\leq&\alpha(1 + N(t))^{\alpha-2}\Big[-\mu N^2(t) + (\theta - \mu)N(t) + \theta\Big].
\end{aligned} \tag{4.35}$$

Then,

$$\begin{aligned}
\mathrm{d}V(t) \leq&\alpha(1 + N(t))^{\alpha-2}\Big[-\mu N^2(t) + (\theta - \mu)N(t) + \theta\Big]\mathrm{d}t + \alpha(1 + N(t))^{\alpha-1}\Big[\sqrt{\hat{r}_1^{\delta}(X(t))}\mathrm{d}W_1(t) \\
&+ \sqrt{\hat{r}_2^{\delta}(X(t))}\mathrm{d}W_2(t) - \sqrt{\varphi(r_3(X(t)))}\mathrm{d}W_3(t) - \sqrt{\varphi(r_4(X(t)))}\mathrm{d}W_4(t) - \sqrt{\varphi(r_5(X(t)))}\mathrm{dW} \\
&- \sqrt{\varphi(r_6(X(t)))}\mathrm{d}W_6(t) - \sqrt{\varphi(r_7(X(t)))}\mathrm{d}W_7(t)\Big].
\end{aligned} \tag{4.36}$$

For $0 < \eta < \mu\alpha$, we have

$$\begin{aligned}
\mathrm{d}\big[e^{\eta t}V(t)\big] =&\eta e^{\eta t}V(t)\mathrm{d}t + e^{\eta t}\mathrm{d}V(t)\\
=&(\eta e^{\eta t}V(t) + e^{\eta t}LV(t))\mathrm{d}t + e^{\eta t}\alpha(1+N(t))^{\alpha-1}\Big[\sqrt{\hat{r}_1^\delta(X(t))}\mathrm{d}W_1(t) + \sqrt{\hat{r}_2^\delta(X(t))}\mathrm{d}W_2(t)\\
&- \sqrt{\varphi(r_3(X(t)))}\mathrm{d}W_3(t) - \sqrt{\varphi(r_4(X(t)))}\mathrm{d}W_4(t) - \sqrt{\varphi(r_5(X(t)))}\mathrm{d}W_5(t)\\
&- \sqrt{\varphi(r_6(X(t)))}\mathrm{d}W_6(t) - \sqrt{\varphi(r_7(X(t)))}\mathrm{d}W_7(t)\Big]. \qquad (4.37)
\end{aligned}$$

Moreover,

$$\begin{aligned}
\eta e^{\eta t}V(t) + e^{\eta t}LV(t) \leq&\alpha e^{\eta t}(1+N(t))^{\alpha-2}\Big[\frac{\eta}{\alpha}(1+N(t))^2 - \mu N^2(t) + (\theta-\mu)N(t) + \theta\Big]\\
\leq&\alpha e^{\eta t}(1+N(t))^{\alpha-2}\Big[-\Big(\mu - \frac{\eta}{\alpha}\Big)N^2(t) + \Big(\theta - \mu + \frac{2\eta}{\alpha}\Big)N(t) + \theta + \frac{\eta}{\alpha}\Big]\\
\leq&\alpha e^{\eta t}H,
\end{aligned}$$

where we observe that the function $N \longmapsto (1+N)^{\alpha-2}\Big[-\Big(\mu-\frac{\eta}{\alpha}\Big)N^2+\Big(\theta-\mu+\frac{2\eta}{\alpha}\Big)N+\theta+\frac{\eta}{\alpha}\Big]$ is uniformly bounded on $\mathbb{R}_+$ and let $H := \sup_{N\in\mathbb{R}_+}(1+N)^{\alpha-2}\Big[-\Big(\mu-\frac{\eta}{\alpha}\Big)N^2 + \Big(\theta-\mu+\frac{2\eta}{\alpha}\Big)N + \theta + \frac{\eta}{\alpha}\Big] + 1$.

Then, it follows from (4.37) that

$$\begin{aligned}
\mathrm{d}\big[e^{\eta t}V(t)\big] \leq&\alpha e^{\eta t}H\mathrm{d}t + e^{\eta t}\alpha(1+N(t))^{\alpha-1}\Big[\sqrt{\hat{r}_1^\delta(X(t))}\mathrm{d}W_1(t) + \sqrt{\hat{r}_2^\delta(X(t))}\mathrm{d}W_2(t)\\
&- \sqrt{\varphi(r_3(X(t)))}\mathrm{d}W_3(t) - \sqrt{\varphi(r_4(X(t)))}\mathrm{d}W_4(t) - \sqrt{\varphi(r_5(X(t)))}\mathrm{d}W_5(t)\\
&- \sqrt{\varphi(r_6(X(t)))}\mathrm{d}W_6(t) - \sqrt{\varphi(r_7(X(t)))}\mathrm{d}W_7(t)\Big]. \qquad (4.38)
\end{aligned}$$

Integrations both sides of the above expression, and we can deduce the inequality

$$\mathbb{E}\big[e^{\eta t\wedge\tau_m}V(t\wedge\tau_m)\big] \leq V(0) + \alpha H\mathbb{E}\Big[\int_0^{t\wedge\tau_m} e^{\eta s}\mathrm{d}s\Big], \qquad (4.39)$$

where τ_m is given in (4.33). Letting $m \longrightarrow +\infty$ gives

$$\mathbb{E}\big[e^{\eta t}(1+N(t))^\alpha\big] \leq (1+N(0))^\alpha + \frac{\alpha H}{\eta}e^{\eta t}.$$

Consequently,

$$\limsup_{t\to+\infty}\mathbb{E}\big[(1+N(t))^\alpha\big] \leq \frac{\alpha H}{\eta} =: H_0. \qquad (4.40)$$

Now using the fact that $|X(t)| \leq N(t)$(thanks to the positivity of S_1, S_2, I_1, I_2, R), we have

$$|X(t)|^{\alpha} \leq (1 + N(t))^{\alpha}, \quad \forall t \geq 0$$

combined with (4.40), we deduce

$$\mathbb{E}\left[|X(t)|^{\alpha}\right] \leq H_0, \quad t \geq 0.$$

Then, for $\alpha = \frac{1}{2}$, there exists a constant $H_0 = \kappa > 0$ such that

$$\mathbb{E}\left[|X(t)|^{\frac{1}{2}}\right] \leq \kappa, \quad t \geq 0. \tag{4.41}$$

For any $\epsilon > 0$ set $\delta = \frac{\kappa^2}{\epsilon^2}$, then using the Chebyshev's inequality, we have

$$\mathbb{P}\{|X(t)| \geq \delta\} < \frac{\mathbb{E}\left[|X(t)|^{\frac{1}{2}}\right]}{\delta^{\frac{1}{2}}}$$

in other words,

$$\limsup_{t \to +\infty} \mathbb{P}\{|X(t)| \geq \delta\} < \frac{\kappa}{\delta^{\frac{1}{2}}} = \epsilon,$$

which completes the proof.

4.4.1.3 Extinction

In this section, we derive the conditions required for the extinction of the parasite within the host population. The following notation and definition are provided for convenience. Let

$$\langle x(t) \rangle = \frac{1}{t} \int_0^t x(r) \mathrm{d}r.$$

Definition 12 *For system (3.17), the infected individuals become extinct, if*

$$\lim_{t \to \infty} I_1(t) = 0 \quad a.s. \quad and \quad \lim_{t \to \infty} I_2(t) = 0 \quad a.s..$$

Lemma 6 (Strong law of large number [73]) *Let $M = \{M_t\}_{t \geq 0}$ be a real-valued contin-*

uous local martingale vanishing at $t = 0$*, then*

$$\lim_{t\to\infty}\langle M, M\rangle_t = \infty \quad a.s. \quad \Rightarrow \quad \lim_{t\to\infty}\frac{M_t}{\langle M, M\rangle_t} = 0 \quad a.s. \quad \textit{and also,} \tag{4.42}$$

$$\limsup_{t\to\infty}\frac{\langle M, M\rangle_t}{t} < \infty \quad a.s. \quad \Rightarrow \quad \lim_{t\to\infty}\frac{M_t}{t} = 0 \quad a.s. \tag{4.43}$$

Lemma 7 ([60]) *Let* $f \in C[(0,\infty)\times\Omega,(0,\infty)]$ *and* $F(t) \in C[(0,\infty)\times\Omega,\mathbb{R}]$*. If there exist positive constants* λ_0 *and* T*, such that*

$$\log f(t) \le \lambda t - \lambda_0\int_0^t f(s)\mathrm{d}s + F(t) \quad a.s. \tag{4.44}$$

for all $t \ge T$*, and* $\lim_{t\to\infty}\frac{F(t)}{t} = 0$ *a.s., then*

$$\begin{cases} \limsup_{t\to\infty}\langle f(t)\rangle \le \dfrac{\lambda}{\lambda_0} & a.s., \quad if \quad \lambda \ge 0; \\ \lim_{t\to\infty} f(t) = 0 & a.s., \quad if \quad \lambda < 0. \end{cases} \tag{4.45}$$

The following result provides conditions under which the parasite is eradicated with probability one.

Theorem 14 *Let* $X(t) = (S_1(t), S_2(t), I_1(t), I_2(t), R(t)) \in \mathbb{R}^5_+$ *be the solution of the system (3.17) such that* $S_1(t) + S_2(t) + I_1(t) + I_2(t) + R(t) \le \dfrac{\theta}{\mu}$ *a.s. with the initial value* $X_0 = (S_1(0), S_2(0), I_1(0), I_2(0), R(0)) \in \mathbb{R}^5_+$ *such that* $S_1(0) + S_2(0) + I_1(0) + I_2(0) + R(0) \le \dfrac{\theta}{\mu}$ *a.s.. Suppose one of two condition holds*

(a) $\beta_{21} \vee \beta_{22} < \dfrac{1}{K}\left(1 + \dfrac{1}{2K}\right)d_1 \wedge d_2$, $1 - p < \dfrac{1}{K} + \dfrac{1}{2K^2}$ *and* $S_1(t) + I_1(t) + I_2(t) + R(t) \ge 1$, *a.s.*

(b) $\beta_{11} \vee \beta_{12} < \dfrac{1}{K}\left(1 + \dfrac{1}{2K}\right)d_1 \wedge d_2$, $p < \dfrac{1}{K} + \dfrac{1}{2K^2}$ *and* $S_2(t) + I_1(t) + I_2(t) + R(t) \ge 1$, *a.s.*

Then

$$\lim_{t\to\infty} I_1(t) + I_2(t) = 0 \quad a.s.$$

Remark 4 *Finally, we establish sufficient conditions to ensure that the parasite is strongly persistent in mean with probability one.*

Proof : We only consider the case when (a) is satisfied. The case under (b) is proven analogously. Let consider $V_1(t) = S_1(t) + I_1(t) + I_2(t) + R(t) \geq 1$. To derive the conditions for extinction of the parasite we apply the Itô's formula to $\log(V_1(t))$ and obtain

$$
\begin{aligned}
\mathrm{d}\log(V_1(t)) =& \frac{1}{V_1(t)}\Big[\hat{f}_1(X(t))\mathrm{d}t + \sqrt{\hat{r}_1^{\delta}(X(t))}\mathrm{d}W_1(t) - \sqrt{\varphi(r_3(X(t)))}\mathrm{d}W_3(t) \\
&- \sqrt{\hat{r}_8^{\delta}(X(t))}\mathrm{d}W_8(t)\Big] + \frac{1}{V_1(t)}\Big[\hat{f}_3(X(t))\mathrm{d}t - \sqrt{\varphi(r_5(X(t)))}\mathrm{d}W_5(t) \\
&+ \sqrt{\hat{r}_8^{\delta}(X(t))}\mathrm{d}W_8(t) - \sqrt{\hat{r}_{10}^{\delta}(X(t))}\mathrm{d}W_{10}(t)\Big] + \frac{1}{V_1(t)}\Big[\hat{f}_4(X(t))\mathrm{d}t \\
&- \sqrt{\varphi(r_6(X(t)))}\mathrm{d}W_6(t) + \sqrt{\hat{r}_9^{\delta}(X(t))}\mathrm{d}W_9(t) - \sqrt{\hat{r}_{11}^{\delta}(X(t))}\mathrm{d}W_{11}(t)\Big] \\
&+ \frac{1}{V_1(t)}\Big[\hat{f}_5(X(t))\mathrm{d}t - \sqrt{\varphi(r_7(X(t)))}\mathrm{d}W_7(t) + \sqrt{\hat{r}_{10}^{\delta}(X(t))}\mathrm{d}W_{10} \\
&+ \sqrt{\hat{r}_{11}^{\delta}(X(t))}\mathrm{d}W_{11}(t)\Big] - \frac{1}{2V_1^2(t)}\Big[\hat{r}_1^{\delta}(X(t)) + \varphi(r_3(X(t))) + \varphi(r_5(X(t))) \\
&+ \varphi(r_6(X(t))) + \hat{r}_9^{\delta}(X(t)) + 2\hat{r}_{11}^{\delta}(X(t)) + \varphi(r_7(X(t)))\Big]\mathrm{d}t \\
=& \Big[\frac{\theta(1-p)}{V_1(t)} + \frac{\beta_{21}S_2(t)I_1(t)}{V_1(t)N(t)} + \frac{\beta_{22}S_2(t)I_2(t)}{V_1(t)N(t)} - \frac{\mu V_1(t)}{V_1(t)} - \frac{d_1 I_1(t)}{V_1(t)} - \frac{d_2 I_2(t)}{V_1(t)}\Big]\mathrm{d}t \\
&- \frac{1}{2V_1^2(t)}\Big[\hat{r}_1^{\delta}(X(t)) + \varphi(r_3(X(t))) + \varphi(r_5(X(t))) + \varphi(r_6(X(t))) + \hat{r}_9^{\delta}(X(t)) + \varphi(r
\end{aligned}
$$

$$
\begin{aligned}
&+ \frac{\sqrt{\hat{r}_1^{\delta}(X(t))}}{V_1(t)}\mathrm{d}W_1(t) - \frac{\sqrt{\varphi(r_3(X(t)))}}{V_1(t)}\mathrm{d}W_3(t) - \frac{\sqrt{\varphi(r_5(X(t)))}}{V_1(t)}\mathrm{d}W_5(t) \\
&- \frac{\sqrt{\varphi(r_6(X(t)))}}{V_1(t)}\mathrm{d}W_6(t) + \frac{\sqrt{\hat{r}_9^{\delta}(X(t))}}{V_1(t)}\mathrm{d}W_9(t) - \frac{\sqrt{\varphi(r_7(X(t)))}}{V_1(t)}\mathrm{d}W_7(t) \\
\leq& \Big[\frac{\theta(1-p)}{V_1(t)} + \beta_{21}I_1(t) + \beta_{22}I_2(t) - \mu - \frac{d_1 \wedge d_2}{V_1(t)}(I_1(t) + I_2(t))\Big]\mathrm{d}t - \frac{1}{2V_1^2(t)}\Big[\mu V_1(t) \\
&+ d_1 \wedge d_2(I_1(t) + I_2(t))\Big]\mathrm{d}t + \frac{\sqrt{\hat{r}_1^{\delta}(X(t))}}{V_1(t)}\mathrm{d}W_1(t) - \frac{\sqrt{\varphi(r_3(X(t)))}}{V_1(t)}\mathrm{d}W_3(t) \\
&- \frac{\sqrt{\varphi(r_5(X(t)))}}{V_1(t)}\mathrm{d}W_5(t) - \frac{\sqrt{\varphi(r_6(X(t)))}}{V_1(t)}\mathrm{d}W_6(t) + \frac{\sqrt{\hat{r}_9^{\delta}(X(t))}}{V_1(t)}\mathrm{d}W_9(t) \\
&- \frac{\sqrt{\varphi(r_7(X(t)))}}{V_1(t)}\mathrm{d}W_7(t).
\end{aligned}
$$

Using the almost sure inequalities $1 \leq V_1(t) \leq K$ and $I_1(t) + I_2(t) \leq V_1(t)$, and integrating

from 0 to t give

$$\begin{aligned}
\log(V_1(t)) \leq \log(I_1(0)+I_2(0)) + \int_0^t \Big\{\Big[\theta(1-p)+\beta_{21}\vee\beta_{22}(I_1(u)+I_2(u)) - \mu - \frac{\mu}{2K} \\
- \Big(\frac{1}{K}+\frac{1}{2K^2}\Big)d_1\wedge d_2(I_1(u)+I_2(u))\Big]\Big\}\mathrm{d}u + \int_0^t \frac{\sqrt{\hat{r}_1^{\delta}(X(u))}}{V_1(u)}\mathrm{d}W_1(u) \\
- \int_0^t \frac{\sqrt{\varphi(r_3(X(t)))}}{V_1(u)}\mathrm{d}W_3(u) - \int_0^t \frac{\sqrt{\varphi(r_5(X(u)))}}{V_1(u)}\mathrm{d}W_5(u) \\
- \int_0^t \frac{\sqrt{\varphi(r_6(X(u)))}}{V_1(u)}\mathrm{d}W_6(u) + \int_0^t \frac{\sqrt{\hat{r}_9^{\delta}(X(u))}}{V_1(t)}\mathrm{d}W_9(u) - \int_0^t \frac{\sqrt{\varphi(r_7(X(u)))}}{V_1(u)}\mathrm{d}W_7(u \\
\leq \log(I_1(0)+I_2(0)) + \Big[\theta(1-p)-\mu-\frac{\mu}{2K}\Big]t \\
- \Big[\frac{1}{K}\Big(1+\frac{1}{2K}\Big)d_1\wedge d_2 - \beta_{21}\vee\beta_{22}\Big]\int_0^t (I_1(r)+I_2(r))\mathrm{d}r + M_1(t) \\
- M_3(t) - M_5(t) - M_6(t) + M_9(t) - M_7(t), \qquad (4.46)
\end{aligned}$$

where $M_i(t) = \int_0^t \frac{\sqrt{\varphi(r_i(X(r)))}}{V_1(r)}\mathrm{d}W_i(r)$, $M_j(t) = \int_0^t \frac{\sqrt{\hat{r}_j^{\delta}(X(r))}}{V_1(r)}\mathrm{d}W_j(r)$, $i = 3,5,6,7$, and $j = 1,9$, are local continuous martingales and $M_i(0) = 0$ and $M_j(0) = 0$.

Since $\theta = \mu K$, $1-p < \frac{1}{K}+\frac{1}{2K^2}$, $\beta_{21}\vee\beta_{22} < \frac{1}{K}\Big(1+\frac{1}{2K}\Big)d_1\wedge d_2$ and by using Lemmas 6 and 7, we deduce from (4.46) that

$$\limsup_{t\to\infty}\langle I_1(t)+I_2(t)\rangle \leq \frac{\theta(1-p)-\mu-\frac{\mu}{2K}}{\frac{1}{K}\Big(1+\frac{1}{2K}\Big)d_1\wedge d_2 - \beta_{21}\vee\beta_{22}} \quad \text{a.s.}$$

We conclude by using (4.45) that,

$$\lim_{t\to\infty} I_1(t)+I_2(t) = 0 \quad \text{a.s.},$$

which implies that

$$\lim_{t\to\infty} I_1(t) = 0 \quad \text{a.s.} \quad \text{and} \quad \lim_{t\to\infty} I_2(t) = 0 \quad \text{a.s.}.$$

Remark 5 *Theorem 14 shows that we need a high efficient imperfect vaccine designed to reduce the transmission to eradicate the disease if there is a large vaccination rate. In the case where there is a large number of unvaccinated individuals among the new recruitment*

in the community, we need to implement some strategies to reduce contact between individuals. This implies that the conditions which are needed to have $I_1(t) + I_2(t)$ *to become extinct in the stochastic system (3.17) are more restrictive than in the corresponding deterministic system (3.3).*

4.4.1.4 Persistence in mean

In this section, we establish sufficient conditions to ensure that the parasite is strongly persistent in mean with probability one.

Definition 13 *For system (3.17), the parasite is said to be persistent in mean if*

$$\liminf_{t\to\infty} \langle I_1(t) + I_2(t)\rangle > 0 \quad a.s.$$

Theorem 15 *Let* $X(t) = (S_1(t), S_2(t), I_1(t), I_2(t), R(t)) \in \mathbb{R}^5_+$ *be the solution of system (3.17) such that* $S_1(t) + S_2(t) + I_1(t) + I_2(t) + R(t) < K$ *with the initial value* $X_0 = (S_1(0), S_2(0), I_1(0), I_2(0), R(0)) \in \mathbb{R}^5_+$ *such that* $S_1(0) + S_2(0) + I_1(0) + I_2(0) + R(0) < K$. *Suppose one of two condition holds*

(a) $\beta_{21} \vee \beta_{22} > \frac{1}{K}\left(1 + \frac{1}{2K}\right) d_1 \wedge d_2$, $1 - p < \frac{1}{K} + \frac{1}{2K^2}$ *and* $S_1(t) + I_1(t) + I_2(t) + R(t) \geq 1$, *a.s.*

(b) $\beta_{11} \vee \beta_{12} > \frac{1}{K}\left(1 + \frac{1}{2K}\right) d_1 \wedge d_2$, $p < \frac{1}{K} + \frac{1}{2K^2}$ *and* $S_2(t) + I_1(t) + I_2(t) + R(t) \geq 1$, *a.s.*

Then the solution $(S_1(t), S_2(t), I_1(t), I_2(t), R(t))$ *has the property*

$$\liminf_{t\to\infty} \langle I_1(t) + I_2(t)\rangle > 0 \quad a.s.$$

Proof : We only consider the case when (a) is satisfied. The case under (b) is proven analogously. Let consider $V_1(t) = S_1(t) + I_1(t) + I_2(t) + R(t) \geq 1$. To derive the conditions for persistence in mean of parasites, we apply the Itô's formula to $-\log(V_1(t))$ and obtain

the following lower bound

$$
\begin{aligned}
-\mathrm{d}\log(V_1(t)) = &-\frac{1}{V_1(t)}\Big[\hat{f}_1(X(t))\mathrm{d}t + \sqrt{\hat{r}_1^{\delta}(X(t))}\mathrm{d}W_1(t) - \sqrt{\varphi(r_3(X(t)))}\mathrm{d}W_3(t) \\
&- \sqrt{\hat{r}_8^{\delta}(X(t))}\mathrm{d}W_8(t)\Big] - \frac{1}{V_1(t)}\Big[\hat{f}_3(X(t))\mathrm{d}t - \sqrt{\varphi(r_5(X(t)))}\mathrm{d}W_5(t) \\
&+ \sqrt{\hat{r}_8^{\delta}(X(t))}dW_8(t) - \sqrt{\hat{r}_{10}^{\delta}(X(t))}\mathrm{d}W_{10}(t)\Big] - \frac{1}{V_1(t)}\Big[\hat{f}_4(X(t))\mathrm{d}t \\
&- \sqrt{\varphi(r_6(X(t)))}\mathrm{d}W_6(t) + \sqrt{\hat{r}_9^{\delta}(X(t))}dW_9(t) - \sqrt{\hat{r}_{11}^{\delta}(X(t))}\mathrm{d}W_{11}(t)\Big] \\
&- \frac{1}{V_1(t)}\Big[\hat{f}_5(X(t))\mathrm{d}t - \sqrt{\varphi(r_7(X(t)))}\mathrm{d}W_7(t) + \sqrt{\hat{r}_{10}^{\delta}(X(t))}\mathrm{d}W_{10} \\
&+ \sqrt{\hat{r}_{11}^{\delta}(X(t))}\mathrm{d}W_{11}(t)\Big] + \frac{1}{2V_1^2(t)}\Big[\hat{r}_1^{\delta}(X(t)) + \varphi(r_3(X(t))) + \varphi(r_5(X(t))) \\
&+ \varphi(r_6(X(t))) + \hat{r}_9^{\delta}(X(t)) + \varphi(r_7(X(t)))\Big]\mathrm{d}t
\end{aligned}
$$

$$
\begin{aligned}
=&\Big[-\frac{\theta(1-p)}{V_1(t)}-\frac{\beta_{21}S_2(t)I_1(t)}{V_1(t)N(t)}-\frac{\beta_{22}S_2(t)I_2(t)}{V_1(t)N(t)}+\frac{\mu V_1(t)}{V_1(t)}+\frac{d_1I_1(t)}{V_1(t)}+\frac{d_2I_2(t)}{V_1(t)}\Big]\mathrm{d}t\\
&+\frac{1}{2V_1^2(t)}\Big[\hat{r}_1^{\delta}(X(t))+\varphi(r_3(X(t)))+\varphi(r_5(X(t)))+\varphi(r_6(X(t)))+\hat{r}_9^{\delta}(X(t))+\varphi(r_7(X(t)))\Big]\mathrm{d}t\\
&-\frac{\sqrt{\hat{r}_1^{\delta}(X(t))}}{V_1(t)}\mathrm{d}W_1(t)+\frac{\sqrt{\varphi(r_3(X(t)))}}{V_1(t)}\mathrm{d}W_3(t)+\frac{\sqrt{\varphi(r_5(X(t)))}}{V_1(t)}\mathrm{d}W_5(t)\\
&+\frac{\sqrt{\varphi(r_6(X(t)))}}{V_1(t)}\mathrm{d}W_6(t)-\frac{\sqrt{\hat{r}_9^{\delta}(X(t))}}{V_1(t)}\mathrm{d}W_9(t)+\frac{\sqrt{\varphi(r_7(X(t)))}}{V_1(t)}\mathrm{d}W_7(t)\\
\geq&\Big[-\theta(1-p)-\beta_{21}I_1-\beta_{22}I_2+\mu+\frac{d_1}{K}I_1(t)+\frac{d_2}{K}I_2(t)\Big]\mathrm{d}t+\Big[\frac{1}{2K}\mu+\frac{1}{2K^2}d_1I_1(t)\\
&+\frac{1}{2K^2}d_2I_2(t)\Big]\mathrm{d}t-\frac{\sqrt{\hat{r}_1^{\delta}(X(t))}}{V_1(t)}\mathrm{d}W_1(t)+\frac{\sqrt{\varphi(r_3(X(t)))}}{V_1(t)}\mathrm{d}W_3(t)\\
&+\frac{\sqrt{\varphi(r_5(X(t)))}}{V_1(t)}\mathrm{d}W_5(t)+\frac{\sqrt{\varphi(r_6(X(t)))}}{V_1(t)}\mathrm{d}W_6(t)-\frac{\sqrt{\hat{r}_9^{\delta}(X(t))}}{V_1(t)}\mathrm{d}W_9(t)\\
&+\frac{\sqrt{\varphi(r_7(X(t)))}}{V_1(t)}\mathrm{d}W_7(t)\\
\geq&\Big[\mu+\frac{1}{2K}\mu-\theta(1-p)-\beta_{21}\vee\beta_{22}(I_1(t)+I_2(t))\\
&+\frac{1}{K}\Big(1+\frac{1}{2K}\Big)d_1\wedge d_2(I_1(t)+I_2(t))\Big]\mathrm{d}t-\frac{\sqrt{\hat{r}_1^{\delta}(X(t))}}{V_1(t)}\mathrm{d}W_1(t)\\
&+\frac{\sqrt{\varphi(r_3(X(t)))}}{V_1(t)}\mathrm{d}W_3(t)+\frac{\sqrt{\varphi(r_5(X(t)))}}{V_1(t)}\mathrm{d}W_5(t)+\frac{\sqrt{\varphi(r_6(X(t)))}}{V_1(t)}\mathrm{d}W_6(t)\\
&-\frac{\sqrt{\hat{r}_9^{\delta}(X(t))}}{V_1(t)}\mathrm{d}W_9(t)+\frac{\sqrt{\varphi(r_7(X(t)))}}{V_1(t)}\mathrm{d}W_7(t).
\end{aligned}
\tag{4.47}
$$

Integrating (4.47) from 0 to t on both sides gives

$$
\begin{aligned}
&\Big[\beta_{21}\vee\beta_{22}-\frac{1}{K}\Big(1+\frac{1}{2K}\Big)d_1\wedge d_2\Big]\int_0^t(I_1(r)+I_2(r))\mathrm{d}r\\
\geq&-\log(V_1(0))+\Big[\mu+\frac{1}{2K}\mu-\theta(1-p)\Big]t+\log(V_1(t))\\
&-M_1(t)+M_3(t)+M_5(t)+M_6(t)-M_9(t)+M_7(t),
\end{aligned}
\tag{4.48}
$$

where $M_i(t) = \int_0^t \frac{\sqrt{\varphi(r_i(X(r)))}}{V_1(r)} \mathrm{d}W_i(r)$, $M_j(t) = \int_0^t \frac{\sqrt{\hat{r}_j^{\delta}(X(r))}}{V_1(r)} \mathrm{d}W_j(r)$, $i = 3, 5, 6, 7$, and $j = 1, 9$, are local continuous martingales and $M_i(0) = 0$.

Since $\theta = \mu K$, $1 - p < \frac{1}{K} + \frac{1}{2K^2}$, $\beta_{21} \vee \beta_{22} > \frac{1}{K}\left(1 + \frac{1}{2K}\right) d_1 \wedge d_2$ and by using Lemma 6, we deduce from (4.48) that,

$$\lim_{t\to\infty} \inf \langle I_1(t) + I_2(t) \rangle \geq \frac{\mu + \frac{1}{2K}\mu - \theta(1-p)}{\beta_{21} \vee \beta_{22} - \frac{1}{K}\left(1 + \frac{1}{2K}\right) d_1 \wedge d_2} > 0 \quad \text{a.s.}$$

4.4.2 Numerical simulations

In this section some numerical simulations for the system (3.17) are conducted to illustrate the obtained theoretical results provided in Theorem 14 and Theorem 15. Applying the Euler-Maruyama method used in [5] on (3.17), the system (3.17) can be discretized as follows:

$$\begin{cases} S_1(t_{k+1}) = S_1(t_k) + \hat{f}_1(X(t_k))\Delta + \sqrt{\hat{r}_1^{\delta}(X(t_k))}\eta_{1k}\sqrt{\Delta} - \sqrt{\varphi(r_3(X(t_k)))}\eta_{3k}\sqrt{\Delta} - \sqrt{\hat{r}_8^{\delta}(X(t_k))}\eta_8 \\ S_2(t_{k+1}) = S_2(t_k) + \hat{f}_2(X(t_k))\Delta + \sqrt{\hat{r}_2^{\delta}(X(t_k))}\eta_{2k}\sqrt{\Delta} - \sqrt{\varphi(r_4(X(t_k)))}\eta_{4k}\sqrt{\Delta} - \sqrt{\hat{r}_9^{\delta}(X(t_k))}\eta_9 \\ I_1(t_{k+1}) = I_1(t_k) + \hat{f}_3(X(t_k))\Delta - \sqrt{\varphi(r_5(X(t_k)))}\eta_{5k}\sqrt{\Delta} + \sqrt{\hat{r}_8^{\delta}(X(t_k))}\eta_{8k}\sqrt{\Delta} - \sqrt{\hat{r}_{10}^{\delta}(X(t_k))}\eta_1 \\ I_2(t_{k+1}) = I_2(t_k) + \hat{f}_4(X(t_k))\Delta - \sqrt{\varphi(r_6(X(t_k)))}\eta_{6k}\sqrt{\Delta} + \sqrt{\hat{r}_9^{\delta}(X(t_k))}\eta_{9k}\sqrt{\Delta} - \sqrt{\hat{r}_{11}^{\delta}(X(t_k))}\eta_1 \\ R(t_{k+1}) = R(t_k) + \hat{f}_5(X(t_k))\Delta - \sqrt{\varphi(r_7(X(t_k)))}\eta_{7k}\sqrt{\Delta} + \sqrt{\hat{r}_{10}^{\delta}(X(t_k))}\eta_{10k}\sqrt{\Delta} + \sqrt{\hat{r}_{11}^{\delta}(X(t_k))}\eta \end{cases} \tag{4.49}$$

where $X(t_k) = (S_1(t_k), S_2(t_k), I_1(t_k), I_2(t_k), R(t_k))$, $k = 0, 1, 2, \cdots$, Δ is the step size and η_{ik}(for $i \in \{1; 2; \cdots; 11\}$ and $k = 0, 1, 2, \cdots$) are mutually independent Gaussian random variables which follow the distribution $\mathcal{N}(0, 1)$. In addition, the discretized equations (4.49) are similar to the ones in [74, 114] with the positive preserving truncated Euler–Maruyama method. This ensures that, population sizes remain nonnegative: if at the t_k^{th} time step a calculated population size is negative, it si reset to zero before the t_{k+1}^{th} time step [5]. Notably in [74, 114], the function φ is only use in the numerical implementation to preserve the positivity.

We compute the sample paths with a step size of 0.01. The parameter δ is set to 0.25 and the carrying capacity, representing the maximum population size, K, is set to 100000. The specific parameter values used are summarized in Table 2. The initial values are set as $(S_1(0), S_2(0), I_1(0), I_2(0), R(0)) = (1000, 700, 200, 80, 20)$.

In Figure 20(a), we fix $\theta = 1000$, $\beta_{11} = 0.4$, $\beta_{12} = 0.2$, $\beta_{21} = 10^{-9}$, $\beta_{22} = 10^{-9}$, $\mu = \theta/K$, $p = 1 - 0.00001$ (others as given in Table 2), so that the condition (a) of Theorem 14 is satisfied. For the condition (b) of Theorem 14, we consider parameter values as $\theta = 1000$, $\beta_{11} = 10^{-9}$, $\beta_{12} = 10^{-9}$, $\beta_{21} = 0.4$, $\beta_{22} = 0.3$, $\mu = \theta/K$, $p = 0.00001$ (others as given in Table 2). However, a stochastic solution of the same system yields different outcome for each simulation due to the randomness of the system (see Figures 20(a) and 20(b), upper panel). To address this, in Figure 20(c) (respectively Figure 20(d)), we present the mean value of 1000 simulations of the number of infected $(I_1 + I_2)$ using the parameter values that satisfy condition (a)(respectively condition (b)) of Theorem 14. The result illustrates the extinction of the parasite within the host population.

In Figure 21(a), we choose $\theta = 1000$, $\beta_{11} = 0.6$, $\beta_{12} = 0.5$, $\beta_{21} = 0.4$, $\beta_{22} = 0.3$, $\mu = \theta/K$, $p = 1 - 0.00001$ (others as given in Table 2) to ensure that the condition (a) of Theorem 15 is satisfied. Similarly, the condition (b) of Theorem 15, is satisfied when $\theta = 1000$, $\beta_{11} = 0.5$, $\beta_{12} = 0.6$, $\beta_{21} = 0.2$, $\beta_{22} = 0.1$, $\mu = \theta/K$, $p = 0.00001$(others as given in Table 2). Figure 21(c)(respectively Figure 21(d)) is corresponding to the mean value of 1000 simulations of number infected $(I_1 + I_2)$. This shows the persistence in mean of the parasite in the host population.

4.4.3 Summary

A major question in epidemiology is to account for the effect stochasticity and thus to determine the likely realistic outcome of epidemics. In this chapter, we formulated the stochastic model for the transmission dynamic of an infectious disease in a heterogeneous population of vaccinated and unvaccinated hosts to investigate the effect of demographic variability on the ODE system (3.3). Our work shows that the conditions for the disease to become extinct in the stochastic system are more restrictive than those of the deterministic system, a result which has implications for optimizing vaccination campaigns.

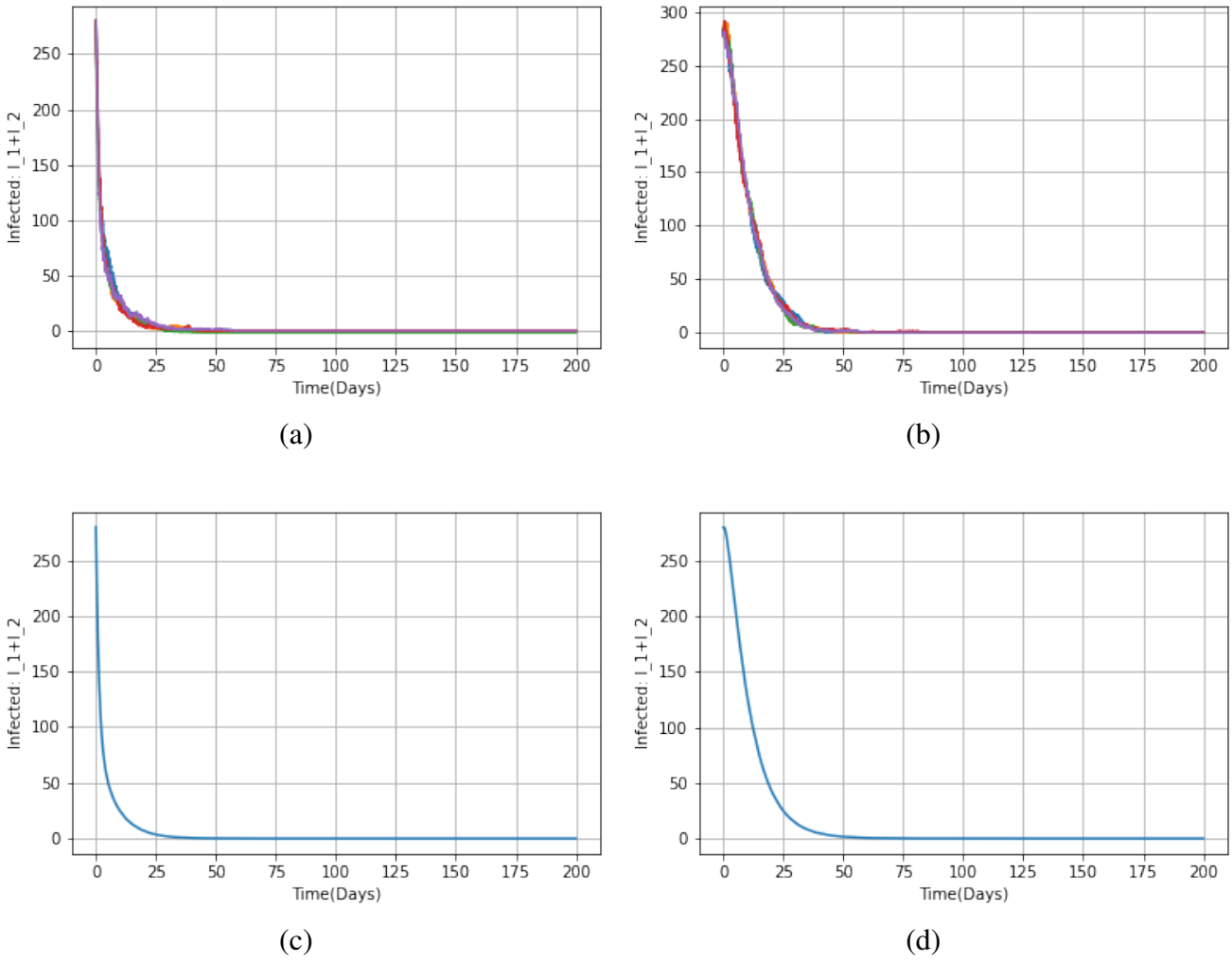

Figure 20: Extinction of the disease with initial conditions $(S_1(0), S_2(0), I_1(0), I_2(0), R(0)) = (1000, 700, 200, 80, 20)$ and a step size 10^{-2}. Upper panel (a) (respectively (b)) represents 5 simulations of infected $(I_1 + I_2)$ of stochastic system (3.17) with parameters which satisfy condition (a) (respectively (b)) of Theorem 14. Lower panel (c) (respectively (d)) represents the average value of 1000 simulations of infected $(I_1 + I_2)$ of system (3.17) with the same parameter values.

4.A Theorem 1.2 of [24]

Consider the operator

$$\mathcal{L}f(x) = \sum_{i,j=1}^{d} \sqrt{x_i x_j}\gamma_{ij}(x)\frac{\partial^2 f}{\partial x_i \partial x_j}(x) + \sum_{i=1}^{d} b_i(x)\frac{\partial f}{\partial x_i}(x), \tag{4.50}$$

on functions in $C_b^2(\mathbb{R}_+^d)$, the space of bounded C^2 functions on the nonnegative orthant with bounded first and second order partial derivatives.

Let ν be a probability on $\mathbb{R}_+^d$. Let $\Omega' = C([0, +\infty); \mathbb{R}_+^d)$ and furnish Ω' with the

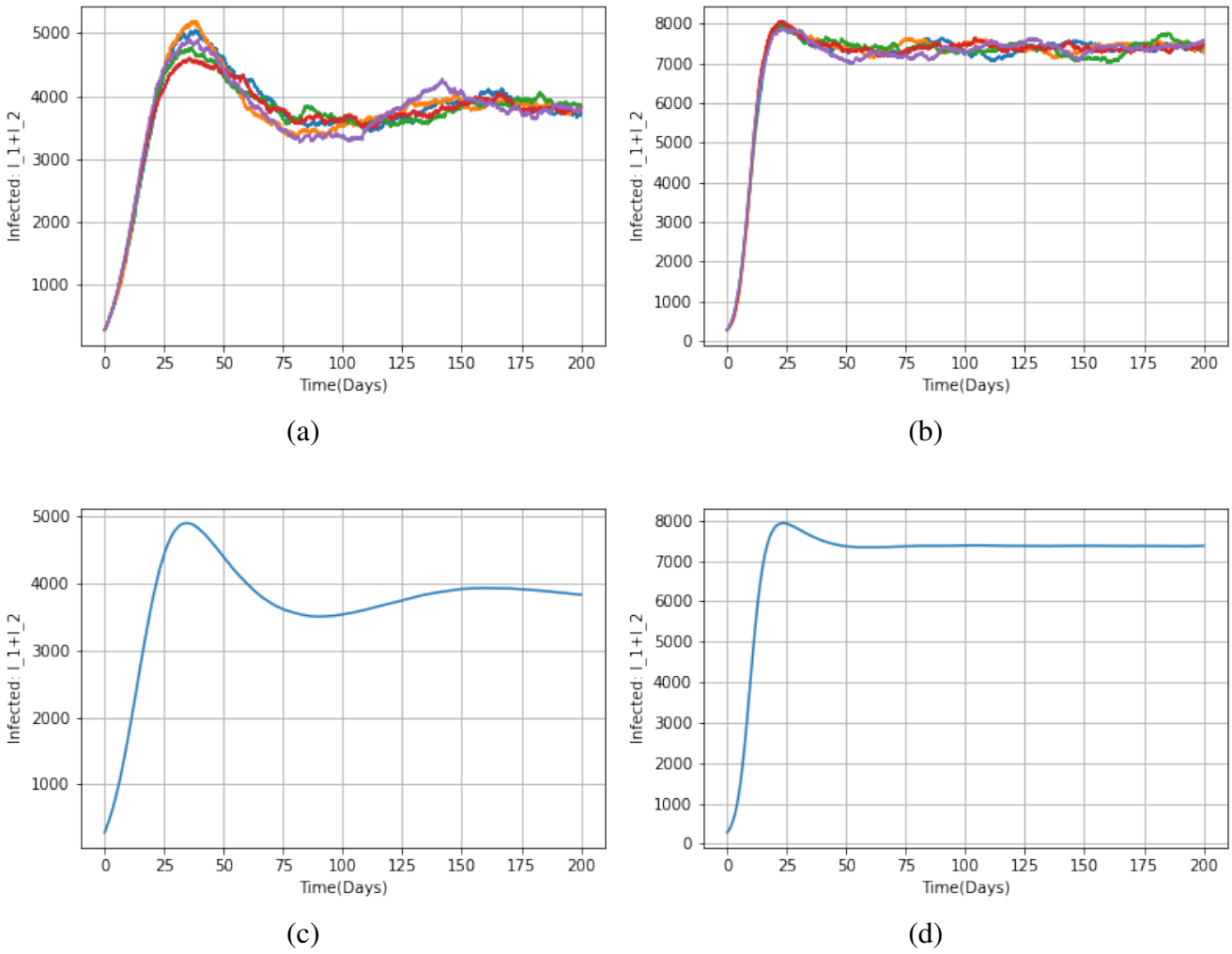

Figure 21: Persistence in mean of the disease with initial conditions $(S_1(0), S_2(0), I_1(0), I_2(0), R(0)) = (1000, 700, 200, 80, 20)$ and a step size 10^{-2}. Upper panel (a) (respectively (b)) represents 5 simulations of infected $(I_1 + I_2)$ of stochastic system (3.17) with parameters which satisfy condition (a) (respectively (b)) of Theorem 14. Lower panel (c) (respectively (d)) represents the average value of 1000 simulations of infected $(I_1 + I_2)$ of system (3.17) with the same parameter values.

cylindrical Borel $\sigma-$ field. Let $X_t(\omega) = \omega(t)$ for $\omega \in \Omega'$. Set $\mathcal{F}'_t = \bigcap_{u>t} \sigma(X_s : s \leq u)$. We say a probability measure $\mathbb{P}$ on $C(\mathbb{R}^d_+)$ solves the martingale problem $MP(\mathcal{L}, \nu)$ if under $\mathbb{P}$ the law of X_0 is equal to ν and for all $f \in C^2_b(\mathbb{R}^d_+)$,

$$f(X_t) - f(X_0) - \int_0^t \mathcal{L}f(X_s)\mathrm{d}s,$$

is a local martingale under $\mathbb{P}$ with respect to $\sigma-$ fields $\mathcal{F}'_t$.

Let $|\ x\ |$ denote the Euclidean norm of $x \in \mathbb{R}^d$ and S^+_d denote the space of $d \times d$ symmetric strictly positive definite matrices. We assume that for some fixed $\alpha \in (0, 1]$,

(H1) $(\gamma_{ij})_{i,j\leq d} : \mathbb{R}^d_+ \to S^+_d$ is $\alpha-$ Hölder continuous on compact sets;

(H2) $(b_i)_{i\leq d} : \mathbb{R}^d_+ \to \mathbb{R}^d$ is $\alpha-$ Höder continuous on compact sets and for all $i \leq d$, $b_i(x) \geq 0$ whenever $x_i = 0$.

We also assume that

$$\mid b(x) \mid \leq C(1+ \mid x \mid) \quad \text{for all} \quad x \in \mathbb{R}^d_+. \tag{4.51}$$

Theorem 16 *Suppose (H1) and (H2) hold. There is a positive constant* $c_{1.1} = c_{1.1}(\alpha, d)$ *such that if*

$$\sum_{i\neq j} \mid \gamma_{ij}(x) \mid \leq c_{1.1} \min_i \gamma_{ii}(x) \quad \textit{for all} \quad x \in \partial\mathbb{R}^d_+, \tag{4.52}$$

then for any probability ν *on* $\mathbb{R}^d_+$*, there is at most one solution to* $MP(\mathcal{L}, \nu)$*. If, in addition, (4.51) holds, then there is exactly one solution to* $MP(\mathcal{L}, \nu)$*.*

Chapter 5

Conclusion and perspectives

5.1 General conclusion

This thesis seeks to deepen the understanding of the interplay between external variability and host defenses in shaping the outcomes of epidemics, with a particular focus on scenarios where parasites do not evolve. By examining the random factors influencing disease dynamics, the research provides valuable insights into the complexities of epidemic control, particularly in world that is rapidly changing. The findings highlight the need for adaptive and flexible public health strategies, that can accommodate to the inherent unpredictability of infectious disease outbreaks.

In Section 4.1, we presented the results of the analysis of a COVID-19 transmission model that incorporated self-quarantined individuals, delays in diagnosis, and environmental transmission. The model was specifically designed to analyze the dynamics of the pandemic in Ghana. Our analysis revealed that the DFE is GAS when the basic reproduction number, $\mathcal{R}_0$, is less than or equal to 1 and the EE is GAS when $\mathcal{R}_0 > 1$. From the sensitivity analysis, we showed that reducing the interaction between susceptible individual, the virus in the environment, and exposed individuals will further reduce the virus spread in the local community or reduce the basic reproduction number more rapidly. As a result, we recommended that all individuals adhere to strict hygiene practices, including regular hand washing with soap and the use of alcohol-based sanitizers when using public facilities. This would help minimize contact with contaminated surfaces or objects. In addition, to reduce the risk of infection from exposed individuals, we advise to improve air quality through increased airflow, air cleaning, or gathering outdoors. Moreover, Figure 8(d) highlighted the importance of timely diagnosis in reducing the number of exposed individuals. Thus, we suggested that the government intensify efforts in diagnosing COVID-19 cases to limit the number of infected individuals in each community. This would significantly contribute to controlling the spread of the virus in Ghana.

When a large proportion of a population becomes immune to a virus, it becomes harder for the disease to spread. This concept constitutes the foundation of herd immunity [22, 35, 72].

However, many individuals choose not to be vaccinated for various reasons (health concerns, lack of information, systemic mistrust, see [83]). Furthermore some vaccines offer only partial protection or are effective only against certain disease variants as seen in the case of COVID-19 where the vaccine efficiency and immunity waning against different variants have been a concern. Therefore, pathogens often encounter a heterogeneous population of vaccinated and unvaccinated hosts [83], and this has consequences in the disease's evolution [2, 48, 45].

In Section 4.2, we employed mathematical modelling techniques, including both analytical methods and numerical simulations, to assess the population-level impact of different types of imperfect vaccines in controlling the spread of a disease transmission within a community. In the first section, we conducted a theoretical analysis of the model, focusing on key epidemiological indicators, such as the basic reproduction number, $\mathcal{R}_0$, and determined the necessary conditions for the stability of the disease-free and endemic equilibria. A key outcome of this analysis was the derivation of a condition related to the proportion of vaccinated individuals required to achieve herd immunity. We defined this as the critical vaccination coverage the threshold at which the reproduction number is reduced to $\mathcal{R}_0 < 1$, ensuring that the disease cannot persist in the population. This condition provides a measurable target for public health interventions aimed at achieving disease eradication through vaccination.

When the vaccine is developed to prevent infection and stop transmission, our results indicates that disease eradication was possible with a strong population turnover, provided that vaccination coverage was greater than 69.6% (48.9%) for weak (strong) vaccine efficiency. However, when population turnover is weak, we observed damped oscillations, and eradication was only achievable with a highly efficient vaccine and a coverage above 75.6%. Otherwise, the disease persisted and became endemic in the community. We emphasized the role of population turnover as an important factor in determining the success of vaccination campaigns (as suggested in [63, 98, 101]). For example, for human population, the turnover can be seen as migration in and out of the community, as birth and death tend to be small and relatively constant. Our results suggested that for a community with strong migration (strong turnover), vaccinating individuals coming in, could help lower the basic reproduction number. However, if there was a weak migration (weak turnover) such as during travel restriction, the vaccination strategy should be enhance with mass vaccination campaigns and the use of high efficiency vaccines. A similar approach applies to domesticated animals (livestock), with the movement of vaccinated individuals between farms influence the dynamics of the epidemic.

We then conducted more detailed analysis of the impact of vaccine type and its efficiency on disease dynamics. The vaccine can reduce transmission and/or enhance the recovery of infected individuals. Disease eradication was achievable if the vaccine reduced transmission by 82%, improved recovery by at least 25%, and a vaccination coverage of 82% was reached provided there was a strong population turnover. In contrast, under weak turnover, maximum vaccine efficiency and coverage were required. This highlights the interaction between the strength of population turnover and the vaccine efficiency and properties. Moreover, we explored the crucial role of vaccine design, specifically the trade-off between its efficiency in preventing transmission (infection) and its ability to accelerate recovery from the disease. By examining three trade-off curves, we found that the convex function ($\nu = \varepsilon^2$) was the most desirable when the vaccine efficiency exceeded 60% under strong population turnover. However, under a weak population turnover, the disease eradication was challenging regardless of the vaccination coverage and the vaccine efficiency combined. Furthermore, we noticed that a smaller vaccination coverage and/or efficiency was sufficient when using a vaccine designed with a convex trade-off between transmission reduction and recovery enhancement compare to vaccines with other trade-offs or no trade-off.

Our model has both limitations and advantages compared to previous work in the literature, as it aims to study the overall behaviour of disease dynamics under various schematic scenarios. First, we used, COVID-19 parameters for illustrative purposes to show the vaccination coverage threshold for a highly transmissible disease. However, we caution against drawing precise recommendations for COVID-19 vaccination solely from these results. Second, our model does not explicitly account for continuous vaccination or large vaccination campaigns in a community. In our model, vaccination is linked to population turnover, which explain the periodic oscillations in disease incidence (known as "honeymoon periods", [22, 51, 98, 101]). These periodic epidemics, as predicted for COVID-19, may be linked to immunity waning of the various vaccines against emerging variants [72]. Third, we used a frequency dependent transmission, which allowed us to derive analytical results in more comprehensively than some earlier model. However, the approach might underestimate the spread of disease and speed of disease dynamics. Thus, to make accurate predictions regarding vaccination efficiency and campaigns for a given disease, the ad hoc parameters of our models must to be correctly calibrated and adjusted.

This model contained some general conclusions that extend beyond human populations to include domesticated animals (livestock), wild animals and even crops. Domesticated animals like human require vaccinations (e.g., [26, 49]), and our study emphasized the

importance of turnover and migration rates within and out of the population. Our results also suggested that in livestock, vaccine types can be adjusted depending on the disease, especially if the goal is to ensure recovery of infected animals rather than focusing only on preventing any transmission (e.g., [26, 49]). Our results could also be relevant for vaccination campaigns aimed at wild, endangered animals [23]. The model can also be applied to crop immunisation. For example, to protect plants from pathogens or pests, biotic or synthetic chemicals can be used to induce immunity in the plant [38] or fungicides [95]. In this context, fungicide application is equivalent to vaccination and is decoupled from population turnover, which in this case refers to the planting and harvesting cycle. Plant epidemiology modelling has been used to predict the efficiency of imperfect fungicide treatments in controlling epidemics and improving crop yield, with results similar to those obtained in our study [95, 99].

A major question in epidemiology is to understand the effect stochasticity and determining realistic outcome of epidemics scenario. In Section 4.4, we formulated the stochastic model to examine the transmission dynamic of an infectious disease within a heterogeneous population of vaccinated and unvaccinated hosts, with the goal to investigate the effect of demographic variability on the ODE system (3.3). The SDE model derived from the approach of Allen et al. [5], does not satisfy the classical global Lipschitz condition when population sizes approaches zero, as it involves square roots of population sizes in the diffusion coefficients. To the best of our knowledge the existence and uniqueness of solutions for such models have not been fully addressed in the stochastic disease modelling literature. We were able to prove the existence and uniqueness of a non-negative weak solution of the SDE by using Theorem 1.2 of [24]. We also discussed the extinction and persistence in mean of the proposed model and providing sufficient conditions for each scenario. Finally, we performed numerical simulations to support our analytical results. Our findings show that the conditions required for disease extinction in the stochastic system are more restrictive than those in the deterministic system, a result that has implications for optimizing vaccination campaigns.

5.2 Perspectives

The thesis concludes with a forward looking exploration on how temperature variability and vaccination strategies affect malaria dynamics within a metapopulation model of malaria. Malaria remains a significant public health challenge, particularly in tropical and subtropical regions, where temperature fluctuations significantly impact mosquito behavior and parasite

development. Rising greenhouse gas emissions are expected to exacerbate climate change in the coming years [78]. As atmospheric CO_2 levels increase, global temperatures are projected rise, enhancing breeding conditions, for vector such as mosquitoes, which transmit malaria. Higher temperatures can expand the geographical range and seasonal duration of mosquito habitats, improving their suitability for reproduction. These results in larger mosquito population and faster parasite development within the vector, whichin turn can lead to increase transmission rates of vector-borne diseases, like malaria.

Regions that experience low transmission rates of vector-borne diseases may face significant changes as temperatures rise to levels more favorable for vector breeding. In areas previously unsuitable for mosquito populations, even modest temperature increases can create condition conducive to mosquito reproduction and survival. As temperatures approach the optimal range for mosquito activity and parasite development, these areas experience a sharp rise in transmission rates, potentially transforming previously low risk regions into hotspots for diseases like malaria. This highlights the need to understand and predict how climate change may alter disease transmission dynamics across various ecological settings. To address this, we will incorporate a temperature model based on an Ornstein–Uhlenbeck process, to capture global warming trend. Depending on the availability of historical temperature data, we will estimated the model's unknown parameters. Coupling this temperature model with the metapopulation model for malaria, we aim to simulate the impact of changing climatic conditions on malaria transmission rates across multiple populations.

The model will also incorporate vaccination strategies, focusing on their effectiveness in reducing malaria transmission within and between populations, particularly in areas with significant variability in mosquito density and human movement. By capturing the stochastic nature of transmission in metapopulations, the model account for local extinctions and reintroductions of the disease, as well as the impact of temperature on the parasite's life cycle. Using both mathematical analysis and numerical simulations, we validate the influence of temperature on mosquito breeding rates and mosquito mortality. In addition, we will investigate and evaluate how these temperature dependent factors interact with vaccination coverage to determine wheter malaria persists or is eradicated in various regions. The study aims to provide more actionable insights into developing more robust malaria control strategies by incorporating environmental variability, the limitation of imperfect vaccines and the challenges posed by population heterogeneity.

Bibliography

[1] Abimbade, S.F., Olaniyi, S., Ajala, O., Ibrahim, M.: Optimal control analysis of a tuberculosis model with exogenous re-infection and incomplete treatment. Optimal Control Applications and Methods **41**(6), 2349–2368 (2020)

[2] Alizon, S., Hurford, A., Mideo, N., Van Baalen, M.: Virulence evolution and the trade-off hypothesis: history, current state of affairs and the future. Journal of evolutionary biology **22**(2), 245–259 (2009). URL https://doi.org/10.1111/j.1420-9101.2008.01658.x

[3] Allen, E.: Modeling with Itô stochastic differential equations, vol. 22. Springer Science & Business Media (2007)

[4] Allen, E.J., Allen, L.J., Arciniega, A., Greenwood, P.: Construction of equivalent stochastic differential equation models. Stochastic analysis and applications **26**(2), 274–297 (2008). URL https://doi.org/10.1080/07362990701857129

[5] Allen, E.J., Allen, L.J., Smith, H.: On real-valued sde and nonnegative-valued sde population models with demographic variability. Journal of Mathematical Biology **81**(2), 487–515 (2020). URL https://doi.org/10.1007/s00285-020-01516-8

[6] Allen, L.J.: An introduction to stochastic processes with applications to biology. CRC press (2010)

[7] Allen, L.J.: A primer on stochastic epidemic models: Formulation, numerical simulation, and analysis. Infectious Disease Modelling **2**(2), 128–142 (2017). URL https://doi.org/10.1016/j.idm.2017.03.001

[8] Allen, L.J., Lahodny Jr., G.E.: Extinction thresholds in deterministic and stochastic epidemic models. Journal of Biological Dynamics **6**(2), 590–611 (2012). URL https://doi.org/10.1080/17513758.2012.665502

[9] Anderson, D.H.: Compartmental modeling and tracer kinetics, vol. 50. Springer Science & Business Media (2013)

[10] Anderson, R.M., May, R.M.: Population biology of infectious diseases: Part 1. Nature **280**(5721), 361–367 (1979). URL https://doi.org/10.1038/280361a0

[11] Anderson, R.M., May, R.M.: The invasion, persistence and spread of infectious diseases within animal and plant communities. Philosophical Transactions of the Royal Society of London. B, Biological Sciences **314**(1167), 533–570 (1986). URL https://doi.org/10.1098/rstb.1986.0072

[12] Anderson, R.M., May, R.M.: Infectious diseases of humans: dynamics and control. Oxford university press (1991)

[13] Anderson, R.M., May, R.M.: Population biology of infectious diseases. Report of the Dahlem workshop on population biology of infectious disease agents Berlin 1982, March 14–19, vol. 50. Berlin:: Springer Science & Business Media (2012)

[14] Arino, J., Brauer, F., Van Den Driessche, P., Watmough, J., Wu, J.: A model for influenza with vaccination and antiviral treatment. Journal of theoretical biology **253**(1), 118–130 (2008). URL https://doi.org/10.1016/j.jtbi.2008.02.026

[15] Asamoah, J.K.K., Bornaa, C., Seidu, B., Jin, Z.: Mathematical analysis of the effects of controls on transmission dynamics of sars-cov-2. Alexandria Engineering Journal **59**(6), 5069–5078 (2020). URL https://doi.org/10.1016/j.aej.2020.09.033

[16] Asamoah, J.K.K., Jin, Z., Sun, G.Q., Li, M.Y.: A deterministic model for q fever transmission dynamics within dairy cattle herds: using sensitivity analysis and optimal controls. Computational and mathematical methods in medicine **2020**(1) (2020). URL https://doi.org/10.1155/2020/6820608

[17] Asamoah, J.K.K., Jin, Z., Sun, G.Q., Seidu, B., Yankson, E., Abidemi, A., Oduro, F., Moore, S.E., Okyere, E.: Sensitivity assessment and optimal economic evaluation of a new covid-19 compartmental epidemic model with control interventions. Chaos, Solitons & Fractals **146**, 110885 (2021). URL https://doi.org/10.1016/j.chaos.2021.110885

[18] Asamoah, J.K.K., Nyabadza, F., Jin, Z., Bonyah, E., Khan, M.A., Li, M.Y., Hayat, T.: Backward bifurcation and sensitivity analysis for bacterial meningitis transmission dynamics with a nonlinear recovery rate. Chaos, Solitons & Fractals **140**, 110237 (2020). URL https://doi.org/10.1016/j.chaos.2020.110237

[19] Asamoah, J.K.K., Nyabadza, F., Seidu, B., Chand, M., Dutta, H.: Mathematical modelling of bacterial meningitis transmission dynamics with control measures. Computational and mathematical methods in medicine **2018**(1) (2018). URL https://doi.org/10.1155/2018/2657461

[20] Asamoah, J.K.K., Oduro, F.T., Bonyah, E., Seidu, B.: Modelling of rabies transmission dynamics using optimal control analysis. Journal of Applied Mathematics **2017** (2017). URL https://doi.org/10.1155/2017/2451237

[21] Asamoah, J.K.K., Owusu, M.A., Jin, Z., Oduro, F., Abidemi, A., Gyasi, E.O.: Global stability and cost-effectiveness analysis of covid-19 considering the impact of the environment: using data from ghana. Chaos, Solitons & Fractals **140**, 110103 (2020). URL https://doi.org/10.1016/j.chaos.2020.110103

[22] Ashby, B., Alex, B.: Herd immunity. Current Biology **31**(4), R174–R177 (2021)

[23] Barnett, K.M., Civitello, D.J.: Ecological and evolutionary challenges for wildlife vaccination. Trends in parasitology **36**(12), 970–978 (2020). URL https://doi.org/10.1016/j.pt.2020.08.006

[24] Bass, R., Perkins, E.: Degenerate stochastic differential equations with hölder continuous coefficients and super-markov chains. Transactions of the American Mathematical Society **355**(1), 373–405 (2003). URL https://doi.org/10.1090/S0002-9947-02-03120-3

[25] Birkhoff, G., Rota, G.: Ordinary differential equations. John Wiley & Sons (1978)

[26] Bitsouni, V., Lycett, S., Opriessnig, T., Doeschl-Wilson, A.: Predicting vaccine effectiveness in livestock populations: A theoretical framework applied to prrs virus infections in pigs. PLoS One **14**(8), e0220738 (2019). URL https://doi.org/10.1371/journal.pone.0220738

[27] Booth, M.T., Hairston Jr, N.G., Flecker, A.S.: How mobile are fish populations? diel movement, population turnover, and site fidelity in suckers. Canadian Journal of Fisheries and Aquatic Sciences **70**(5), 666–677 (2013). URL https://doi.org/10.1139/cjfas-2012-0334

[28] Boots Michael, G.J., Ross, D., Norman, R., Hails, R., Sait, S.: The population dynamical implications of covert infections in host–microparasite interactions. Journal of Animal Ecology **72**(6), 1064–1072 (2003). URL https://doi.org/10.1046/j.1365-2656.2003.00777.x

[29] Bowong, S., Tewa, J.: Mathematical analysis of a tuberculosis model with differential infectivity. Communications in Nonlinear Science and Numerical Simulation **14**(11), 4010–4021 (2009). URL https://doi.org/10.1016/j.cnsns.2009.02.017

[30] Cheng, S., Chen W.and Yang, Y., Chu, P., Liu, X., Zhao, M., Tan, W., Xu, L., Wu, Q., Guan, H., Liu, J.: Effect of diagnostic and treatment delay on the risk of tuberculosis transmission in shenzhen, china: an observational cohort study, 1993–2010. PLoS One **8**(6), e67516 (2013). URL https://doi.org/10.1371/journal.pone.0067516

[31] Cressler, C.E., McLeod, D.V., Rozins, C., Van Den Hoogen, J., Day, T.: The adaptive evolution of virulence: a review of theoretical predictions and empirical tests. Parasitology **143**(7), 915–930 (2016). URL https://doi.org/10.1017/S003118201500092X

[32] Cresson, J., Sonner, S.: A note on a derivation method for sde models: Applications in biology and viability criteria. Stochastic Analysis and Applications **36**(2), 224–239 (2018). URL https://doi.org/10.1080/07362994.2017.1386571

[33] Dagan, N., Barda, N., Kepten, E., Miron, O., Perchik, S., Katz, M.A., Hernán, M.A., Lipsitch, M., Reis, B., Balicer, R.D.: Bnt162b2 mrna covid-19 vaccine in a nationwide mass vaccination setting. New England Journal of Medicine **384**, 1412–23 (2021). DOI 10.1056/NEJMoa2101765

[34] Djaoue, S., Kolaye, G.G., Abboubakar, H., Ari, A.A.A., Damakoa, I.: Mathematical modeling, analysis and numerical simulation of the covid-19 transmission with mitigation of control strategies used in cameroon. Chaos, Solitons & Fractals **139**, 110281 (2020). URL https://doi.org/10.1016/j.chaos.2020.110281

[35] Djatcha Yaleu, G., Bowong, S., Danga, E.H., Kurths, J.: Mathematical analysis of the dynamical transmission of neisseria meningitidis serogroup a. International Journal of Computer Mathematics **94**(12), 2409–2434 (2017). URL https://doi.org/10.1080/00207160.2017.1283411

[36] van den Driessche, P., Watmough, J.: Reproduction numbers and sub-threshold endemic equilibria for compartmental models of disease transmission. Mathematical biosciences **180**(1-2), 29–48 (2002). URL https://doi.org/10.1016/S0025-5564(02)00108-6

[37] Duncan, J.: Two cases of coronavirus confirmed in ghana, citi newsroom (Retrieved 16 March 2020.)

[38] Dyakov, Y.T., Dzhavakhiya, V.G., Korpela, T.: Molecular basis of plant immunization. In Comprehensive and Molecular Phytopathology

[39] Efird, J.T., Davies, S.W., O'Neal, W.T., Anderson, E.J.: Animal viruses, bacteria, and cancer: a brief commentary. Frontiers in Public Health

[40] Fang, Y., Nie, Y., Penny, M.: Transmission dynamics of the covid-19 outbreak and effectiveness of government interventions: A data-driven analysis. Journal of medical virology **92**(6), 645–659 (2020)

[41] Fisman, D.N.: Seasonality of infectious diseases. Annual review of public health **28**(1), 127–143 (2007)

[42] Frank, S.A.: Immunology and evolution of infectious disease. Princeton University Press (2002)

[43] Freedman, H.I., Ruan, S., Tang, M.: Uniform persistence and flows near a closed positively invariant set. Journal of Dynamics and Differential Equations **6**(4), 583–600 (1994). URL https://doi.org/10.1007/BF02218848

[44] Frey-Klett, P., Burlinson, P., Deveau, A., Barret, M., Tarkka, M., Sarniguet, A.: Bacterial-fungal interactions: hyphens between agricultural, clinical, environmental, and food microbiologists. Microbiology and molecular biology reviews **75**(4), 583–609 (2011). URL https://doi.org/10.1128/mmbr.00020-11

[45] Gandon, S., Day, T.: The evolutionary epidemiology of vaccination. Journal of the Royal Society Interface **4**(16), 803–817 (2007). URL https://doi.org/10.1098/rsif.2006.0207

[46] Gandon, S., Day, T.: Evidences of parasite evolution after vaccination. Vaccine **26**, C4–C7 (2008). URL https://doi.org/10.1016/j.vaccine.2008.02.007

[47] Gandon, S., Day, T., Metcalf, C.J.E., Grenfell, B.T.: Forecasting epidemiological and evolutionary dynamics of infectious diseases. Trends in ecology & evolution **31**(10), 776–788 (2016). DOI 10.1016/j.tree.2016.07.010

[48] Gandon, S., Mackinnon, M., Nee, S., Read, A.: Imperfect vaccination: some epidemiological and evolutionary consequences. Proceedings of the Royal Society of London. Series B: Biological Sciences **270**(1520), 1129–1136 (2003). URL https://doi.org/10.1098/rspb.2003.2370

[49] Gulbudak, H., Martcheva, M.: A structured avian influenza model with imperfect vaccination and vaccine-induced asymptomatic infection. Bulletin of mathematical biology **76**, 2389–2425 (2014). URL https://doi.org/10.1007/s11538-014-0012-1

[50] Gumel, A., Enahoro, A., Calistus, N., Gideon, A.: Mathematical assessment of the roles of vaccination and non-pharmaceutical interventions on covid-19 dynamics: a multigroup modeling approach. Frontiers in Public Health **9**, 709369 (2021)

[51] Gumel, A.B., McCluskey, C.C., Watmough, J.: An sveir model for assessing potential impact of an imperfect anti-sars vaccine. Mathematical Biosciences and Engineering **3**(3), 485 (2006). DOI 10.3934/mbe.2006.3.485

[52] Halatoko, W.A., Konu, Y.R., Gbeasor-Komlanvi, F.A., Sadio, A.J., Tchankoni, M.K., Komlanvi, K.S., Salou, M., et al.: Prevalence of sars-cov-2 among high-risk populations in lomé (togo) in 2020. PLoS One **15**(11), e0242124 (2020). URL https://doi.org/10.1371/journal.pone.0242124

[53] Hethcote, H.W., Thieme, H.R.: Stability of the endemic equilibrium in epidemic models with subpopulations. Mathematical biosciences **75**(2), 205–227 (2017). URL https://doi.org/10.1016/0025-5564(85)90038-0

[54] Hwang, J.K., Zhang, T., Wang, A.Z., Li, Z.: Covid-19 vaccines for patients with cancer: benefits likely outweigh risks. Journal of hematology & oncology **14**

[55] Iboi, E., Richardson, A., Ruffin, R., Ingram, D., Clark, J., Hawkins, J., McKinney, M., Horne, N., Ponder, R., Denton, Z., et al.: Impact of public health education program on the novel coronavirus outbreak in the united states. Frontiers in public health **9**, 208 (2021). URL https://doi.org/10.3389/fpubh.2021.630974

[56] Ioannidis, J.P.: Benefit of covid-19 vaccination accounting for potential risk compensation. npj Vaccines **6**(1), 1–5 (2021). URL https://doi.org/10.1038/s41541-021-00362-z

[57] Iseki, N., Sasaki, A., Toju, H.: Arms race between weevil rostrum length and camellia pericarp thickness: Geographical cline and theory. Journal of Theoretical Biology **285**(1), 1–9 (2011). URL https://doi.org/10.1016/j.jtbi.2011.05.033

[58] Jacquez, J.A., Simon, C.P.: Qualitative theory of compartmental systems. Siam Review **35**(1), 43–79 (1993). URL https://doi.org/10.1137/1035003

[59] Jacquez, J.A., Simon, C.P.: Qualitative theory of compartmental systems. Siam Review **35**(1), 43–79 (1993). URL https://doi.org/10.1137/1035003

[60] Ji, C., Jiang, D.: Threshold behaviour of a stochastic sir model. Applied Mathematical Modelling **38**(21-22), 5067–5079 (2014). URL https://doi.org/10.1016/j.apm.2014.03.037

[61] Khan, M.A., Atangana, A., Alzahrani, E., et al.: The dynamics of covid-19 with quarantined and isolation. Advances in Difference Equations **2020**(1), 425 (2020). URL https://doi.org/10.1186/s13662-020-02882-9

[62] Khan, T., Khan, A., Zaman, G.: The extinction and persistence of the stochastic hepatitis b epidemic model. Chaos, Solitons & Fractals **108**

[63] Knight, J., Baral, S.D., Schwartz, S., Wang, L., Ma, H., Young, K., Hausler, H., Mishra, S.: Contribution of high risk groups' unmet needs may be underestimated in epidemic models without risk turnover: A mechanistic modelling analysis. Infectious Disease Modelling **5**, 549–562 (2020). URL https://doi.org/10.1016/j.idm.2020.07.004

[64] Kraef, C., Bentzon A.and Panteleev, A., Skrahina, A., Bolokadze, N., Tetradov, S., Podlasin, R., Karpov, I., Borodulina, E., Denisova, E., Azina, I.: Delayed diagnosis of tuberculosis in persons living with hiv in eastern europe: associated factors and effect on mortality-a multicentre prospective cohort study. BMC infectious diseases **21**(1), 1–12 (2021). URL https://doi.org/10.1186/s12879-021-06745-w

[65] La Salle, J., Lefschetz, S.: Stability by Liapunov's direct method with applications by Joseph L Salle and Solomon Lefschetz. Elsevier (2012)

[66] La Salle, J.P.: The stability of dynamical systems, vol. 25. SIAM (1976)

[67] Lahrouz, A., Omari, L., Kiouach, D., Belmaâti, A.: Deterministic and stochastic stability of a mathematical model of smoking. Statistics & Probability Letters **81**(8), 1276–1284 (2011). URL https://doi.org/10.1016/j.spl.2011.03.029

[68] Lambert, F.: Conditions d'existence et d'unicité de la solution pour une équation différentielle fonctionnelle stochastique. Annales scientifiques de l'Université de Clermont. Mathématiques **61**(14), 43–70 (1976). URL http://www.numdam.org/item?id=ASCFM_1976__61_14_43_0

[69] Li, M.Y., Graef, J.R., Wang, L., Karsai, J.: Global dynamics of a seir model with varying total population size. Mathematical biosciences **160**(2), 191–213 (1999). URL https://doi.org/10.1016/S0025-5564(99)00030-9

[70] Li, Q., Guan, X., Wu, P., Wang, X., Zhou, L., Tong, Y., Ren, R., et al.: Early transmission dynamics in wuhan, china, of novel coronavirus–infected pneumonia. New England journal of medicine **382**(13), 1199–1207 (2020). DOI 10.1056/NEJMoa2001316

[71] Maliyoni, M.: Probability of disease extinction or outbreak in a stochastic epidemic model for west nile virus dynamics in birds. Acta Biotheoretica **69**(2), 91–116 (2021). URL https://doi.org/10.1007/s10441-020-09391-y

[72] Mancuso, M., Eikenberry, S.E., Gumel, A.B.: Will vaccine-derived protective immunity curtail covid-19 variants in the us ? Infectious Disease Modelling **6**, 1110–1134 (2021). URL https://doi.org/10.1016/j.idm.2021.08.008

[73] Mao, X.: Stochastic differential equations and applications. Elsevier (2007)

[74] Mao, X., Wei, F., Wiriyakraikul, T.: Positivity preserving truncated euler–maruyama method for stochastic lotka–volterra competition model. Journal of Computational and Applied Mathematics **394**, 113566 (2021). URL https://doi.org/10.1016/j.cam.2021.113566

[75] Marino, S., Hogue, I.B., Ray, C.J., Kirschner, D.E.: A methodology for performing global uncertainty and sensitivity analysis in systems biology. Journal of theoretical biology **254**(1), 178–196 (2008). URL https://doi.org/10.1016/j.jtbi.2008.04.011

[76] Martcheva, M.: Introduction to Mathematical Epidemiology, vol. 61. Springer (2015). URL https://doi.org/10.1007/978-1-4899-7612-3

[77] Martiny, J.B., Riemann, L., Marston, M.F., Middelboe, M.: Antagonistic coevolution of marine planktonic viruses and their hosts. Annual review of marine science **6**(1), 393–414 (2014). URL https://doi.org/10.1146/annurev-marine-010213-135108

[78] Masson-Delmotte, V., Zhai, P., Pirani, A., Connors, S.L., Péan, C., Berger, S., Caud, N., Chen, Y., Goldfarb, L., Gomis, M., Huang, M.: Climate change 2021: the physical science basis. Contribution of working group I to the sixth assessment report of the intergovernmental panel on climate change **2**(1), 2391 (2021)

[79] Moore, S.E., Nyandjo-Bamen, H.L., Menoukeu-Pamen, O., Asamoah, J.K.K., Jin, Z.: Global stability dynamics and sensitivity assessment of covid-19 with timely-delayed diagnosis in ghana. Computational and Mathematical Biophysics **10**(1), 87–104 (2022). URL https://doi.org/10.1515/cmb-2022-0134

[80] Moore, S.E., Okyere, E.: Controlling the transmission dynamics of covid-19. arXiv preprint arXiv:2004.00443 (2020)

[81] Moriyama, M., Hugentobler, W.J., Iwasaki, A.: Seasonality of respiratory viral infections. Annual review of virology **7**, 83–101 (2020)

[82] Märkle, H., Tellier, A.: Inference of coevolutionary dynamics and parameters from host and parasite polymorphism data of repeated experiments. PLoS Computational Biology **16**(3), e1007668 (2020). URL https://doi.org/10.1371/journal.pcbi.1007668

[83] Müller, J., Tellier, A., Kurschilgen, M.: Echo chambers and opinion dynamics explain the occurrence of vaccination hesitancy. Royal Society Open Science **9**(10), 220367 (2022). URL https://doi.org/10.1098/rsos.220367

[84] Ndaïrou, F., Area, I., Nieto, J.J., Torres, D.F.: Mathematical modeling of covid-19 transmission dynamics with a case study of wuhan. Chaos, Solitons & Fractals **135**, 109846 (2020). URL https://doi.org/10.1016/j.chaos.2020.109846

[85] Nkamba, L.N., Manga, T.T.: Modelling and prediction of the spread of covid-19 in cameroon and assessing the governmental measures (march–september 2020). COVID **1**(3)

[86] Nkwayep, C.H., Bowong, S., Tsanou, B., Alaoui, M.A., Kurths, J.: Mathematical modeling of covid-19 pandemic in the context of sub-saharan africa: a short-term forecasting in cameroon and gabon. Mathematical Medicine and Biology : A Journal of the IMA **39**(1)

[87] Nuismer, S.L., Althouse, B.M., May, R., Bull, J.J., Stromberg, S.P., Antia, R.: Eradicating infectious disease using weakly transmissible vaccines. Proceedings of the Royal Society B **283**(1841), 20161903 (2016). URL https://doi.org/10.1098/rspb.2016.1903

[88] Nuismer, S.L., Basinski, A.J., Schreiner, C., Whitlock, A., Remien, C.H.: Reservoir population ecology, viral evolution and the risk of emerging infectious disease. Proceedings of the Royal Society B **289**(1982), 20221080 (2022). URL https://doi.org/10.1098/rspb.2022.1080

[89] Nyandjo Bamen, H.L., Ntaganda, J.M., Tellier, A., Menoukeu Pamen, O.: Impact of imperfect vaccine, vaccine trade-off and population turnover on infectious disease dynamics. Mathematics **5**(11), 1240 (2023). URL https://doi.org/10.3390/math11051240

[90] Nyandjo Bamen, H.L., Ntaganda, J.M., Tellier, A., Menoukeu Pamen, O.: Stochastic extinction and persistence of a heterogeneous epidemiological model. Journal of Applied Mathematics and Computing **70**(6), 5603–5628 (2024). URL https://doi.org/10.1007/s12190-024-02191-4

[91] Øksendal, B.: Stochastic differential equations

[92] Organization, W.H.: WHO characterizes covid-19 as a pandemic. https://www.who.int/dg/speeches/detail/who-director-general (2020)

[93] Organization, W.H.: WHO weekly operational update on covid-19. https://www.who.int/docs/default-source/coronaviruse/situation-reports (2021)

[94] P., W.: Review total population. https://worldpopulationreview.com/ (2020)

[95] Parnell, S., Van Den Bosch, F., Gilligan, C.A.: Large-scale fungicide spray heterogeneity and the regional spread of resistant pathogen strains. Phytopathology **96**(5), 549–555 (2006)

[96] Perilla-Henao, L.M., Casteel, C.L.: Vector-borne bacterial plant pathogens: interactions with hemipteran insects and plants. Frontiers in plant science **7**

[97] Publishing., H.H.: How long can the coronavirus that causes covid19 survive on surfaces. https://www.health.harvard.edu/diseases-and-conditions/covid-19-basics, (2020)

[98] Pulliam, J.R., Dushoff, J.G., Levin, S.A., Dobson, A.P.: Epidemic enhancement in partially immune populations. PLoS One 2 **2**(1), e165 (2007). URL https://doi.org/10.1371/journal.pone.0000165

[99] Rock, K., Brand, S., Moir, J., Keeling, M.J.: Dynamics of infectious diseases. Reports on Progress in Physics **77**(2), 026602 (2014). DOI 10.1088/0034-4885/77/2/026602

[100] Rong, X., Yang, L., Chu, H., Fan, M.: Effect of delay in diagnosis on transmission of covid-19. Mathematical Biosciences and Engineering **17**(3), 2725–2740 (2020)

[101] Scherer, A., McLean, A.: Mathematical models of vaccination. British medical bulletin **62**(1), 187–199 (2002). URL https://doi.org/10.1093/bmb/62.1.187

[102] Schurz, H., Tosun, K.: Stochastic asymptotic stability of sir model with variable diffusion rates. Journal of Dynamics and Differential Equations **27**

[103] Service, G.H.: COVID-19 Updates, Ghana. www.ghanahealthservice.org. (2020). [Retrieved 23 July 2020]

[104] Shuai, Z., van den Driessche, P.: Global stability of infectious disease models using lyapunov functions. SIAM Journal on Applied Mathematics **73**(4), 1513–1532 (2013). URL https://doi.org/10.1137/120876642

[105] Shuman, E.K.: Global climate change and infectious diseases. New England Journal of Medicine **362**(12), 1061–1063 (2010)

[106] Smith, H.L., Waltman, P.: The Theory of the Chemostat: Dynamics of Microbial Competition

[107] Sorrell, I., White, A., Pedersen, A.B., Hails, R.S., Boots, M.: The evolution of covert, silent infection as a parasite strategy. Proceedings of the Royal Society B: Biological Sciences **276**(1665), 2217–2226 (2009). URL https://doi.org/10.1098/rspb.2008.1915

[108] Tchatat, D., Kolaye, G.G., Alioum, A., Bowong, S., Maïrousgou, C.: Mathematical modelling of the impact of poverty on cholera outbreaks. Mathematical Methods in the Applied Sciences **47**(4), 1940–1960 (2024). URL https://doi.org/10.1002/mma.9727

[109] Temgoua, A., Malong, Y., Mbang, J., Bowong, S.: Global properties of a tuberculosis model with lost sight and multi-compartment of latents. Journal of Mathematical Modeling **6**(1), 47–76 (2020). DOI 10.22124/jmm.2018.2775

[110] Vale, P.F., Fenton, A., Brown, S.P.: Limiting damage during infection: lessons from infection tolerance for novel therapeutics. PLoS biology **12**(1), e1001769 (2014). URL https://doi.org/10.1371/journal.pbio.1001769

[111] Worldometer: https://www.worldometers.info/coronavirus/country/ghana/ (2020)

[112] Wu, J., Dhingra, R., Gambhir, M., Remais, J.V.: Sensitivity analysis of infectious disease models: methods, advances and their application. Journal of The Royal Society Interface **10**(86), 20121018 (2013). URL https://doi.org/10.1098/rsif.2012.1018

[113] Yi, X., Liu, G.: Analysis of stochastic nicholson-type delay system with patch structure. Applied Mathematics Letters **96**

[114] Zhai, X., Li, W., Wei, F., Mao, X.: Dynamics of an hiv/aids transmission model with protection awareness and fluctuations. Chaos, Solitons & Fractals **169**

[115] Zhang, W.: Disease clearance of tuberculosis infection: An in-host continuous-time markov chain model. Applied Mathematics and Computation **413**

[116] Zhao, D.: Study on the threshold of a stochastic sir epidemic model and its extensions. Communications in Nonlinear Science and Numerical Simulation **38**

[117] Živković, D., John, S., Verin, M., Stephan, W., Tellier, A.: Neutral genomic signatures of host-parasite coevolution. BMC Evolutionary Biology **19**